PONTIFICIA UNIVERSIDAD CATÓLICA DE CHILE
Facultad de Ciencias Biológicas
Programa de Doctorado en Ciencias Biológicas
Mención Genética Molecular y Microbiología

DOCTORAL THESIS:

GLOEOCAPSOPSIS AAB1, A CYANOBACTERIUM HIGHLY TOLERANT TO DESICCATION ISOLATED FROM THE ATACAMA DESERT

By

ARMANDO JAVIER AZÚA BUSTOS

PONTIFICIA UNIVERSIDAD CATÓLICA DE CHILE
Facultad de Ciencias Biológicas
Programa de Doctorado en Ciencias Biológicas
Mención Genética Molecular y Microbiología

GLOEOCAPSOPSIS AAB1, A CYANOBACTERIUM HIGHLY TOLERANT TO DESICCATION ISOLATED FROM THE ATACAMA DESERT

Tesis presentada a la Pontificia Universidad Católica de Chile como parte de los requisitos para optar al grado de Doctor en Ciencias Biológicas mención Genética Molecular y Microbiología

Por

ARMANDO JAVIER AZÚA BUSTOS

Director de Tesis: Rafael Vicuña Errázuriz

Comisión de Tesis: Bernardo González
Alexis Kalergis
Luis Larrondo
Osvaldo Ulloa

August 30, 2013

PONTIFICIA UNIVERSIDAD CATÓLICA DE CHILE
Facultad de Ciencias Biológicas
Programa de Doctorado en Ciencias Biológicas
Mención Genética Molecular y Microbiología

La defensa final de la tesis Doctoral titulada:

GLOEOCAPSOPSIS AAB1, A CYANOBACTERIUM HIGHLY TOLERANT TO DESICCATION ISOLATED FROM THE ATACAMA DESERT

Presentada con fecha de hoy por el candidato a Doctor

Armando Javier Azúa Bustos

Ha sido aprobada por el Tribunal Examinador, constituido por los profesores abajo firmantes, calificándose el trabajo realizado, el manuscrito sometido y la defensa oral con nota _____

Prof. Rafael Vicuña E.
Director de Tesis
Facultad de Ciencias Biológicas

Prof. Juan Correa M.
Decano
Facultad de Ciencias Biológicas

Prof. Osvaldo Ulloa
Profesor Invitado
Departamento de Oceanografía
Universidad de Concepción

Prof. Alexis Kalergis
Jefe de la Mención
Facultad de Ciencias Biológicas

Prof. Bernardo González
Profesor Invitado
Facultad de Ingeniería y Ciencias
Universidad Adolfo Ibáñez

Prof. Luis Larrondo
Miembro Comisión de Tesis
Facultad de Ciencias Biológicas

Santiago de Chile, August 30 2013

I dedicate this thesis work to my little daughter, Margarita Azúa Rasmussen.

ACKNOWLEDGMENTS

Work on this thesis would not have been possible without the Scholarship for Graduate Studies received from CONICYT Chile to AAB, the financial support from the Millennium Institute for Fundamental and Applied Biology (MIFAB) and from FONDECYT project nº 1110597.

I am indebted to Rafael Vicuña for all his help and guidance, Marcelo Orellana for his help in HPLC analysis, Jorge Zúñiga for his help in obtaining the isolate, Fabio Rodrigues for his help with Raman analysis, Eduardo Palma for his help with phylogenetic analysis and Loreto Salas and Cristián Arenas for their help in various aspects.

INDEX

FIGURE INDEX

TABLE INDEX

ABBREVIATIONS

AAR: Average annual rains

ABS: Absolute value

a_w: Water activity

CLSM: Confocal laser scanning microscopy

DGGE: Denaturing gradient gel electrophoresis

EPS: Exopolysaccharide

HPLC: High performance liquid chromatography

ITS: Internal transcribed region

PAS: Per-iodic acid Schiff staining

PPFD: Photosynthetic photon flux density

qPCR: Quantitative polymerase chain reaction

RH: Relative humidity

SEM: scanning electron microscopy

TEM: Transmission electron microscopy

RESUMEN

El acabado estudio de los microorganismos que han evolucionado en el Desierto de Atacama, el más seco y antiguo del mundo, permitirían entender el rol clave del agua para la vida en general. Para aproximarse a este fin, primero caracterizamos el microambiente que permite la colonización de cuarzos de la Cordillera de la Costa de este desierto por microorganismos hipolíticos. A continuación describimos la composición de la biodiversidad microbiana de estos biofilms, aislando posteriormente una cepa de cianobacteria desde éstos. Basados en análisis morfológicos y filogenéticos, el aislado (AAB1) fue clasificado como un nuevo miembro del género *Gloeocapsopsis*. Los cambios mostrados por células del aislado AAB1 en condiciones de desecación indicaron que éste es altamente tolerante a esta condición de estrés. Adicionalmente, nuestros resultados indican que el aislado sintetiza sacarosa y trehalosa en respuesta a la desecación. Posteriormente identificamos los dos genes candidatos involucrados en la síntesis de sacarosa (la sacarosa-6-fosfato sintetasa y la sacarosa-6-fosfato fosfatasa). Sin embargo, no pudimos identificar los genes involucrados en la síntesis de trehalosa. Medimos también los niveles de mRNA de los genes candidatos involucrados en la síntesis de sacarosa bajo condiciones de desecación mediante qPCR. Sin embargo, las variaciones detectadas requieren experimentos adicionales para poder ser entendidas a cabalidad. Finalmente, el conjunto de resultados obtenidos sugieren que células del aislado AAB1 pueden encontrarse metabólicamente activas bajo condiciones de desecación extrema. Esta posibilidad fue preliminarmente confirmada con la cuantificación de los niveles de ATP en células aisladas, los que encontramos variaban en respuesta a estímulos ambientales.

ABSTRACT

The comprehensive study of microorganisms that evolved in the Atacama Desert, the driest and oldest on Earth, may be of help to understand the key role of water for life in general. In order to approach this aim, we first characterized the microenvironment that allows the colonization of the underside of quartzes of the Coastal range of this desert by hypolithic microorganisms. We then described the microbial diversity composition of these biofilms, later isolating a cyanobacterial isolate from them. Based on morphologic and phylogenetic analyses, this isolate (AAB1) was classified as a new member of the genus *Gloeocapsopsis*. Physiological, morphological and molecular changes of isolate AAB1 cells under desiccation showed that this isolate is highly tolerant to this stressful condition. Our results indicate that isolate AAB1 synthesizes sucrose and trehalose in response to desiccation. We identified the two candidate genes involved in sucrose synthesis (sucrose-6-phosphate synthase and sucrose-6-phosphate phosphatase). However, we could not identify the genes involved in trehalose synthesis. We then mesured the mRNA levels of the candidate genes involved in sucrose synthesis under conditions of desiccation. However, due to the variations observed, further experiments are required to really interprete the results. Finally, the results obtained suggest that isolate AAB1 cells may be metabolically active under conditions of extreme desiccation. This possibility was preliminary confirmed by the quantification of the pools of ATP in desiccated cells, which we found varied in response to various environmental stimuli.

1. Introduction

1.1 The Atacama Desert

By definition, a desert is a region that receives extremely low rains, far less than the amount required to support the growth of most plants (Noy-Meir, 1973). The majority of Earth's deserts have average annual rains (AAR) lower than 400 millimeters per year. This is the case of the Kalahari and Mojave Deserts, which receive 250 and 330 millimeters of AAR, respectively. In turn, "true deserts" receive less than 250 millimeters of AAR. The Gobi and the Sahara Deserts, with AAR of 194 millimeters and 20-100 millimeters, respectively, classify in this category. In the case of the Atacama Desert, the special category of "hyperarid", in which the Atacama Desert is classified, is assigned to those deserts possessing aridity indexes lower than 0.05 that is, the amount of evapo-transpiration of water from its soil far exceeds the amount of rain that it receives (Houston and Hartley, 2003). There are regions in the Atacama Desert with only one reported rain event in four years, which amounted to 2.3 millimeters (McKay *et al*., 2003).

Located between 17° and 27°S latitude in northern Chile, the Atacama Desert is bordered on the east by the Andes Mountains and on the west by the Coastal Range. With AAR of less than 2 mm, in extensive areas of the Atacama Desert Desert even the sturdiest plants and microbes can not grow (McKay *et al*., 2003; Azúa-Bustos *et al.*, 2012) (Figure 1).

As part of the NASA's Astrobiology program, during four years McKay's group collected data (temperature, relative humidity, rains, sun irradiation and winds) that

contributed to better understand the origin of the dryness of the Atacama Desert (McKay *et al*., 2003) The rationale was to focus on the moisture sources and their role in creating suitable environments for photosynthetic microorganisms. They found that during the measured period, the average air temperature had been 16.5°C, with extremes of -6°C and 38°C. Annual average sunlight was about 336 Wm^{-2} and wind speeds averaged a few meters per second. Strikingly, during this period only a single rain event was recorded. This event (of only 2.3 mm) led the authors to suggest that it may have corresponded to a heavy fog rainout. Dews were frequently recorded following nights of high relative humidity at the hyperarid areas, but they did not contribute much to the moisture of the soil surface. In addition, they also concluded that groundwater did not contribute to surface moisture.

Additional work by Houston and Hartley contributed to classify the Atacama Desert as a hyperarid desert (Houston and Hartley, 2003). These authors proposed that the west slope of the central Andes exhibits a pronounced rain shadow effect, causing a core zone of hyper-aridity which extends from 15 to 30°S, at elevations from sea level up to 3500 m. They also suggested that the initial onset of hyper-aridity most likely developed progressively with the uplift of the Andes as these mountains reached elevations between 1000 to 2000 m above sea level, coupled with the intensification of a cold, upwelling Peruvian Current about 10-15 million years ago. The Atacama Desert has additionally been proposed to be the oldest desert on Earth. Based on palaeomagnetic data, Hartley *et al.*, (2005) found no significant latitudinal movement since the late Jurassic, 150 million years ago.

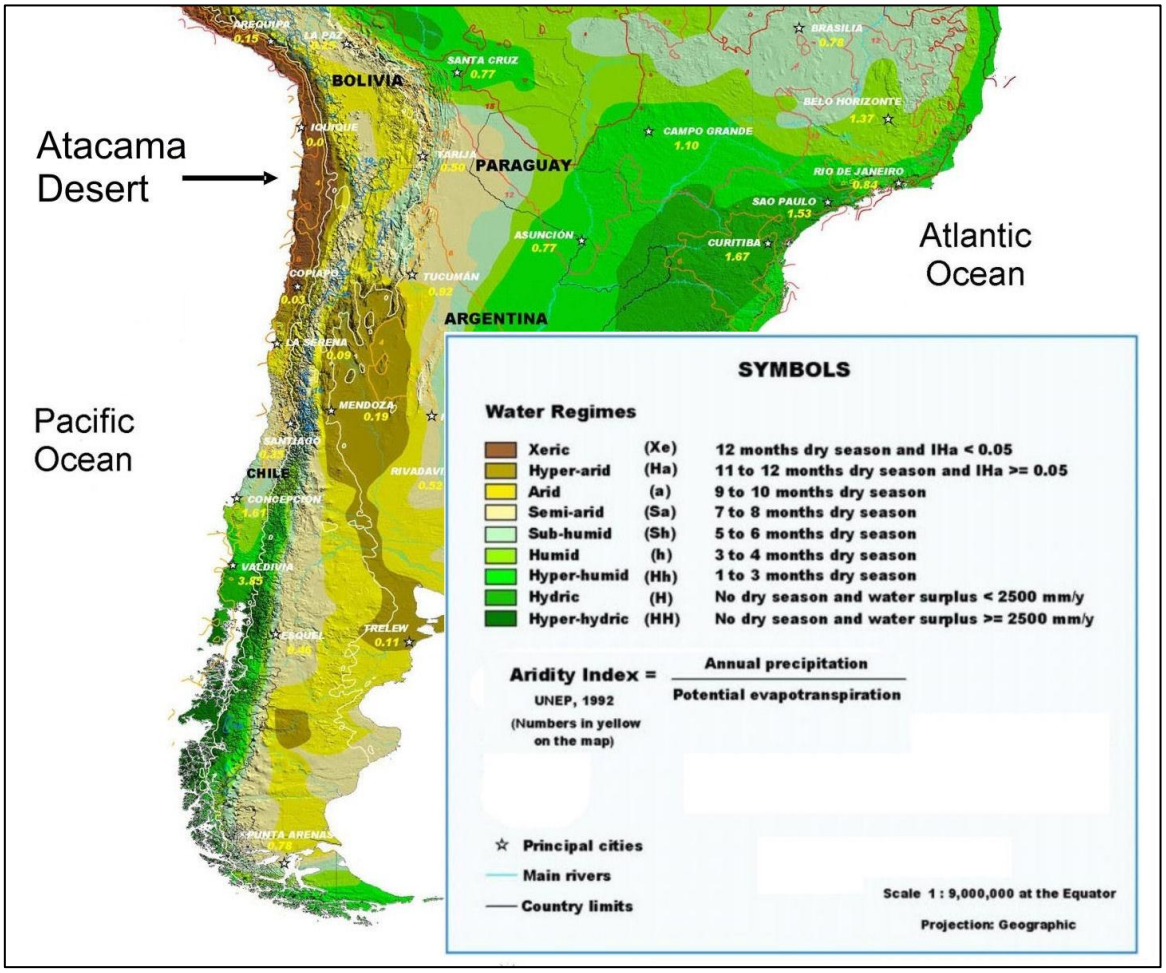

Figure 1.- Map showing the location of the Atacama Desert desert and the water regimes and aridity indexes in the southern tip of South America. *Source: Agriculture and Environmental Center, AGRIMED, Faculty of Agronomical Science, Universidad de Chile.*

This property, along with the location of the Atacama Desert within the dry subtropical climate belt and the presence offshore of a cold, upwelling current dating from at least the early Cenozoic, resulted in conditions promoting climatic stability and the development of this arid desert.

These and other characteristics (in particular high UV irradiation), allowed the Atacama Desert to be considered a valid analog model for the planet Mars (Navarro González *et al*., 2003; Paulino-Lima *et al*., 2013; Azúa-Bustos and Vega-Martínez, 2013)

1.2 Atacama Desert microbiology

For a long time it was thought that extensive regions of the Atacama Desert could not uphold any type of life forms due to its hyperaridity. However, recent culture-independent methods (metagenomics, transcriptomics, *in situ* hybridization, etc) have greatly improved the sensitivity for life detection. Thus, microorganisms have been found even in the driest regions of this desert, which makes scientists wonder about the true limit of water availability needed to sustain life as we know it.

Hypolithic (*under stones*) microbial habitats allow the development of complex and active biological communities in desert environments (Azúa-Bustos *et al*., 2011; Warren-Rhodes *et al*., 2006; Warren-Rhodes *et al*., 2007). Besides the well-known importance of light availability under translucent substrates for the photosynthetic component of the hypolithic community, other factors like temperature and water availability have been investigated. These efforts advance the interesting idea that the benefit of translucent rocks for cyanobacterial communities is the transmission of light to a substrate that is sheltered from the high evaporative water loss of bare soil surfaces.

In the hyperarid deserts of China, Pointing *et al*. (2007) found that the availability of liquid water for hypolithic cyanobacterial communities may be the key determinant of biological diversity, as it was also suggested by Warren Rhodes *et al*. (2006, 2007) in quartzes of the hyperarid areas of the Atacama Desert.

Warren-Rhodes *et al*. (2006) showed that as mean rainfall declines from 21 mm/year to less than 2 mm/year along a south to north transect performed in the central valley of the Atacama Desert, the abundance of hypolithic cyanobacteria under quartz rocks dropped from 28% (Copiapo) to less than 0.1% (Antofagasta).

However, at the extreme western limit of the hyperarid zone in the Atacama Desert, where the arid Coastal Range acts as a topographic barrier to clouds and moisture-rich marine air moving eastwards from the Pacific Ocean, sites are comparatively more humid. Here, fog water allows the presence of "fog oases" in the southern parts of the Coastal Range, able to support a high number of endemic plant species which have been even proposed as a source of water for human consumption (Cereceda *et al*., 2002; Larraín *et al*., 2002). These clouds show a daily cycle with a maximum expansion over the coastal hills during the early morning hours (Farías *et al*., 2005). Consequently, the dry hills and mountains of the Pacific Coastal Range offer relatively more benign sites for the development of microbial life. Although much has been published about the hyperarid areas of the Atacama Desert, there are no reports on the microbial life present in zones where there is some water availability due to fog, as it is the case of the Coastal Range.

For a review on the microbiology in habitats in the Atacama Desert other than hypolithic biofilms under quartzes, see our article attached to this thesis (Azúa *et al*.,

2012), or our papers on Atacama Desert caves microbiology (Azúa-Bustos *et al*., 2009; Azúa-Bustos *et al*., 2010), or soil microbiology (Paulino-Lima *et al*., 2013).

1.3 Cyanobacteria in desert environments

Cyanobacteria in desert environments have been reported in hypolithic, epilithic and endolithic biofilms (Warren-Rhodes *et al*., 2006; Warren-Rhodes *et al*., 2007; Azúa-Bustos *et al*., 2011). Cyanolichens have also been found, although in deserts with moderate temperatures (Büdel, 1997). Cyanobacteria described in these studies include species of the genus *Chroococcidiopsis, Calothrix, Gloeocapsa, Nostoc, Phormidium, Scytonema* and *Stigonema,* among others. These species are highly adapted to desiccation (Potts, 1999) and to high solar radiation (Büdel *et al*., 1997). To date, just a handful of groups have attempted to culture cyanobacteria from arid environments, in particular from the Atacama Desert. Hence, there is virtually no information concerning cyanobacteria of this desert, other than tentative genotypic identification through 16S rRNA profiling.

1.4 Molecular mechanisms allowing tolerance to low availability of water

Water is essential for maintaining the proper structure of macromolecules inside a cell. Its removal from non tolerant organisms leads to irreversible macromolecular aggregations which result in a complete loss of intracellular structure (Alpert, 2005). With the notable exception of some plant seeds, most organisms die when desiccated to a water content of about 20% and are therefore considered sensitive to desiccation. However, some organisms are tolerant to desiccation since they can endure water content

up to 10%. Thus, desiccation tolerance is defined as the ability of an organism to dehydrate in equilibrium with dry air and then reassume the usual physiological functions when rehydrated. Desiccation tolerance, although rare, is widespread among bacteria, fungi and plants (Alpert, 2006).

A good quantitative definition of desiccation is dehydration to less than 0.1 g H_2O per gram of dry matter (equivalent to a water content below 10%) (Tweddle *et al*., 2003). This threshold value of 10% seems to have a biological explanation, since it corresponds to the point in which there is not enough water to form a monolayer around macromolecules inside the cell, preventing proper enzyme activity and therefore active metabolism (Billi *et al*., 2001).

Most of the knowledge related to desiccation tolerance has been gained from plants (Ashraf, 2010). The need of the biotechnology industry to obtain drought tolerant crops has been the main drive for the understanding of molecular and physiological adaptations of life to low water availability (Bhatnagar-Mathur *et al*., 2008).

In general, three main mechanisms have been described that allow organisms to tolerate conditions of low water availability (Potts, 1999; Gorbushina, 2007): 1) intracellular accumulation of compatible solutes that replace water by forming low fluidity “glasses”; 2) synthesis of exopolyssacharides that capture and retain water leading to a more humid microenvironment and 3) synthesis of proteins known as dehydrins (LEA proteins or hydrophilins) that stabilize macromolecules and membranes.

1.4.1 Compatible solutes

Numerous physiological studies have shown that several species accumulate sugars (sucrose, trehalose, fructans), sugar alcohols (mannitol, sorbitol, glucosylglycerol), aminoacids (prolin) and amines (glycine betaine) under conditions of low water availability (Marín *et al*., 2002; Buitink and Leprince, 2004: Avonce *et al*., 2006; Klähn and Hagemann, 2011). These metabolites, also known as compatible solutes, may act as osmolites and antioxidants, or they may even neutralize the action of toxic compounds that interfere with tolerance to water stress. It has been proposed that sugars stabilize cells by directly interacting with macromolecules and membranes by means of reversibly immobilizing the citosol in a liquid state in which the flux of solutes is extremely low. Hence its resemblance to glasses (Buitink, and Leprince, 2004). Interestingly, sugars in seeds tend to form "glasses" at water contents near 10% (Walters *et al*., 2005).

Under conditions of water stress, cyanobacteria like *Phormidium*, *Anabaena*, *Nostoc* and *Chroococcidiopsis* accumulate sucrose and trehalose (Hershkovits *et al*., 1991; Potts, 1999; Higo *et al*., 2006), whereas *Synechocystis* accumulates glucosylglycerol (Marin *et al*., 2002). Genes involved in the biosynthesis of compatible solutes have not been described for any *Gloeocapsopsis* species. In fact, only 5 genes of this entire genus have been reported in Genbank, two of them being 16S rRNA.

Experimental evidence demonstrates that tolerance to water stress can be transferred by means of recombinant DNA techniques. Several transgenic organisms show an increased tolerance after transformation with genes encoding enzymes involved in the production of compatible solutes like glicine betaine (Holmstrom *et al*., 2000), mannitol, trehalose, myo-inositol, sorbitol (Cortina and Culianez-Macia, 2005; Ge *et al*., 2008) and proline (Yamada *et al*., 2005). Genes transferred include those encoding

sucrose-6-phosphate synthase from *Synechocystis* sp. isolate PCC 6803 (Billi *et al*., 2000); phosphethanolamine N-methyltransferase from spinach and choline oxidase from *Arthrobacter pascens*, both from the biosynthetic pathway of glycine betaine (McNeil *et al*., 2001); mannitol phosphate dehydrogenase from *E. coli* involved in mannitol biosynthesis (Tarczynski *et al*., 1992); trehalose-6-phosphate synthase from *E. coli* and yeast and trehalose-6-phosphate phosphatase from *E. coli*, involved in the synthesis of trehalose (Jang *et al*., 2003) and Δ1-pyrroline-5-carboxylate synthetase from Arabidopsis and rice, γ-glutamyl kinase from *Bacillus subtilis* and yeast and proline oxidase from yeast, all from the proline biosynthetic pathway (Chen *et al*., 2007).

1.4.2 Exopolysaccharides

Many microbial communities in arid regions are found to be immersed in exopolyssacharide (EPS) rich matrixes (De Philippis and Vincenzini, 1998). These sugar polymers have the ability to retain water from the atmosphere for long periods of time (Neu, 1996; Azúa-Bustos *et al*., 2011), thus increasing the viability of the microbial cells in arid environments (Gorbushina, 2007). In the cyanobacteria *Anabaena*, the expression of genes encoding enzymes from the metabolic pathway leading to the biosynthesis of exoplyssacharides is activated in response to desiccation (Yoshimura *et al*., 2007).

1.4.3 Dehydrins

An additional mechanism allowing survival under water limitation is the expression of dehydrins or LEA (Late Embryogenesis Abundant) proteins (Hong-Bo *et al.*, 2005; Kovacs *et al*., 2008). This is a group of highly hydrophilic proteins that accumulate during the late stages of embryo maturation in plant seeds. Some authors have suggested calling them “hydrophilins” (Garay-Arroyo *et al*., 2000), although the

generic name dehydrin has prevailed (Close, 1997). Dehydrins are also expressed under conditions of water stress or other types of abiotic stresses in vegetative tissues (Garay-Arroyo *et al*., 2000). Further studies have shown that dehydrins are produced by organisms belonging to all domains of life, namely arquea, bacteria and eukarya (Tweddle *et al*., 2003; Wise and Tunnacliffe, 2004; Kovacs *et al*., 2008). Dehydrins have been grouped in several families based on sequence similarity (Wise, 2003; Wise and Tunnacliffe, 2004). Dehydrin-like proteins have been detected using antibody based assays in cyanobacteria such as *Anabaena* sp. isolate PCC 7120, *Calothrix* sp. isolate PCC7601 and *Nostoc* sp. isolate Mac-R2 (Close and Lammers, 1993). Nevertheless, the genes encoding these proteins are unknown.

There is ample evidence showing the involvement of dehydrins in adaptive responses to water stress. It has been found that heterologous expression of dehydrins in plants, yeast, nematodes and human cells confers tolerance to water deficit (Menze *et al*., 2009; Swire-Clark and Marcotte, 1999). *In vitro* assays, in which the activities of various enzymes were measured both in the presence and in the absence of dehydrins, showed that these proteins (from plants, bacteria and yeast) are able to protect these enzymes from denaturation after a dehydration event (Goyal *et al*., 2005). Transgenic organisms expressing dehydrins also show a better tolerance to water stress (Liu *et al*., 2009; Sivamani *et al*., 2000). Proteins used for these purposes include HVA1 from barley (Oraby *et al*., 2005), Le4 from tomato (Ge *et al*., 2008), BhLEA1 and BhLEA2 from *Boea hygrometrica* (Liu *et al*., 2009) and BN115m from *Brassica napus* (Singh *et al*., 2009).

1.5.- Hypothesis and General Objective of this work:

Given the findings shown above, we postulate the following hypotheses:

Being the Atacama Desert the driest desert on Earth, there are unreported cyanobacteria in this desert that are highly tolerant to desiccation, with molecular mechanisms that can be described and give more details about the tolerance phenomenon in general

The general objective of this thesis is:

To find and isolate a cyanobacterium inhabiting the extremely arid Atacama Desert and characterize its physiological and molecular responses under desiccating conditions.

1.6.- Specific Objectives:

1.-To find and identify a new cyanobacterial isolate and describe its basic physiological and cytological characteristics.

2.-To determine the physiological, molecular and cytological responses of the cyanobacterial isolate under conditions of desiccation.

3.- To gain an improved understanding of the metabolic strategies used by life in general in the desiccated state using the new cyanobacterial isolate as a model.

2. Materials and Methods

2.1. Site description and sampling

Two transects, one 30 m long and the other 25 m long, were set in one of these quartz fields (23º48’57’’ S, 70º29’21’’ O). A square grid (1 × 1 m) was placed twice to the left and twice to the right side randomly along each of these two transects, and all types of rocks over 0.5 g inside the grid were counted and collected. In total, 275 rocks were collected in the eight 1-m^2 quadrants. The fraction of rocks corresponding to quartzes was then separated and weighed. All rock samples were kept in sterile bags until further analysis. The presence of hypolithic microorganisms under all quartz rocks was determined by inspection using a Nikon Optiphot-2 microscope equipped with a Qimaging MicroPublisher 3.3 RTV digital camera.

Temperature and relative humidity measurements

In situ (in the field) and *ex situ* (under lab conditions) infrared temperatures of quartz rocks, soil, and other rocks were taken with a Raytek MiniTemp MT4 non-contact infrared thermometer equipped with a laser pointer in 2007 (Raytek Corporation Santa Cruz, CA, USA). Miniature temperature loggers (17 mm diameter × 6 mm height) ACR SmartButtons, ACR Systems Inc., Surrey, BC, Canada) were used to measure temperatures during 2005 and 2007, under quartz and other rocks, at the quartz–soil interface and at the soil surface adjacent to quartz rocks. The loggers were set up to record the temperature every 30 min, for periods of up to 2 months. In some cases, a total of eight continuous months of data were recorded during 2008. The accuracy of these

loggers was verified by comparing its readings with a mercury thermometer used as a reference standard under simulated *in situ* conditions. Relative humidity measurements at the quartz–soil interface were taken with miniature-sized loggers (16 mm diameter × 6 mm height) (Maxim Integrated Products, Inc., Sunnyvale, CA, USA). The loggers were set up to record the temperature every 30 min for 30 d. When taking measurements with microsensors at the quartz–soil interface, care was taken when placing the sensors under the quartz stones so to rebury them as they were, leaving the hypolithic community as intact as possible. Infrared thermography of quartz rocks, other rock types, and adjacent soils were taken with a ThermaCAM B20HSV (FLIR Systems, Boston, MA, USA). For a quantitative appraisal of the thermographs, 18 to 20 pixels (measuring points) of the thermographs were randomly chosen using the "flying point" feature of the analysis software of the camera. Air temperatures were taken with a DO 9406 thermometer–hygrometer data logger (Delta Ohm, Padua, Italy).

Photosynthetic photon flux density (PPFD) measurements

For PPFD, an Apogee Quantum Meter QMSW-SS calibrated for sunlight was used as instructed by the manufacturer. The sensor was placed on the ground for ambient PPFD measurements and then quartz rocks were placed over it. A black plasticine ring was placed around the sensor and tightly fitted against the quartz in order to measure only the light passing through the quartz. Each reading was recorded when the sensor showed a stable value for at least 10 s. As quartz rocks differed in size, the number of measurements possible to be taken per rock differed as well, due to sensor size.

Determination of the water absorption by biofilm samples

Biofilms samples were collected under quartzes, weighed and then incubated with distilled water in a Petri dish in the laboratory. After 30 min, samples were taken out of the Petri dishes and then weighed again, in order to determine how much water they absorbed in this period of time.

2.2. Characterization of the microbial diversity in the hypolithic biofilm and attainment of a Cyanobacterial isolate.

Approximately 100 mg of biofilm material obtained from the underside of the quartz stones were aseptically collected using a sterile knife. Total genomic DNA was extracted using a Soil DNA Isolation Kit (MoBio Laboratories, Solano Beach, CA, USA) according to the manufacturer's instructions. For cyanobacteria, the 16S rRNA genes present in the extracted DNA were amplified using the cyanobacteria specific oligonucleotide primers—CYA359F (5′-GGGGAAT(CT)TTCCGCAATGGG-3′), CYA781R(a) (5′-GACTACTGGGGTATCTAACATT-3′), and CYA781R(b) (5′-GACTACAGGGGTATCTAATCCCTTT-3′) (Nübel *et al*., 1997) in three separate reactions (CYA359F-CYA781R(a), CYA359FCYA781R(b), and CYA359F-CYA781R(a)-CYA781R(b)). For archaea, Arch21F (5′-TTCCGGTTGATCCYGCCGGA-3′) and Arch958R primers (5′-YCCGGCGTTGAMTCCAATT-3′) were used (Luna *et al*., 2008). For heterotrophic bacteria, universal primers Univ515FPL (5′-GCGGATCCTCTA GACTGCAGTGCCAGCAGCCGCGGTAA-3′) and Univ1492RPL (5′-

GGCTCGAGCGGCCGCCCGGGTTACCTTGTTACGACTT-3′) and bacteria specific primers 63f (5′-CAGGCCTAACACATGCAAGTC-3′) and 1387r (5′-GGGCGGWGTGTACAAGGC-3′) were used (Marchesi *et al*., 1998, Reysenbach, *et al*., 1994). For the amplification of the DNA template, the GoTaq Green Master Mix (Promega Corporation, Madison, WI, USA) was used according to the manufacturer's instructions. PCR conditions were as follows: an initial denaturing step at 94°C for 2 min followed by four consecutive cycles of 94°C for 1 min, n ºC for 1 min, and 72°C for 1 min, in which n = 46–47–48–49°C. This was then followed by 31 cycles of 94°C for 1 min, 50°C for 1 min, 72°C for 1 min, and a final extension step at 72°C for 15 min, thus totaling 35 cycles of amplification. The PCR products were ligated to the pGEM-T Easy Vector System (Promega Corporation, Madison, WI, USA), and cloned in *E. coli* XL1-Blue cells. The resulting plasmid vectors were isolated and purified using the Invisorb Spin Plasmid Mini Two (Invitek GmbH, Berlin, Germany) according to the manufacturer's instructions. Automated sequencing of the clones was conducted by Macrogen DNA Sequencing Inc. (Seoul, Korea) using the M13 forward primer site of the pGEM-T Easy Vector.

Denaturing gradient gel electrophoresis (DGGE)

ITS sequences were amplified using the cyanobacterial ITS specific oligonucleotide primers, CS1Fw (5′-G(T/C)CACGCCCGAAGTC(G/A)TTAC-3′), which contains a 40 bp GC clamp (5'-CGCCCGCCGCGCCCCGCGCCCGGCCCGCCGCCCC CGCCCC-3') and 373Rv (5′-CTAACCACCTGAGCTAAT-3′) (Janse *et al*., 1993). For the PCR reactions, the Go Taq colorless Master Mix (Promega Corporation, Madison,

WI, USA) was used in a touchdown PCR with 10 cycles with annealing temperatures from 62ºC to 52ºC, 25 cycles at 52ºC, and a final extension step at 72ºC for 45 min. PCR products were then quantified using a NanoDrop 2000 (Thermo Scientific, Massachusetts, USA). DGGE of the generated PCR products was performed using the Dcode universal mutation detection system (Bio-Rad Dcode, Richmond, VA, USA) at 75 V and 60°C for 16 h in 0.5×TAE buffer. PCR products (8 μg for biofilm samples and 5μg for cell culture samples) were loaded on 6% (w/v) polyacrylamide gels containing a linear gradient ranging from 40 to 60% denaturant (100% denaturant corresponded to 7 M urea and 40% (v/v) formamide), increasing in the direction of electrophoresis. A 7-ml stacking 6% (w/v) polyacrylamide gel without denaturant was added on top. After electrophoresis, the gels were stained with ethydium bromide for 30 min and then photographed in a transilluminator. Bands were cut and DNA extracted overnight by water elution at 4ºC. This DNA was then re-amplified with the same primers used for the DGGE, at an annealing temperature of 60ºC for 30 cycles. The amplified DNA was sent for automated sequencing conducted by Macrogen DNA Sequencing Inc. (Seoul Korea) using CS1Fw and 373Rv primers. To identify the closest relatives of the ITS sequences obtained, nucleotide sequences were analyzed using the Megablast option for highly similar sequences of the BLASTN algorithm against the National Centre for Biotechnology Information non redundant database (www.ncbi.nlm.nih.gov).

Identification of the biofilm species

To identify the closest relatives of the queried 16S rRNA gene sequences, the nucleotide sequence of the isolated 16S rRNA genes were analyzed using the Megablast

option for highly similar sequences of the BLASTN algorithm against the National Centre for Biotechnology Information nonredundant database (www.ncbi.nlm.nih.gov). Assigned phylogeny was determined by observing the maximum identity values of known species in the list of results obtained for each reported new clone.

Isolation of *Gloeocapsopsis* isolate AAB1

Biofilm samples were collected and placed on flasks containing BG-11 liquid media (Stanier *et al*., 1971). These flasks were placed in a temperature (25ºC) and light (16/8 light dark cycle, 30 μmol m^{-2} s^{-1}) controlled room. Sustained growth and reproduction of these biofilms was attained, with a number of morphologically distinct species being identified by bright field microscopy. From these biofilms, cells corresponding to the expected size and morphology reported for *Gloeocapsopsis* were separated and isolated by serial dilution using an inverted bright field microscope, and placed in 2 by 3 well sterile plastic plates. After 4 months, a mono-cyanobacterial culture was obtained as determined by DGGE and bright field microscopy.

2.3. Microscopy techniques

Bright field microscopy

Biofilms samples were suspended in water, a 5 μl aliquot placed in a glass slide and immediately observed with a Nikon Optiphot-2 microscope. Images were recorded with a Panasonic DMC-FX07 camera.

Transmission Electron Microscopy

To verify the characteristics of the isolate, samples of cells in culture were centrifuged at 3,000 rpm on a tabletop centrifuge. The resulting pellet was fixed with 3% glutaraldehyde in sodium cacodylate buffer 0.1 M pH 7.2 during 18 h at room temperature. After three consecutive 20-min washes with sodium cacodylate buffer 0.1 M pH 7.2, the sample was treated with 1% aqueous osmium tetroxide for 60 min. The sample was then dehydrated with a graded acetone series (50% to 100%), 15 min for each concentration used. The sample was pre-embedded overnight with epon–acetone 1:1 and then embedded in pure epon. The polymerization process was done at 60°C for 24 h. Sixty-nm thin sections were obtained with a Sorvall MT-5000 ultramicrotome and stained with 4% uranyl acetate in methanol and lead citrate. Observations were made with a Philips Tecnai 12 transmission electron microscope operated at 80 kV.

Scanning electron microscopy (SEM)

Small rock samples covered with biofilm were fixed with 2% glutaraldehyde in cacodylate buffer overnight and then washed with the same buffer three times, 20 min each. After critical point drying and gold coating, the samples were observed with a scanning electron microscope Jeol JSM 25S-II at 30 kV.

2.4. Per-iodic acid schiff (PAS) staining

Ultra-microtome cuts of approximate 1-2 μm were first obtained, and then placed in a sterile distilled water drop over glass slides which were then dried. NaOH 0.1N was added and after 5 min the samples were washed with distilled water. Then, 1.5% per-

iodic acid was added, and washed with distilled water after 15 min of incubation. The cuts were then stained with the Schiff stain (fuchsin bisulfate) during 45 min at 30ºC. Thereafter, the stain was washed with distilled water for 20 minutes, with a water change after the first 10 min. Finally, the cuts were dried at 60ºC.

2.5. Phylogenetic analysis of 16S and 23S rRNA, ITS and other gene sequences

Total genomic DNA was extracted using a Microbial DNA Isolation Kit (MoBio Laboratories, Solano Beach, CA, USA) according to the manufacturer's instructions. Gene sequences were aligned by Multiple sequence comparison by log- expectation (MUSCLE), analyzed with jModelTest and then analyzed by PhyML, all tools of the Bosque Phylogenetic Analysis software (Ramírez-Flandes and Ulloa, 2008). Only cultured cyanobacterial species, and if available, only species with known genomes were considered in all analyses.

2.6. Determination of the growth rate under different light intensities

Cells were grown on 250 ml flasks containing 100 ml of BG-11 media (Stanier *et al*., 1971). Three OSRAM l18W-765 fluorescent lamp tubes were used as a source of light. To attain different light levels (10, 30, 70 and 100 μmol m^{-2} s^{-1}), flasks were placed at 9, 16, 29 and 37 cm from the light source respectively. Light/dark regime was set at 16/8 h. Temperature was set at 23ºC. All measurements were performed in triplicate.

2.7. Analysis of photosynthetic pigments

Extraction of photosynthetic pigments

Chlorophyll and carotenoids were extracted based on the protocol by Chorus and Bartram (1999). Ten ml of a cell culture with an OD750nm of 0.9 were serially centrifuged in a 2 ml microfuge tube. The resultant pellet was submerged in liquid nitrogen for one min and then heated for two min at 65ºC, repeating the procedure three times. 1.5 ml of methanol 100% preheated at 65ºC was added to the pellet and then vortexed for one min. The microfuge tube was then sonicated in a Cole Palmer water bath for fifty min. The methanol mixture was placed in a 15 ml tube, completing the volume to 4 ml with 100% methanol. The tube was then placed in the dark for 24 h at room temperature. Finally, the sample was centrifuged at 14.000 rpm for two min, and the supernatant (pigment extract) collected.

Absorbance spectra

After pigment extraction, spectra were directly obtained measuring 1ml of the extract in a quartz cuvette using a Shimadzu UV-160 spectrophotometer in the 400-800 nm range.

Identification of photosynthesis related pigments by HPLC

Samples were analyzed with a Shimadzu SPD-M10A Diode Array Detector/ SCL -10A System Detector/ LC 10AT Liquid Cromatograph equipped with a C18 4.6 mm wide by 150 mm long column. The mobile phase for chlorophyll a and carotenoids was

composed of acetonitrile: methanol: isopropanol (750:200:50). Samples were concentrated from 1 ml to 300 μl by evaporating the solvent at 40ºC. Samples were then centrifuged for 5 min and 100 μl were loaded into the equipment. Analysis runs were for 30 min at 25ºC. Chromatograms were analyzed with the LC Solutions software in the 665 and 474 nm channels for chlorophyll *a* and carotenoids, respectively.

Quantification of chlorophyll autofluorescence intensity

Isolate cell samples were suspended in water and immediately observed using an Olympus FV 1000 confocal laser scanning microscope equipped with a ×100 oil immersion objective (Olympus, Hamburg, Germany). The images were analyzed with the Fluoview 5.0 software. Relative intensity of chlorophyll autofluorescence was quantified using the histogram tool of the ImageJ software.

2.8. Raman spectroscopy

The spectra were obtained in a FT-Raman Bruker RFS-100/s spectrometer with Nd:YAG Coherent laser (excitation at 1064 nm) and equipped with a solid state Ge detector. The spectral resolution was 4 cm^{-1} and the spectra was obtained with 256 accumulations and a laser power of 30 mW.

2.9. Assembly of the desiccation chamber

The chamber consisted of a standard Petri dish. Samples were placed on a glass slide used as support and different amounts of silica, calcium chloride or sodium chloride were used as desiccating agents. To prevent direct contact between the glass slide

containing the samples and the desiccating agent, bundles of sterilized toothpicks were placed in between. Samples were loaded as water based cell suspensions in volumes of up to 500 μl, or as pellets of cells. Relative humidity and temperature inside the desiccation chamber were monitored with miniature-sized loggers (16 mm diameter × 6 mm height) (Maxim Integrated Products, Inc., Sunnyvale, CA, USA). The loggers were set up to record the temperature every 10 min for the duration of the desiccation experiment. Parafilm (Wisconsin, USA) was used to ensure complete seal of the chambers.

2.10. Determination of viability

For viability determinations, the LIVE/DEAD BacLight Bacterial Viability Kit (Molecular Probes, Oregon, USA) was used. Equal volumes of SYTO9 and propidium iodide were combined in a microfuge tube and thoroughly mixed. Three μl of the dye mixture for each ml of the cell suspension were used. The suspension was thoroughly mixed and incubated at room temperature in the dark for 15 min. Five μl of the stained bacterial suspension were placed between a slide and an 20 mm square coverslip and thereafter observed in a Olympus FV 1000 confocal laser scanning microscope (Olympus, Hamburg, Germany) equipped with a ×100 oil immersion objective. The images were recorded with the Fluoview 5.0 software, and dead and live cells counted.

2.11. DNA fragmentation analysis

Determination of genomic PCR fragmentation was based on the protocol of Billi *et al*., (2009). Dried cells were rewetted with sterile distilled water, then they were immediately subjected to three cycles of freeze/thawing and boiled for 5 min. After

centrifugation, the supernatant was used for genomic PCR amplifications using the primer HIP1-CA (5'-GCGATCGCCA-3') (Bruno *et al*. 2005). PCR conditions were as follows: one cycle at 94ºC for 3 min; 30 cycles at [94ºC for 30 s, 35ºC for 30 s and 72ºC for 1 min], and 1 cycle at 72ºC for 7 min. Genomic DNA extracted from desiccated and non-stressed *Gloeocapsopsis* isolate AAB1 and isolate N76 was used as a control. For each species, equal amounts of DNA were used. DNA fragments were resolved in agarose 2% (w/v) gels at 50V.

2.12. Extraction and identification of sugars

A cell pellet was first obtained by centrifuging 10 ml of a cell culture at an OD750nm of 0.9. Two hundred µl of 80% ethanol were then added and the tubes were submerged in liquid nitrogen for one min and then heated for two mins at 65ºC, repeating the procedure three times. To the resulting mixture, additional 1.8 ml of 80% ethanol were added. The tubes were then heated for three h at 65ºC and afterwards incubated at 4ºC for twelve h. The tubes were then centrifuged at 14.000 pm for three min and the supernatant (sugar extract) collected. The ethanol present in the extracts was then evaporated in an AES1000 Savant speedvac. Once all ethanol was evaporated, 1 ml of sterile water was added.

Identification and quantification of sugars by high performance liquid chromatography (HPLC)

One ml samples of sugar extracts were transferred to glass vials. These were capped with PTFE septa and perforated screw caps to allow the injection needle to access

the sample. Vials were placed into the autosampler module of a D-7000 Merck Hitachi HPLC system. This was equipped with an Aminex HPX-87H anionic exchange column. The mobile phase was 5 mM H_2SO_4 and the run lasted 30 min per sample. Sugars were detected in a Refraction Index detector (L-7490 Merck Hitachi). For quantification, standards of known concentration were run before each batch of samples. Using these standards, calibration curves and peak quantification were automatically performed by the equipment operating software. For conversions of μg of sugar per mg of dry weight (this work) to μg of sugar per μg of chlorophyll *a* (reported in other works), we used the conversion in which 1 mg of dry weight contains 1.55 μg of chlorophyll *a*.

2.13. Quantification of the maximum photosynthetic efficiency of the Photosystem II

Maximum photosynthetic efficiency of the Photosystem II of control and desiccated cells was quantified with a Handy PEA system (Hansatech Instrument Ltd., Norfolk, England) after dark adaptation for 30 min. Every experiment was repeated at least three times, with 10 replicas per experimental condition.

2.14. Identification of the candidate genes involved in sucrose and trehalose biosynthesis

Sucrose synthase and sucrose phosphate candidate genes were identified by primer walking, using primer pairs based in orthologous genes reported for phylogenetically close species in which some level of knowledge was available; *e.g.;* annotated genomes, functional properties, etc., like *Gloeocapsa* PCC7428, *N. punctiforme* PCC73102 and *Anabaena variabilis* ATCC 29413. For the amplification of

the DNA template, the GoTaq Green Master Mix (Promega Corporation, Madison, WI, USA) was used according to the manufacturer's instructions. PCR conditions were as follows: an initial denaturing step at 94°C for 2 min followed by four consecutive cycles of 94°C for 1 min, n ºC for 1 min, and 72°C for 1 min, in which n = 46–47–48–49°C. This was then followed by 31 cycles of 94°C for 1 min, 50°C for 1 min, 72°C for 1 min, and a final extension step at 72°C for 15 min, thus totaling 35 cycles of amplification.

Candidate genes involved in trehalose synthesis were searched by primer walking, using degenerate and no-degenerate primers based in orthologous genes reported for phylogenetically close species in which some level of knowledge was known; *e.g.;* annotated genomes, functional properties, etc., like *N. punctiforme* PCC73102 and *A. variabilis* ATCC 29413. The genes involved in the two routes reported for other Cyanobacteria, the *treY* (maltooligosyltrehalose synthase)-*treZ* (maltooligosyltrehalose Trehalohydrolase) gene pathway and the *treS* (trehalose synthase) gene were searched. Additionally, this search was enlarged for other close species like *Calothrix* sp. PCC 6303, *Cyanothece* sp. PCC 7424 and *Nostoc* sp. PCC7120. The gene enconding for trehalase, based on orthologous sequences of *Nostoc* sp. PCC7120 was also searched for. For the amplification of the DNA template, the GoTaq Green Master Mix (Promega Corporation, Madison, WI, USA) was used according to the manufacturer's instructions. PCR conditions were as follows: an initial denaturing step at 94°C for 2 min followed by four consecutive cycles of 94°C for 1 min, n ºC for 1 min, and 72°C for 1 min, in which n = 46–47–48–49°C. This was then followed by 31 cycles of 94°C for 1 min, 50°C for 1 min, 72°C for 1 min, and a final extension step at 72°C for 15 min, thus totaling 35 cycles of amplification.

2.15. RNA extraction, visualization and reverse transcription

RNA was extracted with the RNeasy Plant Mini Kit (Qiagen, USA) according to manufacturer's instructions. To 10 μg of RNA, a solution containing 3-(N-morpholino) propanesulfonic acid, (MOPS) 1X, 2.2 M formaldehyde, 50% deionized formamide, 2 μl of ethidium bromide (2 mg/ml) and a 10X loading buffer containing 50% glycerol, 50 mM EDTA, 0.1% xylencyanol and 0.1% bromophenol blue was added. This RNA solution was heated at 70ºC for 10 min, cooled for 2 min and then analyzed by electrophoresis in 1.2% agarose gels, which contained 20% formaldehyde and a MOPS 1X solution containing MOPS 20 mM, 50 mM sodium acetate and 10 mM EDTA at pH 7. After electrophoresis RNA was visualized by exposing it to UV.

DNAse treatment of extracted RNA

In the case that a particular RNA sample was found to be contaminated with DNA, it was treated with RQ1 RNase-Free DNase Transcriptase (Promega Corporation, Wisconsin, USA) as instructed by the manufacturer.

Reverse transcription of RNA molecules

cDNA from the extracted RNA was obtained with the M-MLV Reverse Transcriptase (Promega Corporation, Wisconsin, USA) as instructed by the manufacturer.

2.16. qPCR analyses

All qPCR analyses were performed in a StepOnePlus Real-Time PCR System (Applied Biosystems, Foster City, USA) thermocycler. All experiments were performed

with at least six replicas and all experiments were performed at least three times. The SensiMix SYBR green Kit (Bio-Lines Reagents, Taunton, USA) was used in all cases, as instructed by the manufacturer. Experiments were analyzed with the StepOnePlus software v 2.2. Primers for the different genes analyzed were: Sucrose synthase; SSqPrimer2Fw GCCGAATGCTTTGGTAAGAG, SSqPrimer2Rv TCGTCACGTTCTTCGTTGTC. Sucrose phosphatase; SppqPrimer2Fw ATGACTTCACGGGCAACTTC, SppqPrimer2Rv CAAGTGCGCATTTTGCTG. *rnpB*: rnpBCAABFw ACCAAACTTGCTGGGTAACG, rnpBCAABRv CTTTAGCGGCGGTATGTTTC. *psbA4*: qD1Cyan-126Fw CGTTAGTGCGTGAAACAAGC, qD1Cyan-225Rv AAGTAACCGTGTGCCGCTAC.

2.17. Quantifications of ATP pools.

ATP was quantified with the BacTiter-Glo Microbial Cell Viability Assay (Promega Corporation, Madison, WI, USA) as instructed by the manufacturer. Ten μl cell samples were deposited in 96 well plates, with four replicas per experimental condition. Experiments were performed three times. The luminescent signal was detected by a Pixis 1024 CCD digital camera, with 1024x1024 resolution and 1 s of exposition time (Princeton Instruments, New Jersey, USA). A control of 1 μM of freshly prepared ATP (Sigma, St. Louis, USA) was used in all experiments.

2.18. Statistical analyses.

For all statistical analyses, the Graphpad software (La Jolla, USA) was used. One-way analysis of variance or Tukey's Multiple Comparison Test were used. Values shown

are the means of at least three replicates. Independent experiments were performed in all cases at least three times.

3.- Results and Discussion

3.1. Site location and description of the quartz-hypolithic biofilm system

The site is located 22 km southwest of the city of Antofagasta, in the eastern slope of the hills of the Coastal Range (23° 48′59″ S, 70° 29′25″ W, elevation 537 m), and about 1.5 km from the Pacific Ocean (Figure 2). Here, moisture-rich air masses coming from the Pacific Ocean advance inland during late evening and night, supporting the ephemeral growth of a few plant species (Farías *et al*., 2005). Quartz rocks are found on the surface and originate from one of several surfacing quartz veins. These quartz rocks are primarily distributed over an area of approximately 1,300 m^2. The detailed description of this site was already published by us (Azúa-Bustos *et al*., 2011, attached to this thesis).

3.2 Characteristics of the quartz-hypolithic biofilm system

Temperature and relative humidity measurements

An infrared thermometer revealed that the tops of quartz rocks exposed to full sunlight during midday hours undertake a smaller temperature increase than other types of rock of similar size, weight, and shape (Figure 3). The top surface of quartz rocks were 3.6°C cooler than white color non-quartz rocks and 12.6°C cooler than opaque rocks of similar characteristics.

Microsensors able to simultaneously log relative humidity (RH) and temperature conditions under quartz rocks showed that temperature fluctuated daily.

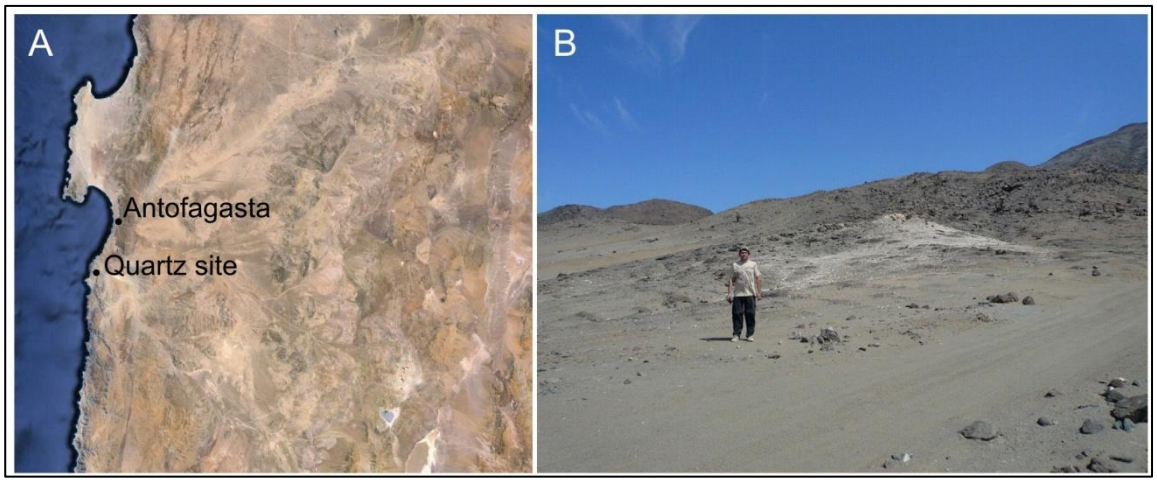

Figure 2.- Site location. A, map depicting the location of the site. B. view of the quartz field.

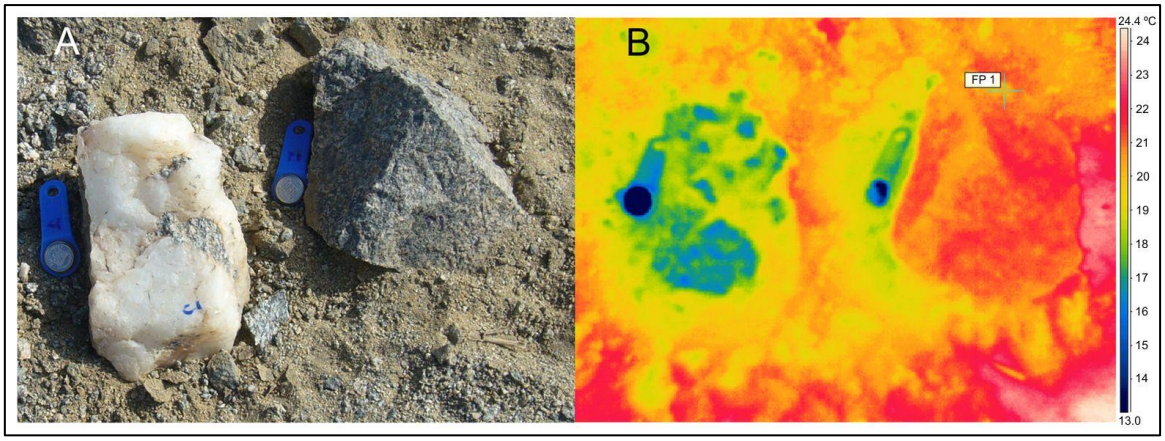

Figure 3.- Infrared thermograph of quartz rocks *in situ*. A, normal view of quartz and other rocks types in the field. B, *in situ* thermograph showing the quartz rock seen in A.

When comparing the temperatures at the quartz–soil interface with the temperatures taken by sensors buried in the soil at a similar depth, the quartz–soil interface remained much cooler during the day and somewhat warmer during the night (Figure 4).

Depending on the atmospheric conditions recorded for a specific day, the hypolithic zone at the quartz–soil interface could be up to 8°C cooler than the surrounding soils during the day and up to 1.5°C warmer during the night. When comparing mean daily temperatures, the quartz–soil interface remained colder than the soil around it. Combined with the infrared temperature data, this shows that quartz rocks (as assessed by the sensors placed both below and above them) were cooler during the day than the surrounding environment (as assessed by the sensors placed on top of the soil surface and buried in its proximity). When comparing the temperatures in the hypolithic zone with the temperatures in similar zones under other types of opaque rock of similar shape, size and weight, a similar trend was observed: the quartz– soil interface was up to 3°C cooler than other rock–soil interface during the day and up to 1°C warmer at night (data not shown).

These microsensors also showed that RH fluctuated daily. RH under the quartz reached values above 80% in 19 out of the 30 days that measurements were conducted (Figure 5). Minimum recorded values of 22% occurred around sunset and maximum values reached 95% around midday, being consistently high (>50%) during part of the afternoon, night, and most of the morning.

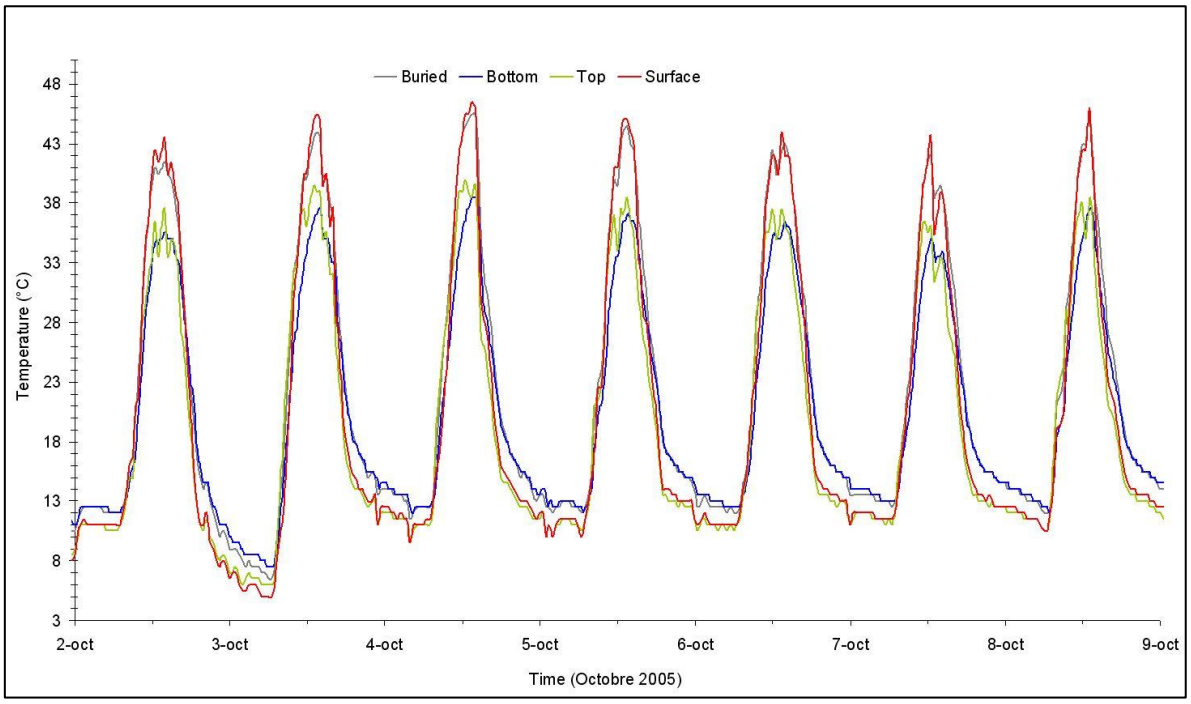

Figure 4.- *In situ* thermal environment around a quartz rock. A representative period of 7 days during spring time is shown. Temperatures were autonomously recorded by microsensors placed around a quartz rock; sensor placed at the quartz–soil interface (bottom), *blue*. Sensor placed over the quartz top, *green*. Sensor placed at the soil surface, *red*. Sensor buried in the soil at the same depth of the sensor labeled as bottom, *gray*.

Then, they dropped in the afternoon and began to rise again early in the evening. No rain events were recorded during or before the time period in which this study was conducted.

It has been suggested that microclimatic changes may have important ecological implications by means of changing photosynthetic productivity in the fog-driven Namib Desert communities (Lalley and Viles, 2006). Our results support this assertion; irrespective of the season of the year, the higher albedo and higher thermal conductivity of the quartz rocks results in lower daytime temperatures and somewhat warmer temperatures during the late evening and nighttime hours at the quartz–soil interface when compared to the nearby desert soil (Figure 3). When comparing mean daily temperatures (7 AM–7 PM) during spring time (September–November) recorded by microsensors placed around a quartz rock, it can be seen that the quartz–soil interface containing the hypolithic community clearly remains colder than the environment around it: quartz–soil interface, 19.8°C; quartz top, 25.7°C; soil surface, 27.9°C; soil (buried sensor), 30.5°C. The maximum mean temperature delta was that of the quartz–soil interface and an equivalent soil stratum (10.7°C). Considering the virtually complete absence of rain at our site, the relative humidity values recorded under quartz rocks at this site are surprisingly high. They reach values higher than 90% during certain days, being consistently high (>50%) during part of the afternoon, night, and most of the morning (Figures 4 and 5), reaching 80% most of the days. Thirty-six percent of the time (402 h), RH was between 70% and 79.9%, and 4% of the time (46 h) RH was between 80% and 89.9%. Interestingly, lichen fields of the Central Namib Desert also frequently experience more than 80% humidity at night, allowing them to conduct net photosynthesis during the following day (Lange *et al*., 2006).

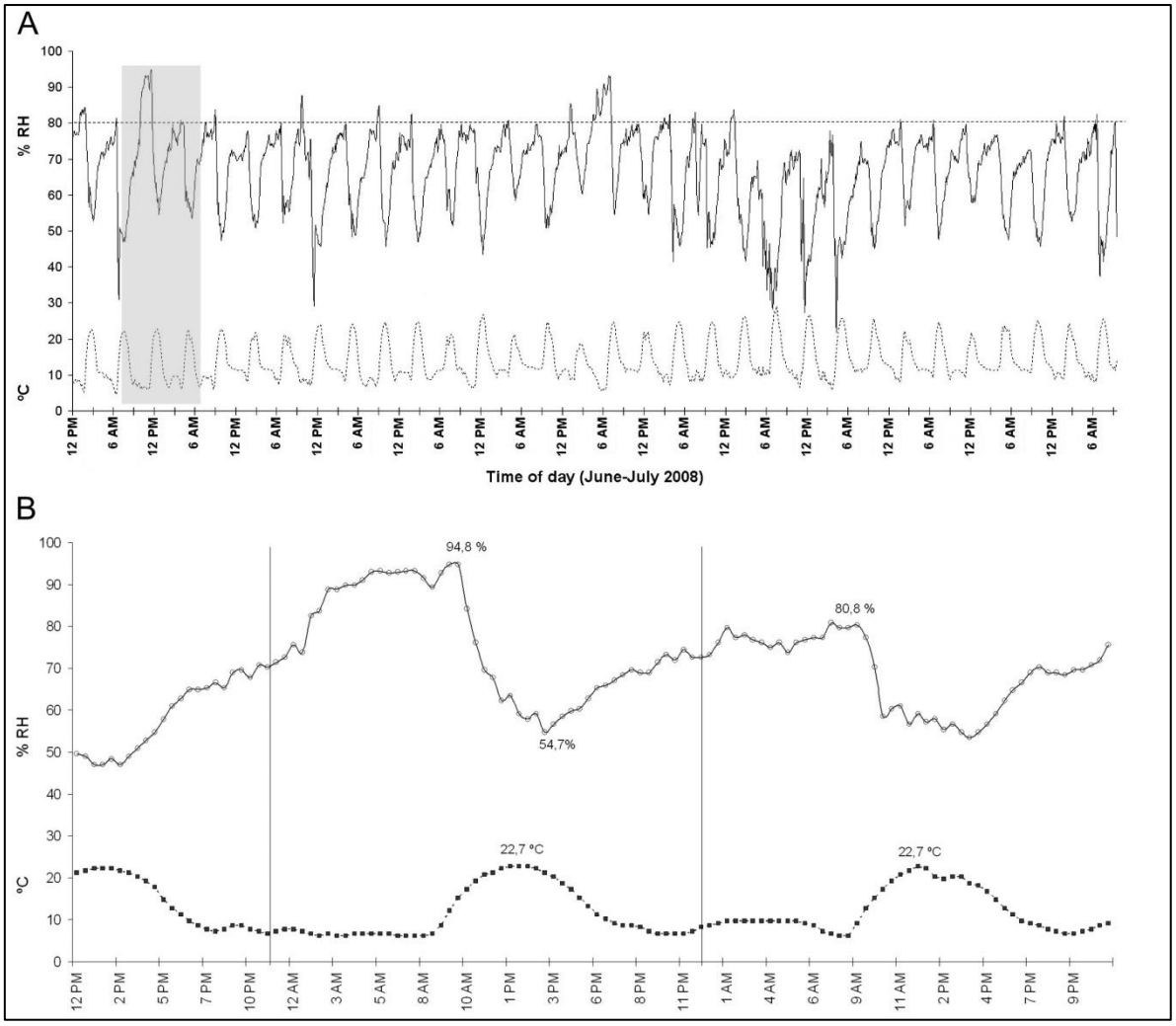

Figure 5.- *In situ* temperature and relative humidity profiles under quartz stones. A, 30-day period of winter time. Solid line, percent RH; dashed line, temperature (degrees Celsius). Straight dashed line at 80% RH shows days at which this RH value was reached. The shaded box indicates zoomed in data period of panel B. B, Time profile of *in situ* temperature and RH changes at the quartz–soil interface (hypolithic zone). -○- RH; -■- temperature. Vertical solid lines mark midnight.

Fog is very important for the arid soil ecology of the coastal Namib Desert, supplying over 50% of total "non-rainfall" atmospheric water at this site (Kaseke-Farai, 2009). Nocturnal hydration events supply daily net input averages of 1.67 to 13.16 mm of water in spring and 0.47 to 9.93 mm of water per cubic centimeter of soil in summer at the Namib Desert (Kaseke-Farai, 2009) This exceeds the theoretical threshold for water availability to microorganisms (Kappen *et al*., 1979), therefore fog and dew events supply small but critical amounts of water important for soil ecology, in agreement with previous findings (Malek *et al*., 1999).

Satellite-based fog detection systems (Gultepe *et al*., 2007) also record an average of 80% RH during fog episodes. RH is not necessarily a good indicator of liquid water in soils. Previous studies have used conductivity sensors in addition to RH (Delong, 1992; McKay *et al*., 2003), since conductivity sensors directly detect the liquid phase. These studies have also shown that in desert soil moisture levels vary sharply between very dry and very wet, and that time under high RH values (>80%) is essentially the same time under liquid water conditions. It has also been shown that in the Namib Desert high RH causes fogs which supply a critical amount of water important for its soil ecology (Kaseke-Farai, 2009). At the Negev Desert, lichens absorb appreciable amounts of dew and briefly photosynthesize during the early morning hours using this water source (Lange and Bertsch, 1965). The occurrence of maximum RH under the quartz rocks around noon and of minimum RH at sunset is counterintuitive and may be related to the influence of the hypolithic community under it. Since the EPS being produced by the microbial community are highly efficient in absorbing water, high RH values around noon time may be reflecting the thermal inertia of the water contained in the biofilm

which was gained during the previous night. Only after the highest temperatures of the day have been reached, a concomitant drop in RH occurs. The rate of water use by the microbial component of the biofilm could also be playing a role. This decrease in RH continues until sunset, when fog usually arrives at the site and reverses the trend. Alternatively, fogs on the Coastal Range persist quite late in the morning, so this also may be reflected in the later maximum of RH. Thus, the observed temporal variations under the quartz rocks are consistent with the temporal presence of the fogs at the Coastal Range hills. Interestingly, RH under the quartz reached values above 80% in 19 out of the 30 days that measurements were conducted (Figure 5). These results are in contrast to those obtained previously in the much drier site of Yungay in the hyperarid core of the Atacama Desert (McKay *et al*., 2003). For Yungay (which is 80 km inland from the study site), high nighttime or early morning RH and in this case, dew also, were recorded during a 4-year interval. Dew by itself did not produce measurable moisture in the soil or under the stones, with one rain event that resulted in soil moisture being recorded. On the contrary, at our study site, heavy fog events have an almost daily frequency and appear to be the most important source of water.

All together, the light, temperature and RH data shown above allow us to postulate a model that could explain the development of a hypolithic community under quartz stones at this site. Since the fog coming from the Pacific Ocean usually advances inland during late evening and night, water condenses onto all surface types of the Coastal Range hills. During the day, as the surface gets heated by the sun, water quickly evaporates back to the atmosphere, but with lower rates of evaporation from the slightly

cooler quartz rocks. It has been previously shown that other types of rocky material, like gravel, reduce the amount of soil surface in direct contact with the atmosphere, shielding the underlying soil from wind and solar radiation, thus favoring moisture conservation (Kemper *et al*., 1994; Li, 2002; Katra *et al*., 2008). In the Namib Desert, quartz desert pavement showed evidence of enhanced nocturnal cooling, thereby promoting dew formation (Graf *et al*., 2008). This condensation process allows the colonization of quartz by the hypolithic microorganisms, which by producing water-retaining EPS start a positive feedback cycle allowing further and more sustained water retention and colonization.

The essence of our model concurs with the one proposed by Warren-Rhodes *et al*. (2007) for the hyperarid deserts in China. In this case, precipitation over the quartz stones results in water runoff from the top surface to the hypolithic habitat, where it is retained by the hypolithic community with the help of EPS. As growth and survival of cyanobacteria is highly dependent on the availability of water (Alpert, 2005; Gupta and Agrawal, 2006; Higo *et al*., 2007), one of the known mechanisms described for efficient water capture and retention is the production of highly hygroscopic EPS (Whitford, 2002; Schlesinger *et al*., 2003; Or *et al.*, 2007). In our case, water condensation from fog events seems to be the primary source of water. In addition, we found that the EPS constituting the matrix of the hypolithic biofilm can absorb up to 5.2 times their own weight in water, thus helping to keep water available for cells later.

Our results show that hypolithic cyanobacteria thriving in the seaward face of the Coastal Range in the hyperarid region of the Atacama Desert may survive with fog as the main regular soil source of moisture. It is difficult to quantitatively compare fog to mean

annual rain events, but we note that the level of colonization we find (80%) corresponds to colonization rates associated with significantly higher rainfall levels. Thus, the Atacama Desert hypolithic community described here occupies an ecological niche intermediate between the Atacama Desert hypolithic communities described by Warren-Rhodes *et al*. (2006) which depend on rain and the Atacama Desert haloendolithic communities described by Wierzchos *et al*., (2006), which derive their water from subsaturated atmospheric humidity.

Photosynthetic photon flux density (PPFD) measurements taken under quartz stones

The PPFD measured at the soil surface of the quartz outcrop reached a mean value of 1,030 μmol m^{-2} s^{-1} at noon. The PPFD measured beneath 29 randomly selected quartz stones varied from 1 to 88 μmol m^{-2} s^{-1}, representing 0.1% to 8.5% of the incident surface PPFD, with a mean value of 2.9% (Fig. 6, Table 1). These values, which are determined by the thickness and the coloration of the quartz, were in the range of those obtained in previous measurements made elsewhere under this type of stones (Rundel *et al*., 1990; Smith *et al*., 2000; Thomas, 2005).

Quartz hypolithic biofilm colonization rates

We found that the distribution of quartz rocks is highly heterogeneous across the Coastal Range hills, and it is associated with quartz outcrops from surfacing veins that produce rock fragments suitable for hypolithic colonization (Fig. 2, panel B).

Table 1. PPFD values measured under 29 randomly selected quartz rocks.

Quartz	PPFD μmol m^{-2} s^{-1}	% of Incident Light
1	1	0.10
2	3	0.29
3	4	0.39
4	5	0.49
5	5	0.49
6	5	0.49
7	7	0.68
8	8	0.78
9	11	1.07
10	12	1.17
11	13	1.26
12	16	1.55
13	17	1.65
14	23	2.23
15	29	2.82
16	32	3.11
17	33	3.20
18	39	3.79
19	40	3.88
20	44	4.27
21	44	4.27
22	48	4.66
23	48	4.66
24	49	4.76
25	51	4.95
26	58	5.63
27	58	5.63
28	77	7.48
29	88	8.54
Mean	29.93	2.91

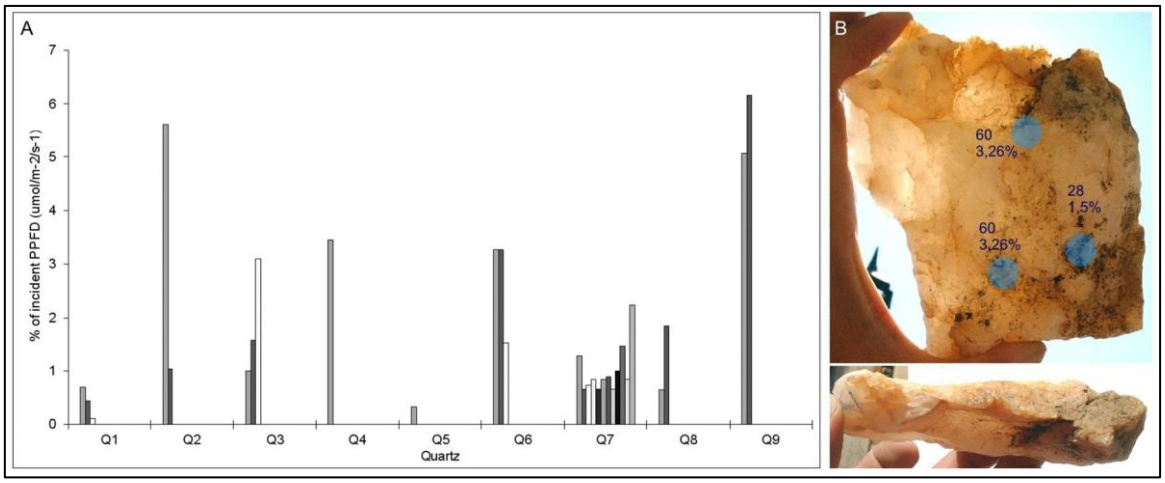

Figure 6.- PPFD values under selected quartz stones. Values of PPFD and the corresponding percentage of the full incident PPFD (1,82 $\mu mol/m^{-2}/s^{-1}$) reaching the top of the quartz are shown. A, Bars show PPFD levels measured under nine randomly chosen quartz rocks, the number of measurements per quartz being a function of its size. B, Backlight image of one of these quartz rocks (Q6). Blue dots show the points where the three measurements were taken.

Of all rock types counted in the transect grids at one of these outcrops, 83.2% corresponded to quartz stones. Among these, about 80% showed hypolithic colonization (Figure 7), as based on inspection using a stereoscopic microscope. Hypolithic colonization was only observed on quartz stones weighing >1 g. The size of quartz stones in these transects varied from small splinters of less than 1 g to rocks of 471 g of weight. As the size of the quartz rock increased, a concomitant increase in hypolithon colonization was observed. All quartz rocks over 20 g were colonized.

Hypolithic microorganisms are only found under quartz rocks associated with outcrops that are dispersed on the surrounding hills of the Coastal Range. The latter are also found inland, randomly distributed on the hills, although they exhibit much lower rates of colonization (Warren-Rhodes *et al*., 2007). When analyzing the extent of the hypolithic colonization in the Coastal Range hills, we found that it is exclusively restricted to quartz rocks since no colonization was observed associated to other rock types, as it has been described for opaque rocks in the Arctic (Cockell and Stokes, 2004). About 80% of the 275 quartz stones counted in one of these outcrops showed some degree of hypolithic colonization. At this site, the colonization pattern is always hypolithic, i.e., no perilithic colonization was observed. The colonization rate of 80% at our site is significantly higher than the colonization rate inland in the hyperarid zone at this same latitude, reported by Warren-Rhodes *et al*., (2006) to be <0.1%. It is even higher than the colonization rate found in sites much further south with mean annual rainfalls of up to 100 mm/year (Warren-Rhodes *et al*., 2007). This is somewhat surprising since this site receives virtually no rain, but mainly fog. According to the data collected by the Meteorological Chilean Service (http://www.meteochile.cl/ precipitacion.html), an

annual mean of only 1.7 mm of rain has been recorded for the last 30 years at the area where this study site is located. With monthly averages of 1 mm during summer and 4 mm in winter, several months show no rain recordings. Thus, it is clear that fog is an effective source of moisture for the hypolithic habitat. Warren-Rhodes *et al*. (2007) suggested that the efficiency of moisture captured from fog by surface rocks increased with increasing rock size. Our results confirmed this trend. The sizes of these stones vary from small fragments of less than 1 g to rocks of almost half a kilogram. We observed an increase in the hypolithic colonization rate concomitant with the increase of quartz size. This finding is in agreement with colonization patterns elsewhere in the world. For example, in China's hyperarid deserts, hypolithic cyanobacteria also tend to colonize larger rocks (Warren-Rhodes *et al*., 2007). In the site here described, all quartz rocks over 20 g are well colonized. In this regard, there seems to be a threshold of hypolithic colonization: quartz fragments of less than 1 g in weight show no colonization.

Fragments of hypolithic biofilms taken from randomly chosen quartz rocks efficiently absorbed water after suspension in distilled water in the laboratory. The amount of absorbed water varied from 0.77 to 5.20 times the original weight of the biofilm section, with an average value of 3.20. This volume increase was accompanied by a rapid greening of the biofilm.

Biofilms species composition

Most of the quartz stones buried in the soil showed abundant colonization of hypolithic microorganisms that formed a mat up to 5 mm thick in some places.

Figure 7.- Example of biofilm at the underside of a quartz rock. Note the characteristic green color of chlorophyll and the agglomeration of soil particles by the exopolysaccharides produced by the biofilm.

In some cases, the biofilm extended outwards from the underside surface of the quartz, with the EPS produced by the microorganisms agglomerating the soil particles under the rock (Figure 7). Observations with a stereoscopic microscope showed a variety of colored patches and filaments corresponding to different members of the hypolithic community.

Scanning electron microscopy (SEM) applied to the underside quartz surface confirmed the presence of a well-formed biofilm with numerous cells embedded in an EPS matrix (Figure 8, panel A). Monolayers of individual cell groups firmly attached to the rock surface were also observed (Figure 8, panel B).

Transmission electron microscopy (TEM) showed the characteristic ultra structural elements of the cyanobacterial component of the hypolithic biofilm, such as thylakoid membranes with embedded phycobillisomes and thick sheets of EPS surrounding the cell wall (Figure 9). In turn, confocal laser scanning microscopy (CLSM) examination of the hypolithic components resuspended in aqueous solution showed the autofluorescence typical of phycobillisomes, revealing a highly diverse population of cyanobacteria and algae (Figure 10).

Analyses of gene clone libraries of 16S and 18S rRNA prepared with DNA obtained from the hypolithic community showed the presence of at least fifty six species of Bacteria, of which fifteen were species of Cyanobacteria, twelve species of Archaea and two species of microalgae (Table 2), totaling 70 different microbial species.

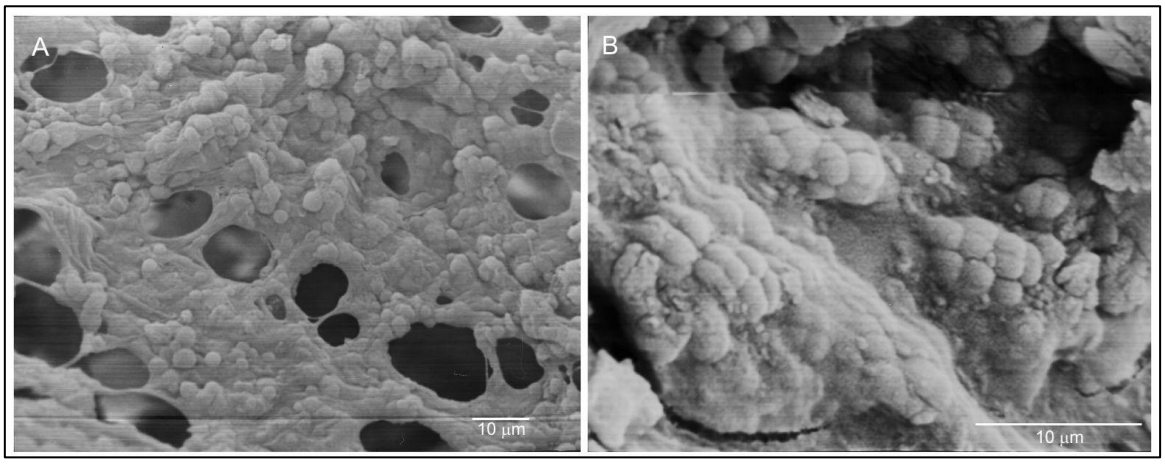

Figure 8.- Scanning electron microscopy (SEM) of the hypolithic biofilm. A, SEM micrograph of groups of cells embedded in an exo polysaccharide (EPS) rich matrix. B, Colonies of unicellular cells adhered to the underside of a quartz stone.

Among the Cyanobacteria, both unicellular (*Cyanothece, Pleurocapsa, Gloeocapsopsis*) and filamentous (*Calothrix, Leptolyngbya, Microcoleus, Nostoc*) members were found. Five additional hits with uncharacterized uncultured species were also obtained. Among the Archaea, members of the Halobacteriaceae *(Haladaptatus, Haloferax, Halococcus, Haloarchaeon*) plus five other uncultured species were found. The greatest diversity was observed among the Bacteria, with species closely related to *Actinomycetospora, Bacillus, Bacteroides, Brevundimonas, Clostridium, Deinococcus, Flavobacterium, Fulvivirga, Fusobacterium, Geobacillus, Halomonas, Kaistobacter, Planctomyces, Pontibacter* and *Streptococcus*, plus eighteen another uncultured bacteria.

Two species of single cell microalgae were found, related to the *Oocystis* and *Chlorella* genera. These results are consistent with other habitats in the Atacama Desert where similar composition of cyanobacterial, archaeal and bacterial species have been reported (Drees *et al*., 2006; Warren *Rhodes et al*., 2006; de los Ríos *et al*., 2010; Lacap *et al*., 2001). In addition, these findings highlight the importance of the concept of "microbial oasis", in terms of sampling strategies and the understanding of microhabitats in extreme environments (Parro *et al*., 2011).

Gloeocapsopsis is a genus of the Cyanobacteria of marine origin, typically found in stony littorals at the surf zone, but also reported in close-by subaerial habitats (stones wetted by water, seepages, stony surface on edges of temporary creeks, Komárek, 1993). To date, there are 10 species named, of which 6 have been taxonomically accepted (Komárek, 2003).

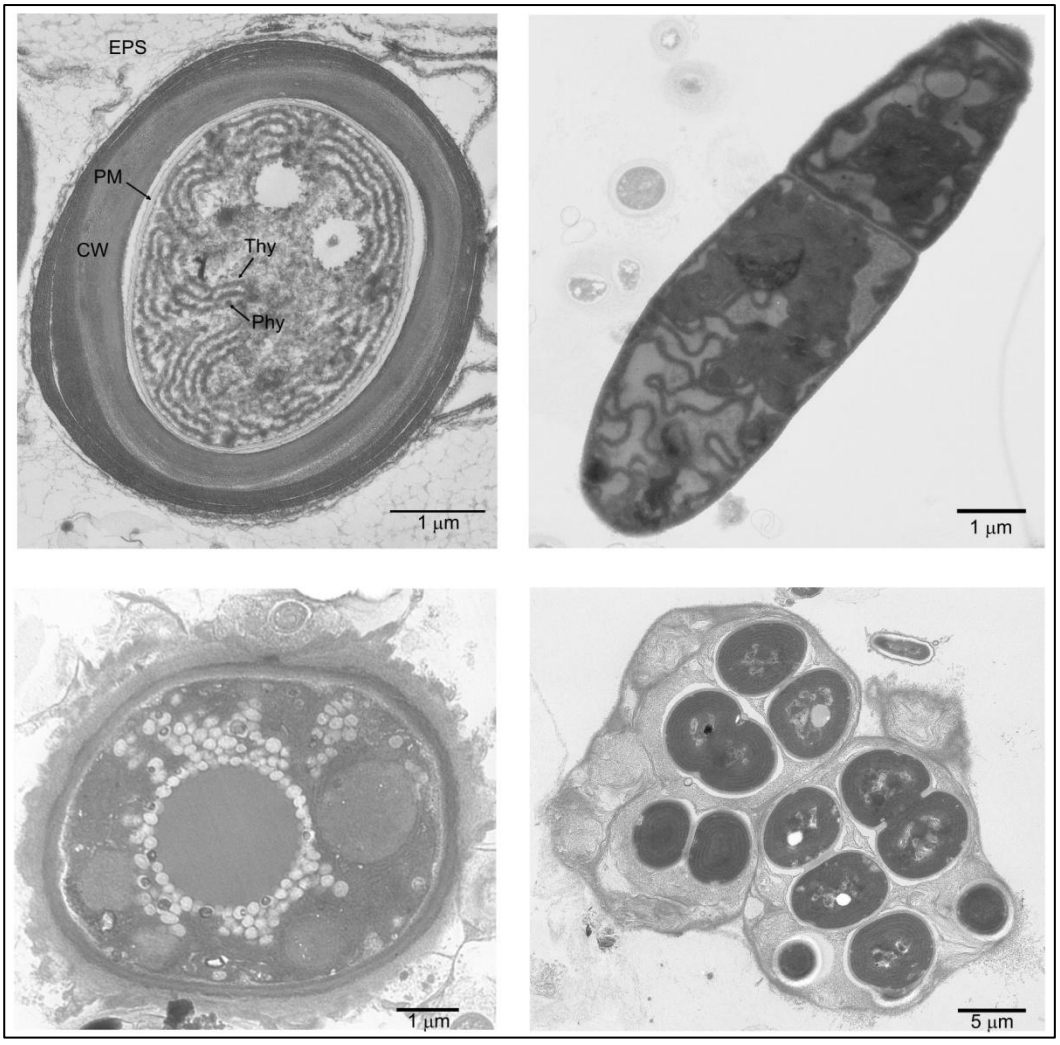

Figure 9.- TEM micrographs of hypolithic microorganisms. EPS, exopolysaccharide; PM, plasma membrane; CW, Cell wall; Thy, Thylakoidal membrane; Phy, Phycobilisome.

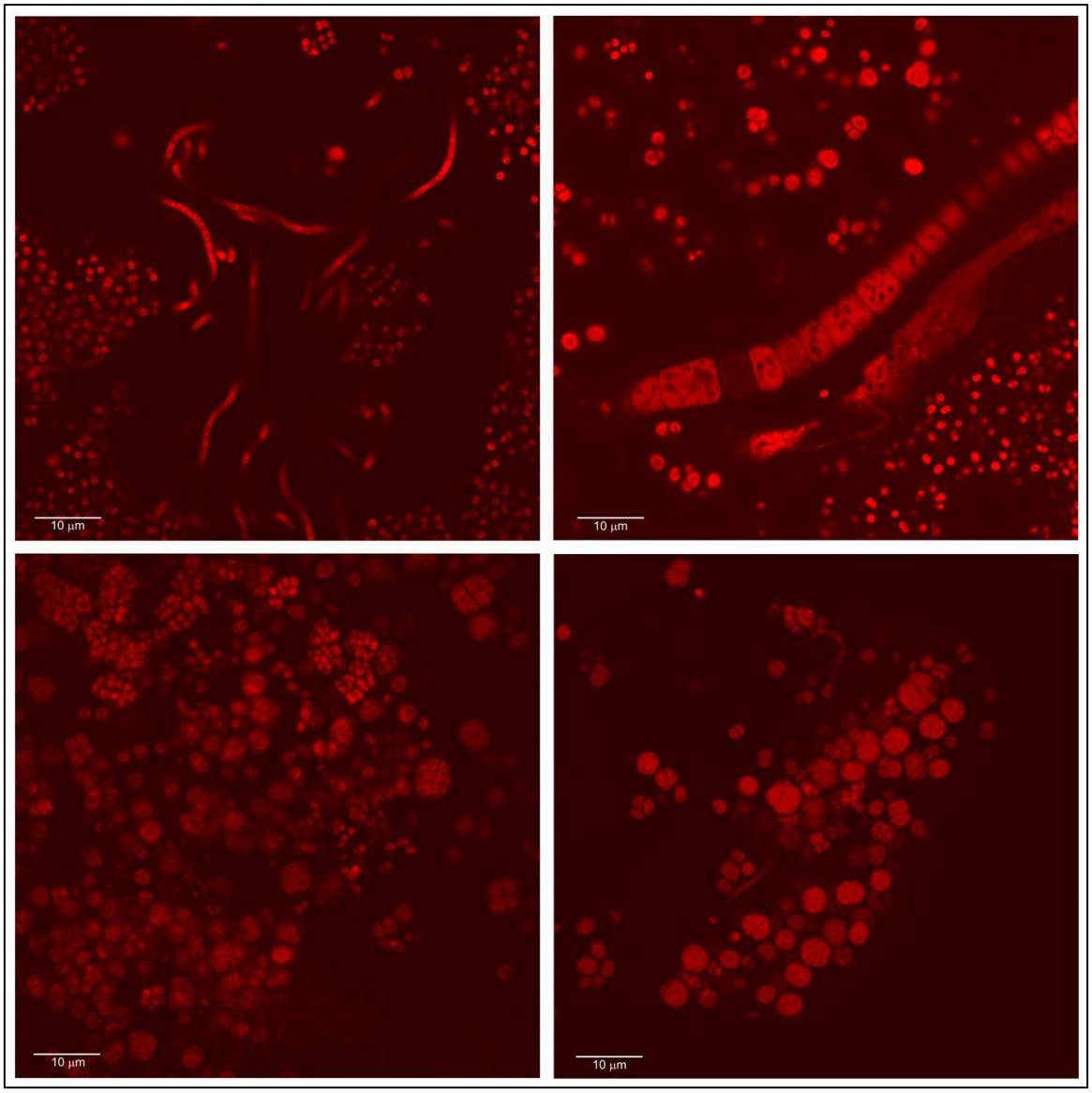

Figure 10.- Morphology of the various photosynthetic components of the hypolithic community. The four panels show confocal laser scanning microscopy (CLSM) micrographs of aqueous suspension of hypolithic biofilm samples taken from the underside of quartz stones. The red fluorescence is due to the autofluorescence emitted by chlorophyll *a*. Scale bar 10 = µm.

The type species *Gloeocapsopsis crepidinum* (Thuret) Geitler ex Komárek) is the phylogenetically closest species to our isolate AAB1 (see below). Interestingly, the quartz field from where isolate AAB1 was isolated is about 600 mt from the Pacific Ocean.

Microorganisms in the form of biofilms and microbial mats similar to the ones presently found in modern desert or intertidal systems are thought to be among the first settlers of land rocks (Costerton and Stoodley, 2003). As *Gloeocapsopsis* species are found in intermittently desiccated intertidal pools, desiccation and high solar irradiance tolerance could be expected. This set of adaptations may have allowed the colonization of arid lands, explaining the presence of isolate AAB1 in its current hypolithic habitat (Azúa-Bustos *et al*, 2012).

3.3. Isolation, identification, and description of the new isolate.

Higher resolution SEM images of the underside of quartzes showed cells with the reported morphology of *Gloeocapsopsis*, that is, tetrads of cells in which the separating cell walls could be seen (Figure 11). Biofilm samples placed on BG-11 liquid media rapidly attained sustained growth and reproduction under growing chamber conditions. A number of morphologically distinct species were identified by bright field microscopy, among them, cells corresponding to the expected size and morphology reported for *Gloeocapsopsis* (Figure 12). From these biofilms, which were grown for several months, a successful serial isolation procedure with an inverted microscope was performed, as cells corresponding to the morphology of *Gloeocapsopsis* were able to separately grow under chamber conditions.

Table 2. Microbial biodiversity of the quartz hypolithic biofilms. (This work).

Blastn highest hit	GenBank Top hit ID
Cyanobacteria	
Cyanothece sp. HSC26	EF150795.1
Pleurocapsa minor, strain SAG 4.99	AJ344564.1
Pleurocapsa sp. CALU 1126	DQ293994.1
Calothrix sp. HA4236-MV1	HQ847575.1
Uncultured Cyanobacterium clone VERDEA75	FJ902644.1
Chroococcales cyanobacterium LEGE 06123	FJ589716.1
Uncultured Cyanobacterium clone AY6_17	FJ891047.1
Leptolyngbya sp. Kovacik.	EU528669.2
Uncultured Cyanobacterium clone AY6_2	FJ891032.1
Uncultured Cyanobacterium clone CAR-K11c-B10	FN298068.1
Nostoc commune NC5 clone 11	EU586728
Microcoleus steenstrupii, clone 177-1	AJ871982.1
Uncultured Cyanobacterium clone CA-C04	EU751471.1
Pleurocapsa minor, strain SAG 4.99	AJ344564.1
Uncultured Cyanobacterium clone AY6_21	FJ891051.1
Archaea	
Haladaptatus cibarius strain D43	EF660747.3
Uncultured archaeon clone DRV-A006	AY923076.1
Haloferax sp. GSP107	FJ696384.1
Haladaptatus litoreus strain RO1-28	EU887285.2
Halococcus sp. FC211	EU308208.1
Uncultured marine archaeon clone Au-Fg10-Arch4	EU377209.1
Uncultured archaeon, clone ss_010b	AJ969889.1
Haloarchaeon Nie 10-2	AB291219.1
Halobacteriaceae archaeon TNN28	GQ282621.1
Uncultured euryarchaeote, clone ST-3K67A	AJ347778.1
Halococcus sp. , strain 004/1-2	AM902588.1
Halococcus thailandensis, strain: JCM 13552	AB549236.1
Haladaptatus cibarius strain D43	EF660747.3
Halococcus sp. , strain 004/1-2	AM902588.1
Halococcus thailandensis, strain: JCM 13552	AB549236.1
Algae	
Uncultured eukaryote clone ncd896b08c1	HM298751.1
Uncultured alga clone ESS-G4	FJ946598.1

Blastn highest hit	GenBank Top hit ID
Bacteria	
Bacillus sp. NCCP-132	AB562920.1
Uncultured bacterium (*Deinococci*?) clone AKIW1046	DQ129340.1
Uncultured bacterium clone WET-E09	EF658856.1
Uncultured *Kaistobacter* sp. clone Plot17-B04	EU440713.1
Uncultured bacterium clone LL141-7G13	FJ675260.1
Halobacillus sp. H57B77	FJ746574.1
Flavobacteriaceae bacterium JLT639	EU581830.1
Uncultured Planctomycetaceae bacterium clone A07-09F 1	FJ542882.1
Halomonas phoceae strain CCUG 5096	AY922995.1
Uncultured bacterium clone 16slp119-1f04.p1k	GQ159672.1
Uncultured bacterium clone F2_162X	GQ263040.1
Uncultured bacterium clone 16slp93-1g08.p1k	GQ158970.1
Fulvivirga kasyanovii strain KMM 6220	DQ836305.1
Uncultured bacterium clone nbw1024d02c1	GQ033083.1
Uncultured *Clostridia* bacterium clone Clept35	DQ350803.1
Uncultured bacterium clone LL141-8A15	FJ675358.1
Uncultured Bacteroidetes bacterium clone D-16S-64	GU552178.1
Uncultured bacterium clone FFCH3058	EU133552.1
Brevundimonas sp. KLE1218	GU644355.1
Uncultured Bacteroidetes bacterium clone 01D1X22	DQ330399.1
Uncultured bacterium clone JSC9-E3	DQ532248.1
Uncultured Bacteroidetes bacterium clone OCSS037	EF522485.1
Uncultured endolithic bacterium clone: 28B-WNS	AB374378.1
Streptococcus australis strain C89 1	GU907517.1
Uncultured bacterium clone nbw116g09c1	DQ129336.1
Uncultured bacterium clone ncd952b01c1	HM330617.1
Uncultured bacterium, clone A5	AM746683.1
Uncultured bacterium clone 16slp92-01a05.p1k	GQ159512.1
Uncultured bacterium clone JSC8-B11	DQ532226.1
Uncultured actinobacterium clone HPIRR2H06	AY852127.1
Fusobacterium nucleatum clone OCU024	GU407893.1
Streptococcus sp. sp2-iso-AG14x2	GQ900836.1
Uncultured bacterium clone Pillow45	HM119355.1
Uncultured bacterium clone C4D10-2	FJ930441.1
Uncultured bacterium clone nbw115f05c1	GQ008290.1
Uncultured bacterium clone Bas-7-39	GQ495396.1
Uncultured bacterium clone NV26_8c10	FJ595565.1
Uncultured bacterium clone MuztB30-9	GU246955.1
Uncultured bacterium clone MVT-B78	EU335864.1
Actinomycetospora sp. TT00-04 , IY07-53	AB514515.1

Note: "Chroococcales cyanobacterium LEGE 06123" was later reclassified as Gloeocapsopsis crepidinum LEGE 06123".

Growth was detected about three months after isolation, by both visual inspection and bright field microscopy (Figure 13). This part of this work was completed with the help of Jorge Zúñiga, (by that time) an undergraduate student of Biochemistry at the Faculty of Biological Sciences of the Pontificia Universidad Católica de Chile. The presence of a single type of cyanobacteria in the final culture, identified as *Gloeocapsopsis*, was confirmed by denaturing gradient gel electrophoresis (DGGE) in which primers specific for cyanobacteria (Janse *et al*., 2003) were used for the internal transcribed sequence (ITS) between 16S rRNA and 23S rRNA (Figure 14).

To confirm the identity of the isolate as a novel *Gloeocapsopsis* species, both morphologic parameters and molecular methods were used. The entire cell cycle of the new isolate was captured in a single, unaltered, TEM micrograph (Figure 15, panel A). From lower left to lower right, cell wall covered and uncovered baeocytes, first stage and second stage division of the tetrad and a "phantom" of cell walls after baeocyte liberation can be seen. This TEM micrograph shows the size, shape and ultrastructure previously reported for the *Gloeocapsopsis* genus by Komárek & Anagnostidis (1998) and Komárek (1993): "*Cell division irregularly in various planes in successive generations. Reproduction by liberation of divided and unsheathed cells from ruptured mother sheaths. Occasional presence of enlarged resting cells with thick, firm and usually intensely colored envelopes"*. A close up of the internal ultrastructure showed thylakoidal membranes with the characteristic arrangement and size corresponding to phycobilisomes in cyanobacteria (Figure 15, Panel B).

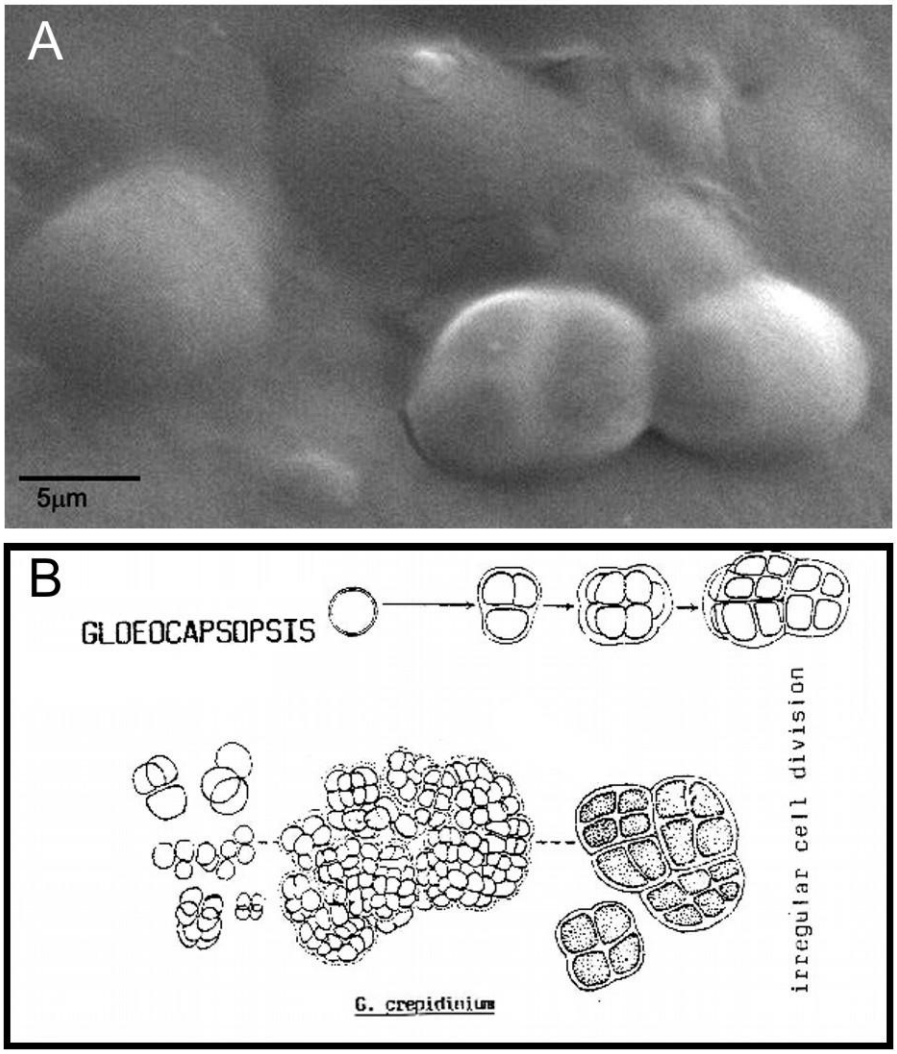

Figure 11.- Quartz underside SEM image and *Gloeocapsis crepidinum* morphology. A, SEM micrograph in which *Gloeocapsopsis*-like cells may be seen. B, Reported morphology for *Gloeocapsopsis crepidinum*. Source; modified from Komárek (1993) which was in turn based in Geitler (1932), Hollerbach *et al*., (1953), Novácek *et al*., (2003) and Komárek and Agnoistidis (1986).

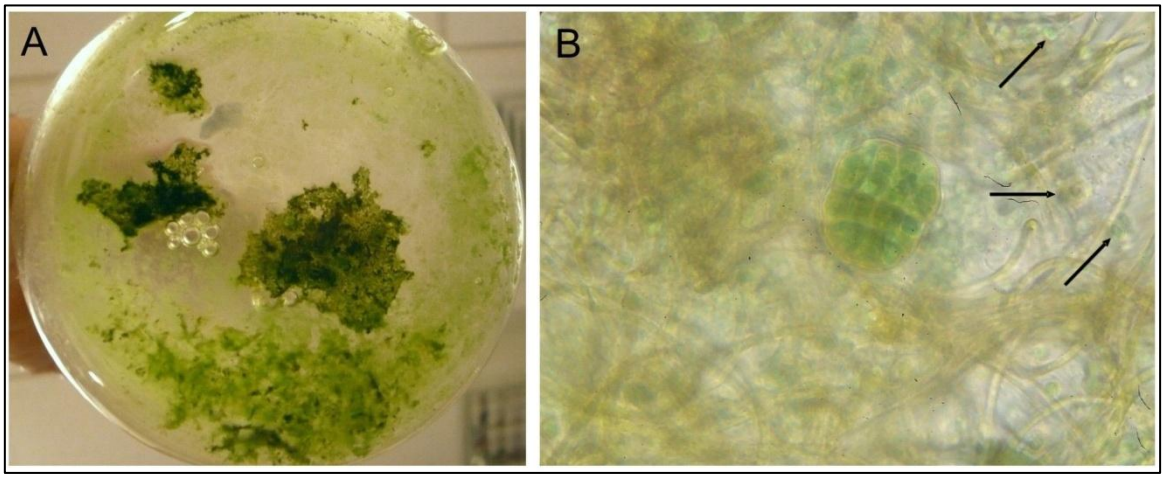

Figure 12.- Bright field micrograph of hypolithic biofilm cells in culture. A, view of biofilms samples in a culture container. B, bright field micrograph of hypolithic biofilm cells. The arrows points to cells with the reported morphology of *Gloeocapsopsis*.

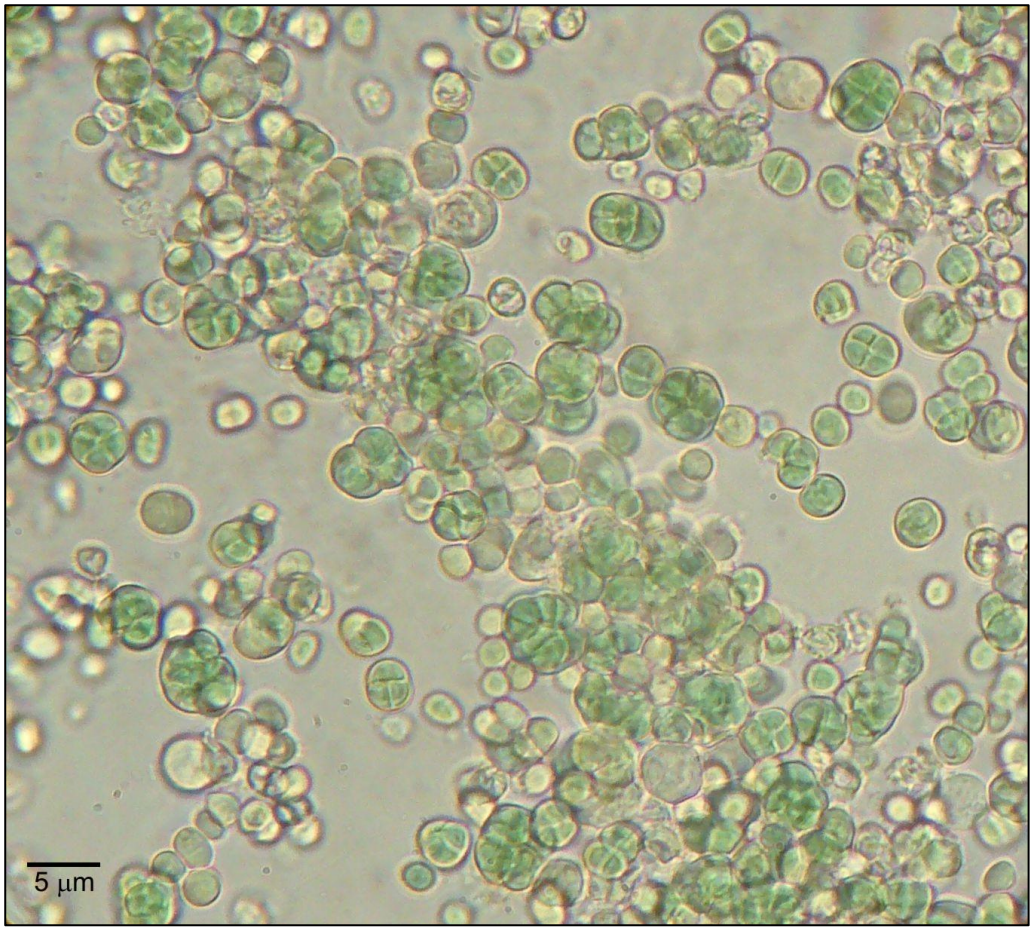

Figure 13.- Bright field micrograph of *Gloeocapsopsis* isolate ABB1 cells in culture.

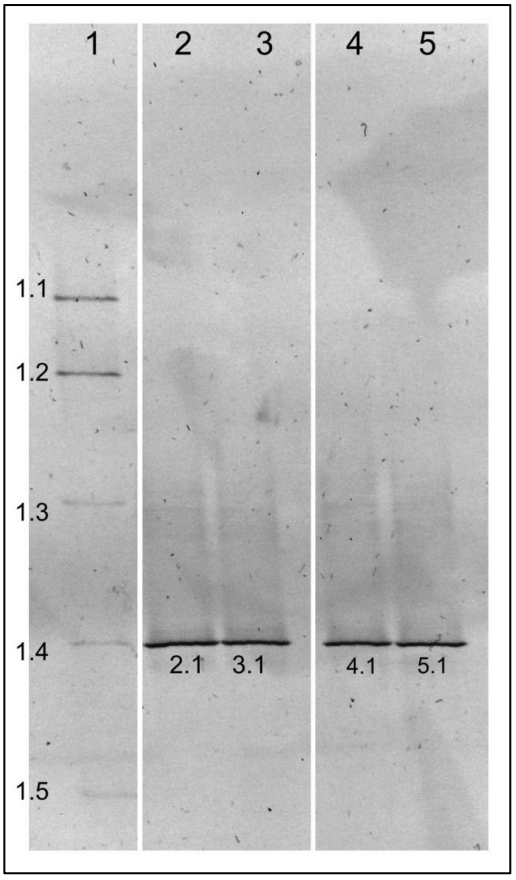

Figure 14.- Denaturing gradient gel electrophoresis (DGGE) gel of ITS DNA sequences. DGGE gel in which DNA samples obtained from the amplification of the gene sequences encoding the ITS were run. Lane 1, Hypolithic biofilm. 1.1: *Calothrix* sp. HA4236-MV1. 1.2: *Leptolyngbya* sp. Kovacik. 1.3: *Nostoc commune* NC5 clone 11. 1.4: *Gloeocapsopsis* isolate AAB1. Lanes 2 – 5, different samplings in time of the cultured isolate. 2.1, 3.1, 4.1 and 5.1, *Gloeocapsopsis* isolate AAB1.

Details of cell division could also be seen, including the formation of the septum and redistribution of the thylakoidal membranes (Figure 16). Per-iodic acid Schiff (PAS) staining detected thick exopolysaccharides, in many cases up to 1 μm thick (data not shown).

Molecular Identification

It is important to note that the isolate was first classified as a new member of the *Chroococcidiopsis* genus of the Cyanobacteria. When the first classification was undertaken three years ago, the highest Blast match (99% similarity) was annotated as "Chroococcales cyanobacterium LEGE 06123", with no further details about its potential genus or species assignation. When this particular sequence was blasted, closest hits belonged to the genus *Chroococcidiopsis* (albeit with lower percentages of similarity). Thus, given that the morphology of the isolate closely matched that of *Chroococcidiopsis*, we assigned our isolate to this genus. However, three years later, *Chroococcales cyanobacterium* LEGE 06123 was then reclassified as *Gloeocapsopsis crepidinum* LEGE 06123. Thus, given the analyses explained in detail below, we reasaigned our isolate to the *Gloeocapsopsis* genus.

The Maximum Likelihood phylogenetic analyses of 16S rRNA, 23S rRNA, ITS, the entire 16S-ITS-23S operon sequences along other three other genes tested confirmed our isolate as a previously unreported *Gloeocapsopsis* species.

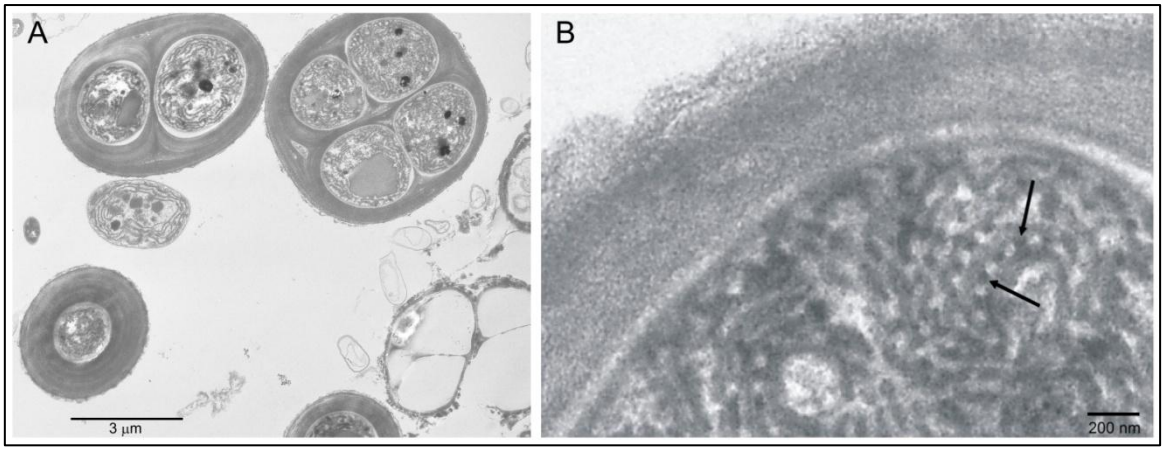

Figure 15.- TEM micrograph of *Gloeocapsopsis* isolate AAB1 cells. A, different stages of the *Gloeocapsopsis* life cycle. B, detail of the thylakoidal membranes with phycobilisomes (arrows) inserted on them. Note the thick walls in cells of panel A and the unsheated cell in the left center of this same panel .

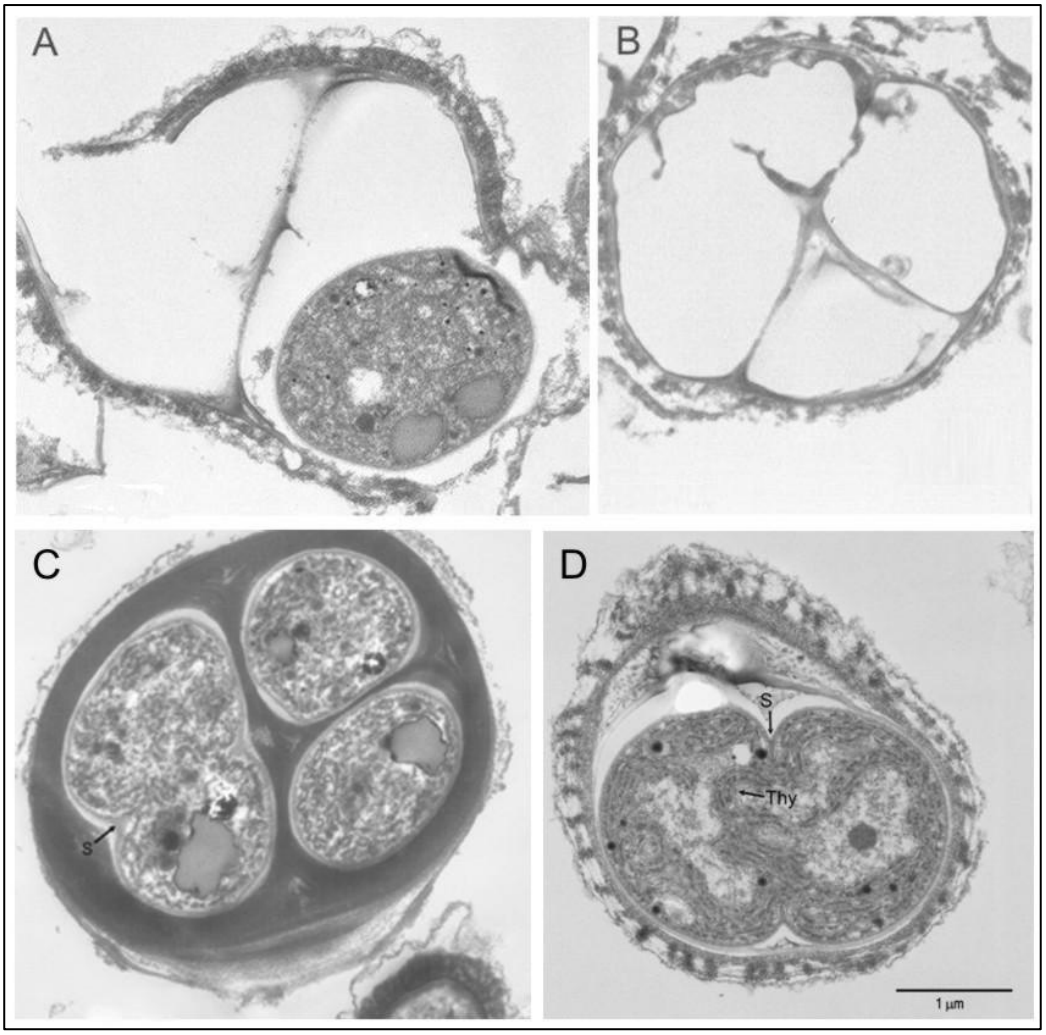

Figure 16.- TEM micrograph of *Gloeocapsopsis* isolate AAB1 cells showing details of cell division. A, baeocyte liberation. B, "phantom" of cell walls left after the liberation of cells of a tetrad. C, formation of the septum (S) at the beginning of the cell division. D, redistribution of the thylakoidal (Thy) membranes during the cell division. Note the liberation of an unsheathed cell from a ruptured mother sheath, as described by Komárek (1993).

The 16S rRNA and 23S rRNA phylogenetic trees show that the closest species to *Gloeocapsopsis* isolate AAB1 is *Gloeocapsopsis crepidinum* LEGE 06123, with a nucleotide similarity of 99% (Figure 17 and Table 3). A similar result was obtained after analyzing the ITS region (Figure 18) and the entire 16S-ITS-23S operon sequences (Figure 19). The GC content of the 16S rRNA-ITS-23S rDNA 3618 bp operon from *Gloeocapsopsis* isolate AAB1 differs by 0.1% with that of *Gloeocapsopsis crepidinum* LEGE 06123 (Table 4). Other known *Gloeocapsopsis* genes analyzed [*cpmA* (circadian phase modifier), *rpoB* (RNA polymerase B subunit), *cpcB* (Phycocyanin beta subunit)], confirmed that our isolate is a new member of the *Gloeocapsopsis* genus (data not shown).

3.4. Characterization of the new isolate under non-stressed conditions

Since hypolithic photosynthetic species evolved to grow under restricted access to light, which for quartzes of this site falls in the range of 1 to 88 μmol m^{-2} s^{-1} (Azúa-Bustos *et al*., 2011), we then determined the optimal light intensity for growing isolate AAB1 under laboratory conditions. As can be seen in panel A of Figure 20, there is no significant change in the growth rate between 10 to 70 μmol m^{-2} s^{-1}. However, since the cultures frequently turned yellow when grown at 100 μmol m^{-2} s^{-1}, we set the light conditions of the growing chamber at 30 μmol m^{-2} s^{-1}, as this value matched the mean intensity light value measured *in situ* under colonized quartzes.

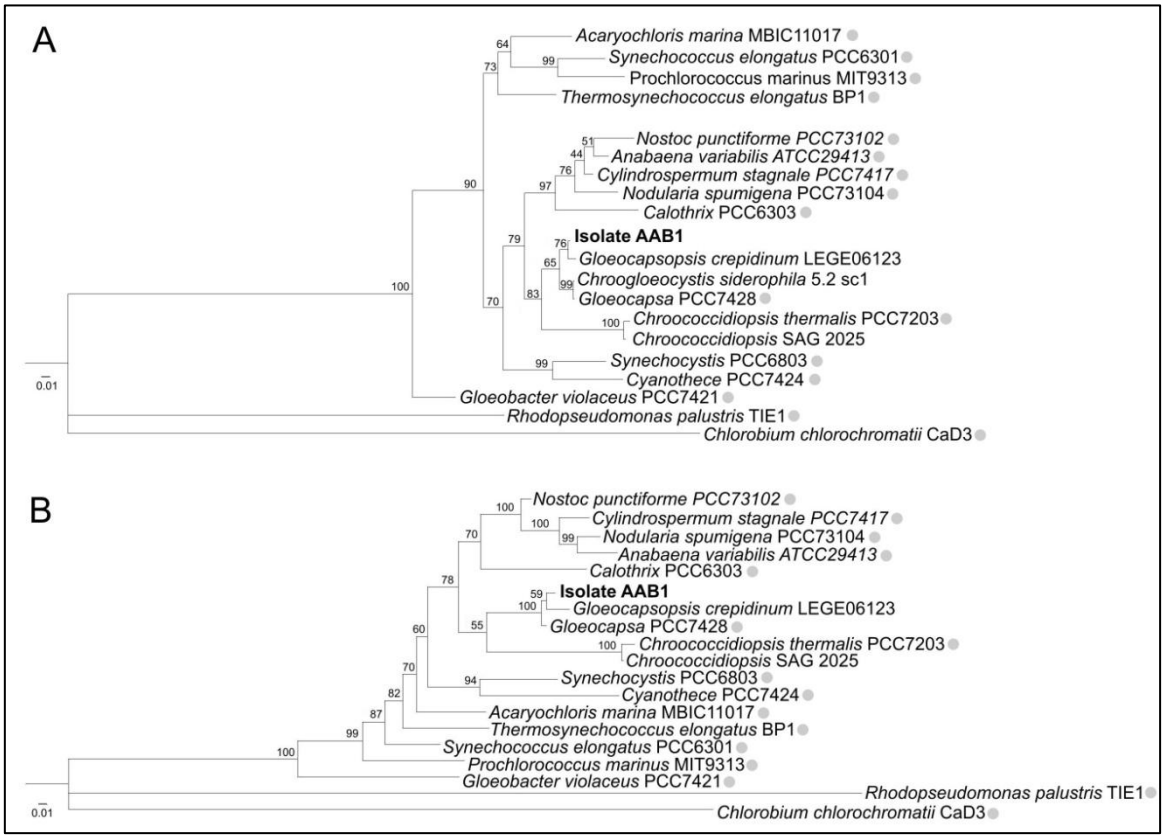

Figure 17.- Phylogenetic tree of 16S rRNA and 23S rRNA *Gloeocapsopsis* gene sequences. Maximum likelihood phylogenetic trees obtained from the aligned 16S rRNA (A) and 23S rRNA (B) *Gloeocapsopsis* gene sequences using BOSQUE (Ramírez-Flandes and Ulloa, 2008). The numbers on the nodes represent bootstrap values in % with 1000 replicates. Grey circles besides names denote species with known genomes.

Table 3. Similarity percentage of 16S rRNA and 23S rRNA isolate AAB1 sequences.

	% Similarity with isolate AAB1	
Species	16S	23S
Gloeocapsopsis crepidinum LEGE 06123	99	98
Gloeocapsa sp. PCC 7428	98	97
Chroogloeocystis siderophila 5.2 s.c. 1	98	n.a.
Chroococcidiopsis sp. SAG 2025	93	86
Cylindrospermum stagnale PCC 7417	93	87
Chroococcidiopsis thermalis PCC 7203	92	86
Nodularia spumigena strain PCC73104	92	87
Nostoc punctiforme PCC 73102	92	88
Anabaena variabilis ATCC 29413	92	86
Calothrix sp. PCC 6303	90	85
Cyanothece sp. PCC 7424	90	84
Synechocystis sp. PCC 6803	90	85
Acaryochloris marina MBIC11017	90	86
Thermosynechococcus elongatus BP-1	90	85
Gloeobacter violaceus PCC 7421	89	81
Prochlorococcus marinus str. MIT 9313	89	83
Synechococcus elongatus PCC 6301	89	86
Chlorobium chlorochromatii CaD3	77	66
Rhodopseudomonas palustris TIE-1	77	69

n.a: not available

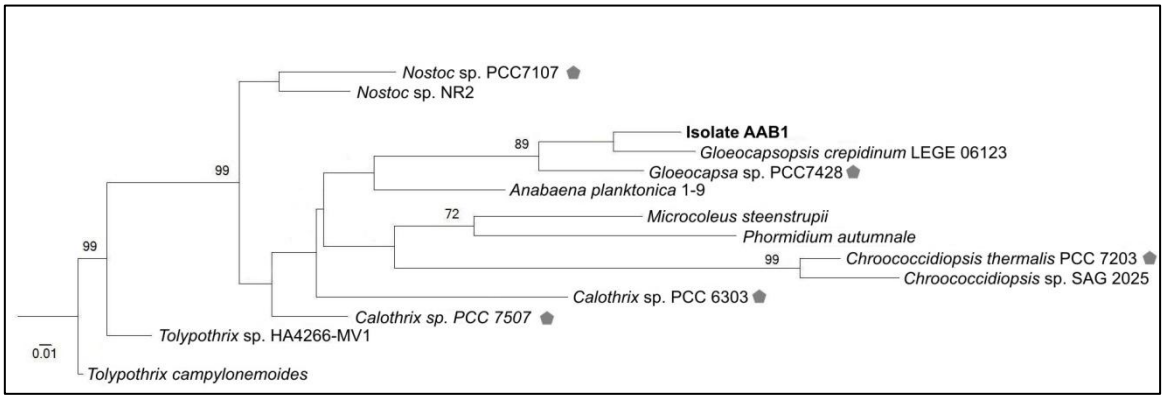

Figure 18.- Phylogenetic tree of ITS *Gloeocapsopsis* gene sequences. Maximum likelihood phylogenetic tree obtained from the aligned ITS region *Gloeocapsopsis* gene sequence using BOSQUE (Ramírez-Flandes and Ulloa, 2008). The numbers on the nodes represent bootstrap values in % with 1000 replicates. Grey pentagons besides names denote species with known genomes.

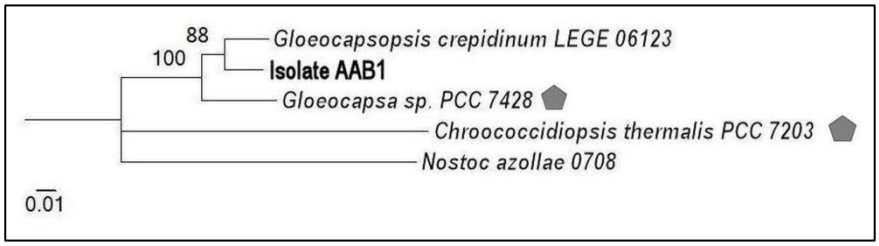

Figure 19.- Phylogenetic tree of 16S rDNA-ITS-23S rRNA operon *Gloeocapsopsis* gene sequences. Maximum likelihood phylogenetic tree obtained from the aligned 16S rRNA-ITS-23S rRNA operon *Gloeocapsopsis* sequence using BOSQUE (Ramírez-Flandes and Ulloa, 2008). The numbers on the nodes represent bootstrap values in % with 1000 replicates. Grey pentagons besides names denote species from which sequences were obtained from its genomes.

Table 4.- GC content percentages of 16S rRNA-ITS-23S rRNA operon sequences. The left column shows the percentage difference in GC content in relation to the sequence of *Gloeocapsopsis* isolate AAB1.

ITS	% GC	Dif % GC
Chroococcidiopsis thermalis	52,8	0,9
Gloeocapsa sp. PCC 7428	52,3	0,4
Gloeocapsopsis crepidinum	52,0	0,1
Gloeocapsopis strain AAB1	51,9	0,0
Nostoc azollae 0708	50,0	1,9

The absorbance spectra of a methanolic pigment extract of isolate AAB1 in liquid culture showed the typical peaks for chlorophyll *a* (440 and 665 nm) and carotenoids (475 nm) found in most Cyanobacteria (Figure 20, panel B). This was confirmed by high performance liquid chromatography (HPLC), in which the expected peak of chlorophyll *a* was observed with a retention time of 11.2 min (data not shown). A minor peak corresponding to phaeophytin was also observed at 13.3 min. The observed peaks in HPLC also suggested that four different carotenoids were present under normal hydration conditions, including the peak at 23.1 min corresponding to β-carotene. Raman spectroscopy also confirmed the presence of chlorophyll *a* and carotenoid compounds (see below) (Edwards *et al*., 2005).

3.5. Physiological, morphological and molecular changes shown by isolate AAB1 under desiccation.

Development of a practical and controllable desiccation assay

In order to study the response of the isolated isolate to low water availability, a controllable and practical method to impose this kind of stress was first developed. For this purpose, we built a simple desiccation chamber using standard Petri dishes (Figure 21, panel A). Different hygroscopic agents such as silica, calcium chloride or sodium chloride were used in order to set the internal RH inside the chamber. Samples of our model isolate were placed onto glass slides, either by a pellet of cells or a concentrated water solution containing the cells.

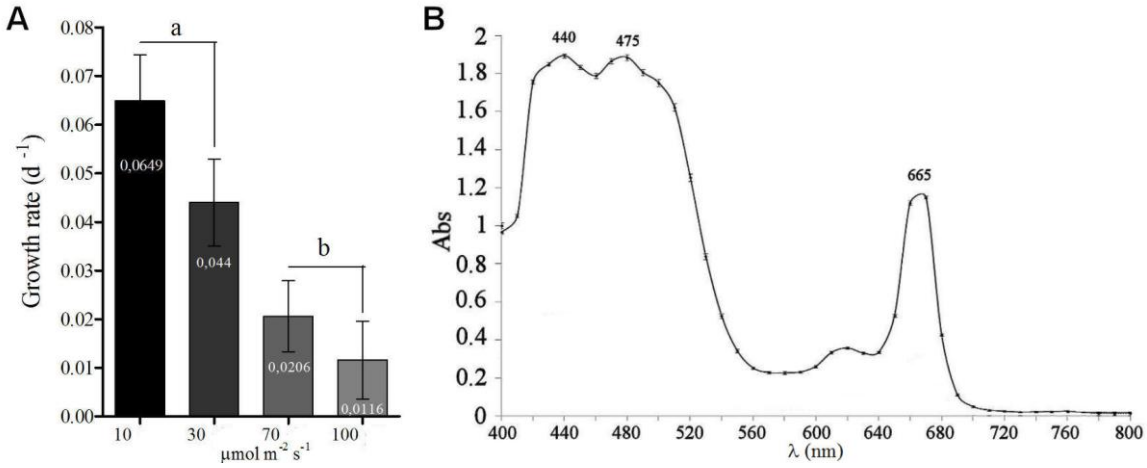

Figure 20.- Light related growth parameters of isolate AAB1. A, Growth rates of isolate AAB1 at four light intensities. The diferent letters denote a significant statistical difference (one way ANOVA with Tukey's post test, $p < 0.05$, a>b). B, Absorption spectra in the range of 400 to 800 nm of a pigment extract of isolate AAB1 cells. Note the characteristic peaks of chlorophyll *a* (440-665) and β-carotene (475). Black line, control. Dark grey line, Desiccated sample (water activity (a_w) 0,4 for twenty days). Light gray line, Desiccated sample (a_w 0.4 for five months).

To prevent direct contact of the desiccating agents with the cells, a support for the glass slide inside the Petri dish was used. In addition, a dual RH/temperature micro-logger was placed attached to the Petri dish lid in order to permanently record the internal RH. Usually, the loggers were set to take measurements of both parameters every ten minutes. Petri dish plates were then sealed with two pieces of parafilm, creating an effectively airtight atmosphere. Using this approach, the internal RH could be adjusted by changing the type and amount of desiccating agent, thus effectively controlling the water activity available for the sample cells.

As seen in Figure 21, panel A, each desiccating agent behaved differently in terms of both the stable RH that can be reached inside the chamber and the initial kinetics of water absorption during the first 36 hours, period after which internal RH became stable. The latter behavior can be explained by the highly dynamic interplay among a) the internal humidity of the air volume inside the chamber, b) the type and amount of the desiccating agent and c) the amount of water placed with the cell solution. Interestingly, all desiccating agents tested showed a lower limit of relative humidity that could be reached, which resulted from a balance among the aforementioned factors. Thus, depending on the amount, silica attained between 40 and 95 % RH in the internal chamber atmosphere.

A similar trend was observed with sodium chloride, with the difference that this salt absorbed water in a more restricted range, with final values of RH between 74 and 78 %. Lower RH end values could be reached with calcium chloride, between 26 and 51 %, depending on the amount used. In our experiments, silica was often the desiccating agent of choice, as it was more manageable and due to its color change (blue to purple) while

absorbing water. In addition, the weight difference of this substance pre and post desiccation allowed the quantification of the total amount of water originally present in the chamber. Altogether, an ample spectrum of % RH could be attained inside the experimental chamber, thus facilitating the control of the desiccation experiments. This method has the advantage of being easily adapted for other micro, and even macro organisms, making comparisons possible.

As the term water activity, which may be defined for practical purposes as a_w=1/(ABS RH) is better suited for the understanding of the biological tolerance to dessication, we will refer to a_w instead of RH in the remaining text.

For comparative purposes, another desert cyanobacterium typically found in hypolithical biofilms, *Chroococcidiopsis* isolate N76 isolated from the Mojave Desert, (obtained from the Culture Collection of Microorganisms of Extreme Environments) was also included in these assays. *Chroococcidiopsis* is a genus of cyanobacteria that has the experimental advantage of being closely related to the *Gloeocapsopsis* genus (see Figure 17). This strategy was adopted as we were not able to use the more closely related species *G. crepidinum*.

The first noticeable effect in desiccated (a_w 0.4) cells of isolate AAB1 was a significant drop in the absorption spectra of photosynthetic pigments after twenty days (Figure 22). However, this decline does not seems to continue in time, as the absorption spectra after five months under the same desiccating conditions is in the same range of what was observed after twenty days. A concomitant drop in chlorophyll *a* autofluorescence was also observed (Figure 23). After 20 days of desiccation, fluorescence intensity dropped to 78% with respect to a control sample.

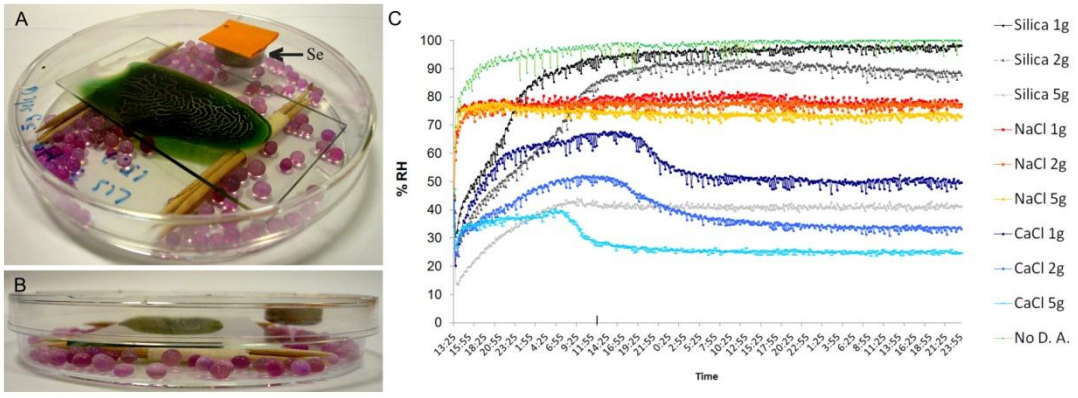

Figure 21.- Desiccation chamber details. A, chamber assembly. The green color represents the cell sample on top of a microscope slide, whereas the blue marbles are the hygroscopic agent. The arrow points to the internal relative humidity sensor attached to the Petri dish lid. B: temporal profile of the percentage of RH inside the chamber in relation to the desiccating agent used. No D.A.: no desiccating agent. 1: Silica, 1 g. 2: Silica, 2 g. 3: Silica, 5 g. 4: NaCl, 1 g. 5: NaCl, 2 g. 6: NaCl, 5 g. 7: $CaCl_2$, 1 g. 8: $CaCl_2$, 2 g. 9: $CaCl_2$, 5 g. Major ticks in the x axis denote days.

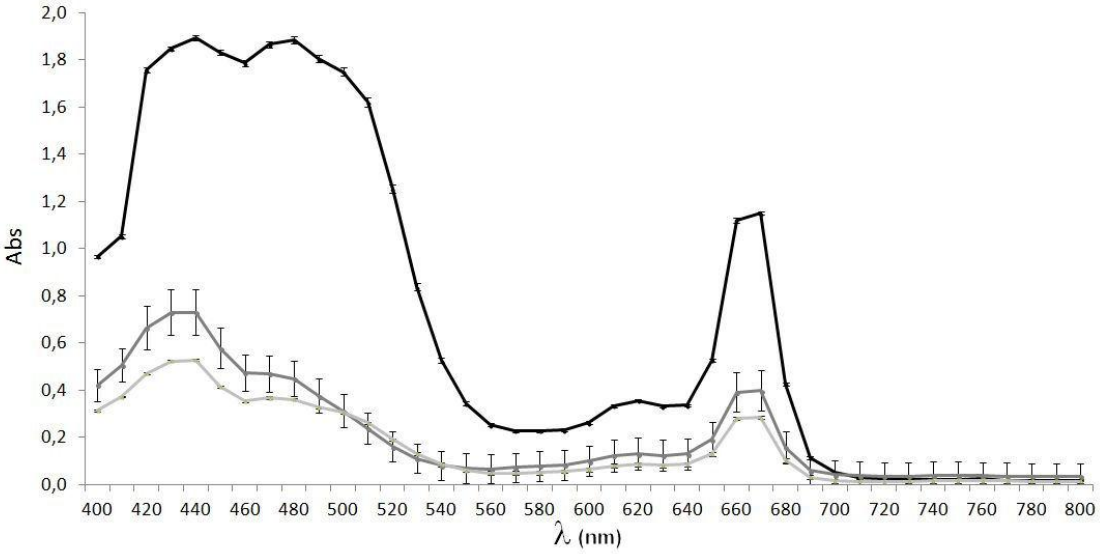

Figure 22.- Absorption spectra in the range of 400 to 800 nm of a pigment extract of isolate AAB1 control and desiccated cells. Black line, control. Dark grey line, desiccated sample (a_w 0.4 for twenty days). Light gray line, desiccated sample (a_w 0.4 for five months).

Interestingly, samples kept desiccated for two years at 0.47 a_w still showed 19% of fluorescence, suggesting that one fifth of the photosynthetic centers remained undamaged under this condition (Figure 23, panel A). Isolate N76 cells behaved in a similar way, with a small drop in chlorophyll *a* fluorescence intensity.

In turn, Raman spectroscopy identified the characteristic double peaks of carotenoids (Edwards *et al*., 2005), seemingly unchanged in samples of isolate AAB1 after two years under desiccation (Figure 24). Raman peaks of chlorophyll *a* (Mathlouthi and Luu, 1980) behaved differently, as they are smaller in the desiccated sample, in agreement with the data obtained by chlorophyll *a* autofluorescence (Figure 23). Raman spectroscopy was conducted with the aid of Iva Paulino-Lima, of the University of Sao Paulo.

Fo (fluorescence origin) and Fm (fluorescence maximum) are parameters which have long been used in measurements of chlorophyll fluorescence (Campbell *et al*., 1998). From these two absolute values, the parameter Fv (fluorescence variable) may be calculated as the difference between the Fm and Fo. In turn, the ratio Fv/Fm has been widely accepted as an indication of the maximum efficiency of photosystem II (Maxwell and Johnson, 2000), as well as an indicator of stress (Bukhov and Carpentier, 2004). When the maximum efficiency of the photosystem II was quantified in cells under desiccating conditions, we found that after five days at an a_w of 0,4 there was a significant drop to 5,6% of the control value (Figure 25). This decline did not vary significantly subsequently, as about the same magnitude was measured after six months of desiccation. A quick recovery up to almost 70% was observed after 40 min of rehydration of the samples desiccated for five days (Figure 25).

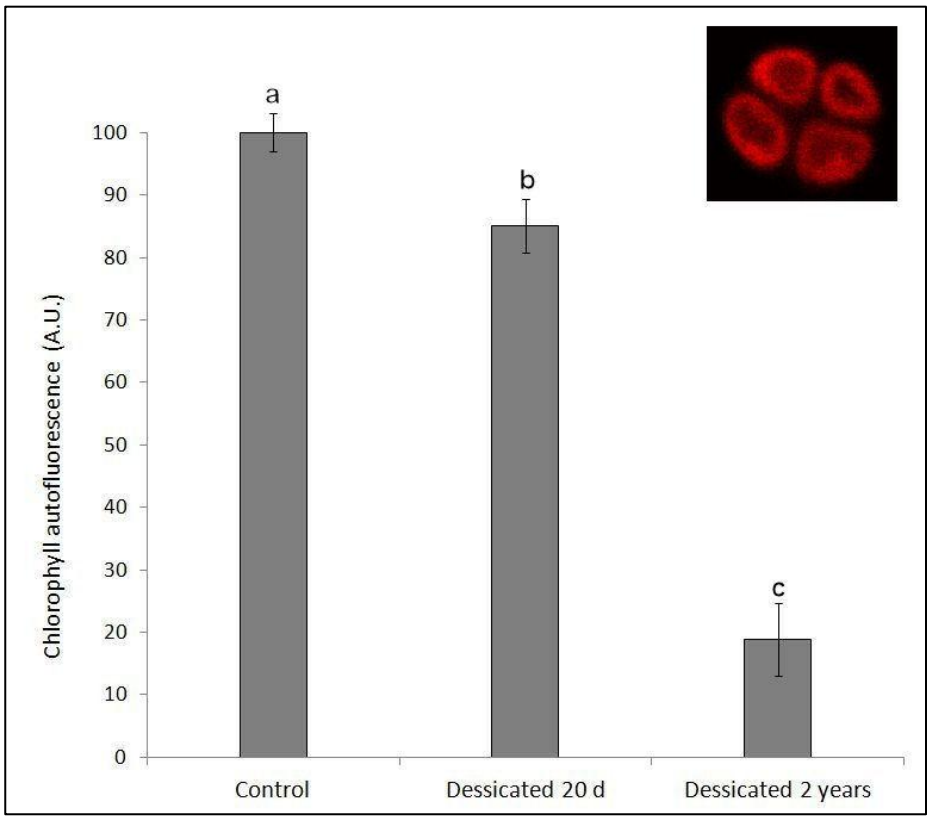

Figure 23.- Chlorophyll *a* autofluorescence decay of isolate AAB1 and *Chroococcidiopsis* isolate N76 cells subjected to desiccation. A: percentage of autofluorescent cells of isolates AAB1 and N76. The inset shows the autofluorescence of a representative tetrad of cells of isolate AAB1 desiccated for two years at a_w 0.4. Means with different letters are statistically different ($P<0.05$; one way ANOVA, Tukey's post test) (a>b>c).

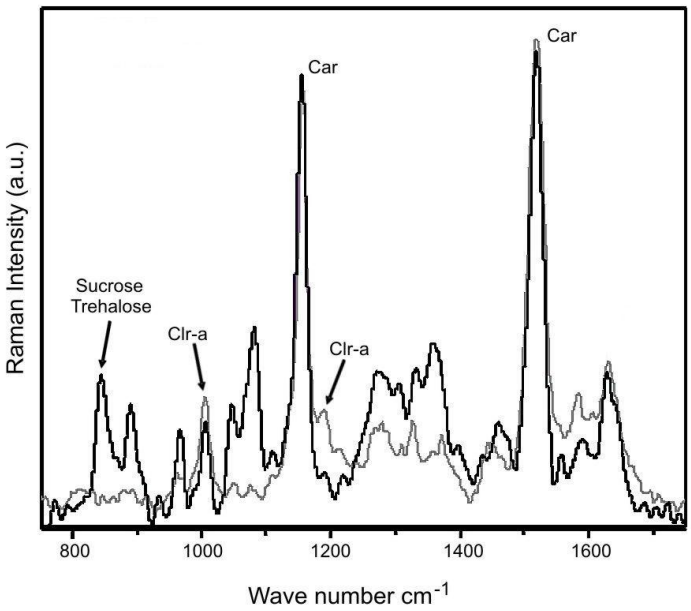

Figure 24.- Raman spectrogram of isolate AAB1 control and desiccated cell samples. Grey line, control. Black line, sample desiccated for two years. Car, carotenoids. Clr-a, Chlorophyll *a*.

This recovery increased up to 84% when the rehydration period lasted 3 h. These results show that although a quick drop in the maximum efficiency of photosystem II quickly follows the onset of desiccation, a rapid recovery (minutes) takes place upon addition of water, a response which has been reported for other desert species that rely on infrequent and unpredictable water inputs (Harel *et al*., 2004; Zeng *et al.*, 2013). Interestingly, the fact that the decline in the maximum efficiency of photosystem II does not reach zero even after six months of desiccation could reflect that there is a low but continuous activity of the photosynthetic apparatus.

As shown in Figure 26, about 80% of isolate AAB1 cells were still viable after 42 d of desiccation at a_w 0.41. After two years under these conditions, cells still showed a viability of 69%, indicating the high tolerance of isolate AAB1 to desiccation stress. All the samples, when placed in liquid BG-11, readily reassumed growth and reproduction (data not shown). In comparison, *Chroococcidiopsis* isolate N76 showed less than 50% viability after 20 d of desiccation at a_w 0.41 (data not shown). TEM micrographs showed little changes in the ultrastructure of cells of isolate AAB1 desiccated for two years (Figure 27). Both cell wall and cell membrane structure seem unchanged. However, phycobilisomes were not evident under desiccating conditions as they were in control samples (Figure 17, panel B). These results are in agreement with previous reports with other desiccation tolerant cyanobacteria such as *Nostoc commune* Utex 584. In this case, after prolonged desiccation, phycobilisomes become dissociated from thylakoids (Angeloni and Potts, 1986; Scherer and Potts, 1989), as a way to diminish the incidence of light into the photosynthetic centers during water stress, thus preventing the formation of ROS (Angeloni and Potts, 1986).

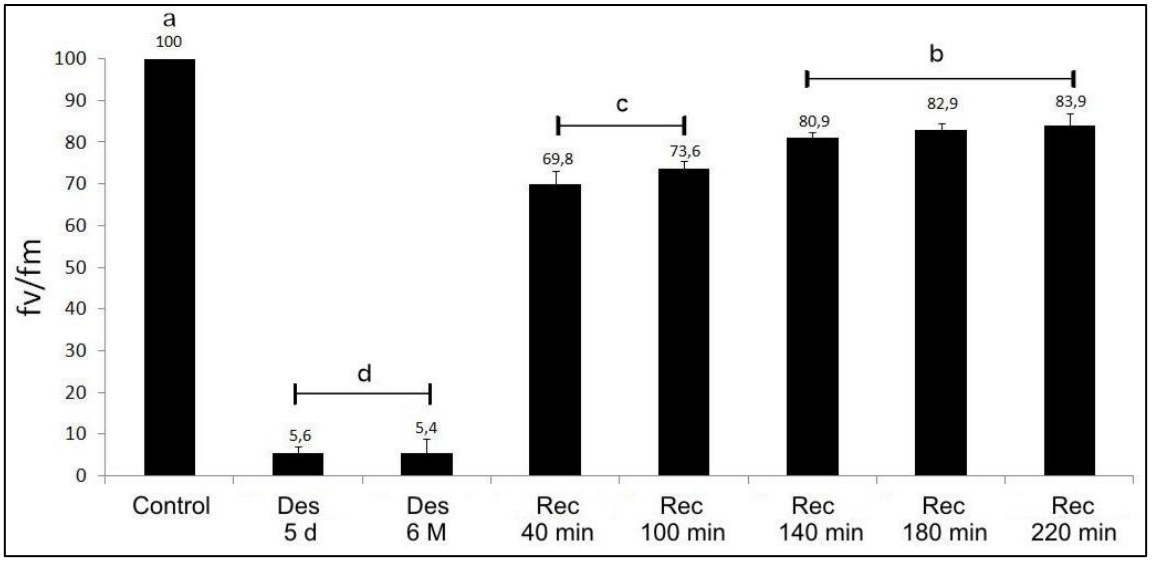

Figure 25.- Maximum photosynthetic efficiency of the Photosystem II of AAB1 cells under desiccating conditions. Des, desiccated. Rec, Recovery. d, days. min, minutes. M, months. Numbers over the bars are means. Means with different letters are statistically different ($P<0.05$; one way ANOVA, Tukey's post test) (a>b>c>d).

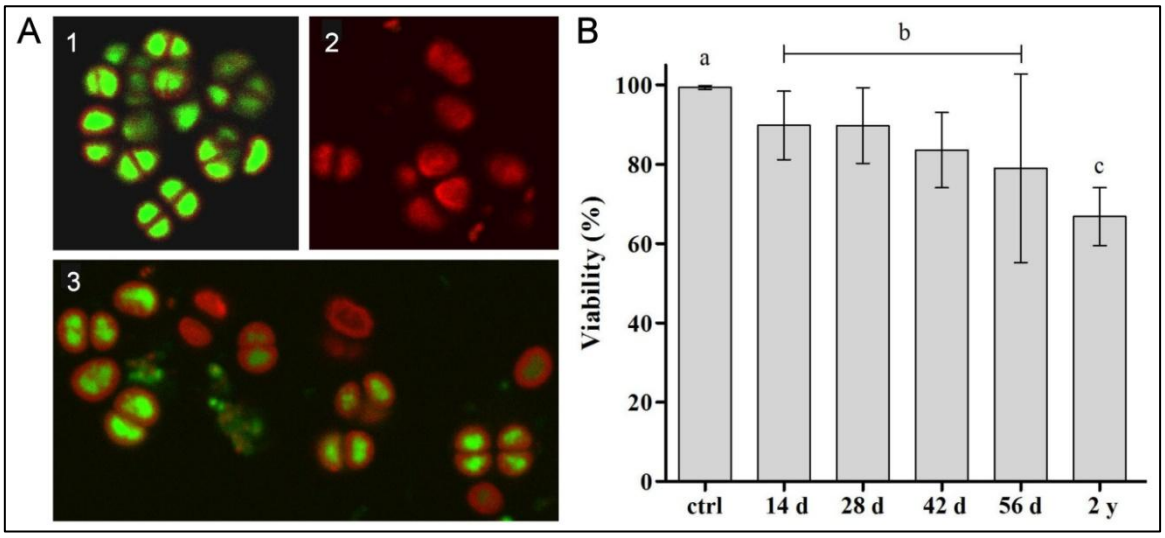

Figure 26.- Viability of *Gloeocapsopsis* isolate AAB1 cells subjected to desiccation. A1: a representative image of viable cells (green) in a control sample of isolate AAB1. A2: a representative image of dead cells (red) in a control sample of isolate AAB1 obtained after boiling for 5 minutes. A3: a representative image of a sample of cells of isolate AAB1 desiccated for 2 years at a_w 0.43. B: percentage of live and dead cells in control and desiccated samples of isolate AAB1. Small letters denote significant statistical differences (t-student $p<0.05$)

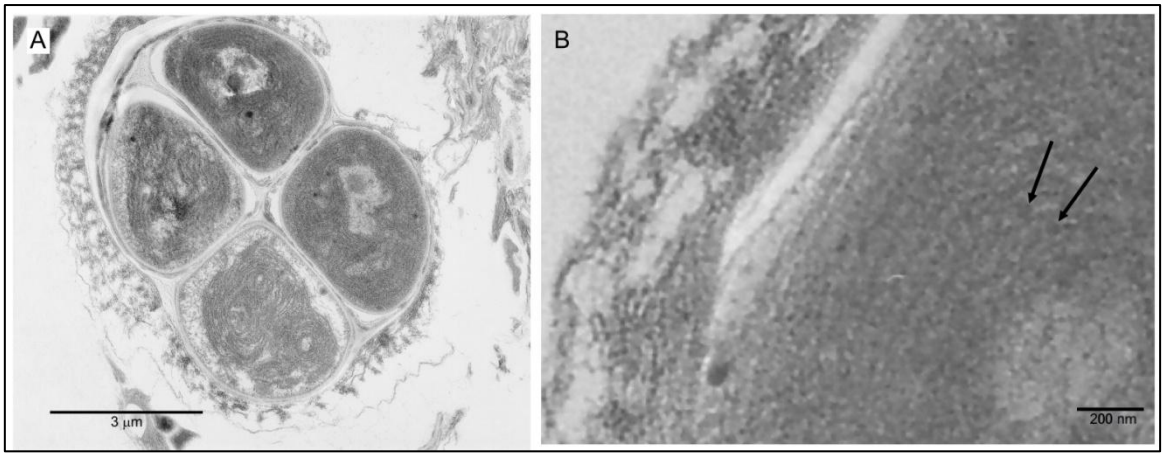

Figure 27.- TEM micrograph of desiccated cells of *Gloeocapsopsis* isolate AAB1. A, TEM micrograph of a two years desiccated cell tetrad. B, Detail of the thylakoidal membranes with a few phycobilisomes (arrows) inserted on them.

Samples of isolates AAB1 and N76 desiccated at a_w 0.40 for 13 days showed no evident changes in the integrity of their DNA (measured as PCR template activity using HIP1 microsatellite-derived primers) and RNA (Figure 28). This agrees with a previous report regarding the genome integrity of isolate *Chroococcidiopsis* CCMEE 123 dried for ten months (Billi *et al*., 2011).

3.6. Identification of compatible solutes synthesized by cells under desiccating conditions.

When desiccated for two weeks at a_w 0.40, cells of our isolate synthesized both sucrose and trehalose, as quantified by HPLC (Figure 29). When desiccated for six months at this same a_w, the biosynthesis of sucrose more than doubled, whereas the synthesis of trehalose was four times higher (Figure 29). In turn, when isolate AAB1 was desiccated for three weeks at a_w 0.8, the level of sucrose biosynthesis attained lower values, which may be expected for an adaptive response. Although it was not the focus of this work, we also found that the isolate synthesizes both sucrose and trehalose when grown in liquid media supplemented with 50 mM NaCl (data not shown), in agreement with other species which synthesize these sugars in both desiccating and ionic conditions (Sakamoto *et al*., 2009; Page-Sharp *et al*., 1999; Hagemann and Marin, 1999). Sucrose and trehalose were also detected as a single peak by Raman spectroscopy (Figure 24).

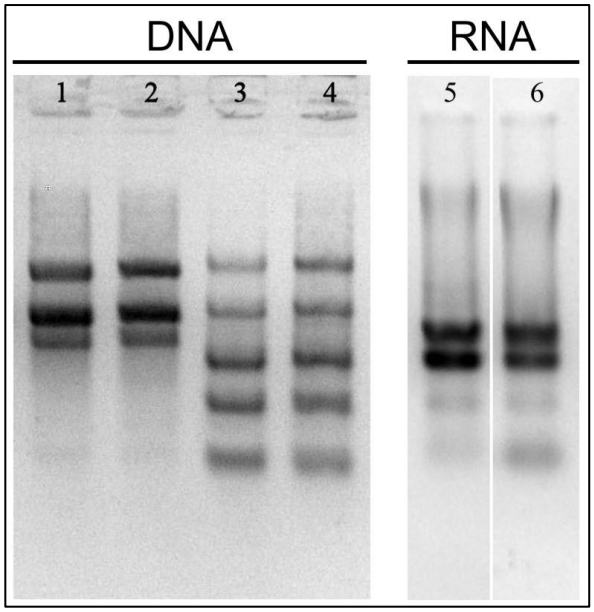

Figure 28.- DNA and RNA fragmentation of isolates *Gloeocapsopsis* AAB1 and *Chroococcidiopsis* N76 cells under desiccation. Lanes: 1, isolate AAB1, control. 2, isolate AAB1 desiccated. 3, isolate N76, control. 4, isolate N76 desiccated. 5, isolate AAB1, control. 6, isolate AAB1 desiccated.

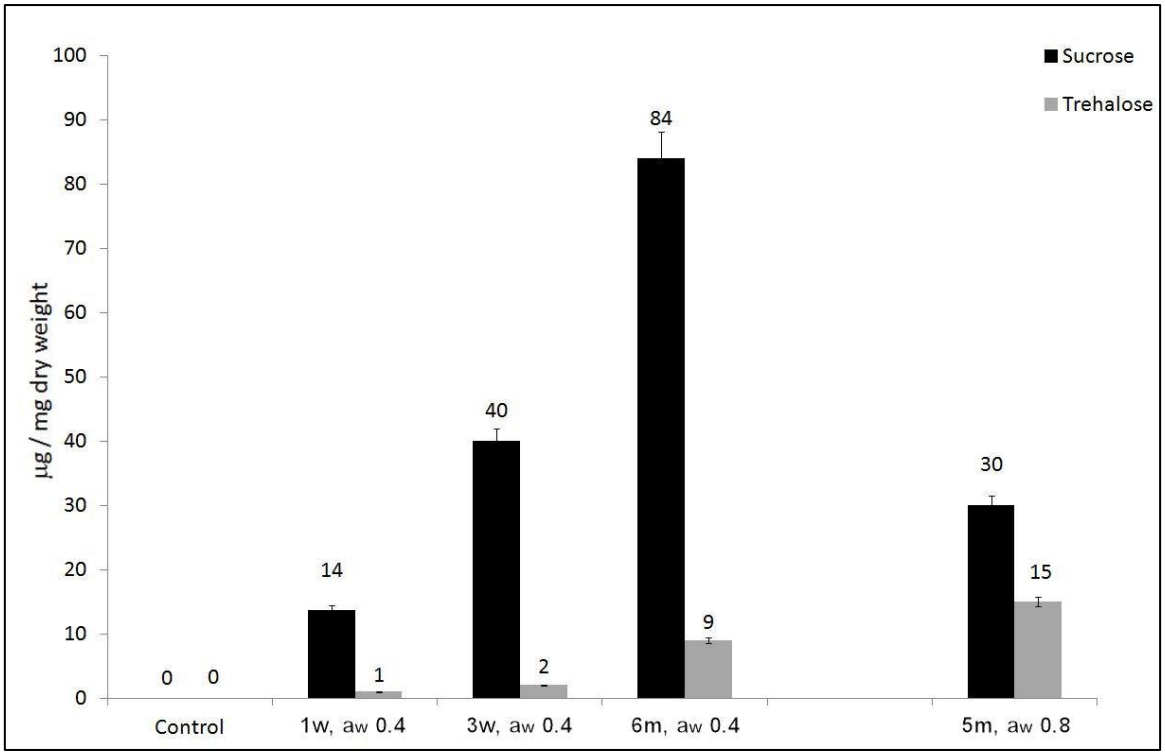

Figure 29.- Synthesis of sucrose and trehalose in cells of isolate AAB1 under desiccation detected by HPLC. Numbers on top of the bars show the synthesis values of sucrose/trehalose in µg of sugar per mg of dry weight. w, weeks; m, months.

These results are not directly comparable with those obtained with other cyanobacteria of previous studies, since other groups measured these sugars under different conditions (water stress, osmotic stress) and at different times and levels of desiccation (Ripka *et al*., 1979; Reed and Stewart, 1983; Warr *et al*., 1987; Yoshida and Sakamoto, 2009). Nevertheless, in very broad terms, after six months of desiccation isolate AAB1 seems to synthesize between forty to eighty times more sucrose and about five to fifteen times more trehalose than other Cyanobacteria (Table 5). In the case of *Chroococcidiopsis* isolate 029, isolated from the Negev Desert, the amounts of sucrose and trehalose reported were obtained only in the range of a_w 0.99-0.84 and at the end of the third day (Hershkovits *et al*., 1995). *Nostoc commune*, another well known model, also synthesizes both sucrose and trehalose under desiccation (Sakamoto *et al*., 2009). However, the amount of trehalose reported for this isolate was eighty times lower than that of isolate AAB1. In desiccated cells of our isolate, no other compatible solutes were detected by HPLC.

3.7. Identification of the candidate genes involved in the synthesis of sucrose and trehalose in isolate AAB1 cells.

Sucrose is synthesized by the action of two enzymes (Lunn, 2002). In the first step, sucrose-6-phosphate synthase catalyzes the synthesis of sucrose-6-phosphate by establishing a glycosidic linkage between C1 of the glucosyl subunit of UDP-glucose and C2 of the fructosyl unit of fructose-6-phosphate.

Table 5.- Synthesis of sucrose and trehalose reported for several cyanobacteria.

Species	µg / mg Dry weight		Reference
	Sucrose	Trehalose	
Gloeocapsopsis AAB1	84	15	This study
Chroococcidiopsis sp. (29-N6904)	3	3	Hershkovitz *et al* ., 1991
Microchaete grisea	n/d	2 - 4	Warr *et al* ., 1987
Rivularia atra	n/d	2 - 4	Reed and Stewart, 1983
Microcoleus chthonoplastes	1	2 - 4	Rippka *et al* ., 1979
Oscillatoria sp.	1.2 - 91	6 - 118	Rippka *et al* ., 1979
Anabaena variabilis	1- 2.4	n/d	Reed *et al* ., 1986
Nostoc entophytum	1- 2.4	n/d	Reed et al., 1986
Nostoc commune	n/d	1.3	Sakamoto *et al* ., 2011
Nostoc punctiforme	0.4	n/d	Yoshida and Sakamoto, 2009
Nostoc verrocosum	n/d	2.3	Sakamoto *et al* ., 2011
Anabaena sp.	1- 2.4	n/d	Warr *et al* ., 1987
Synechococcus sp.	1- 2.4	n/d	Warr *et al* ., 1987
Phormidium autumnale LPP4	4.5	4	Hershkovitz *et al* ., 1991

In the second step, sucrose-6-phosphate is hydrolyzed by sucrose-6-phosphate phosphatase yielding free sucrose and inorganic phosphate. Both exergonic reactions lead to an essentially irreversible pathway providing an efficient production of sucrose even at low substrate concentrations (Salerno and Curatti, 2003). Sucrose is formed only by plants and cyanobacteria.

By using primers based on known sequences of other cyanobacteria, we found in isolate *Gloeocapsopsis* AAB1 the two candidate genes of this metabolic route (Figure 30). Sucrose-6-phosphate synthase is encoded in a 1701 bp intron-less sequence, which contains the GT1 sucrose synthase conserved domain typical of the GT1 family of glycosyltransferases (Coutinho *et al*., 2003). In turn, an intron-less 403 bp sequence encodes sucrose-6-phosphate phosphatase, which contains the sucrose-6-phosphate phosphohydrolase conserved domain found in related enzymes from plants and cyanobacteria (Lunn *et al*., 2000). As already mentioned, genes involved in the biosynthesis of compatible solutes have not been described for any *Gloeocapsopsis* species. In fact, only five genes of this entire genus have been reported.

Thus, we could only analyze our sequences in relation to those of closest species of other phylogenetic related genera, like *Nostoc* and *Anabaena*, as there are no reports neither for other close species like *Chroococcidiopsis* (see Figure 17). As expected, our sequences are found close to sequences of these latter species (Figure 30). We were not able to find in our isolate the genes involved in trehalose synthesis. The search for these genes was complicated by the fact that at least five different routes are known in the microbial word for the synthesis of this sugar (Avonce *et al.*, 2006).

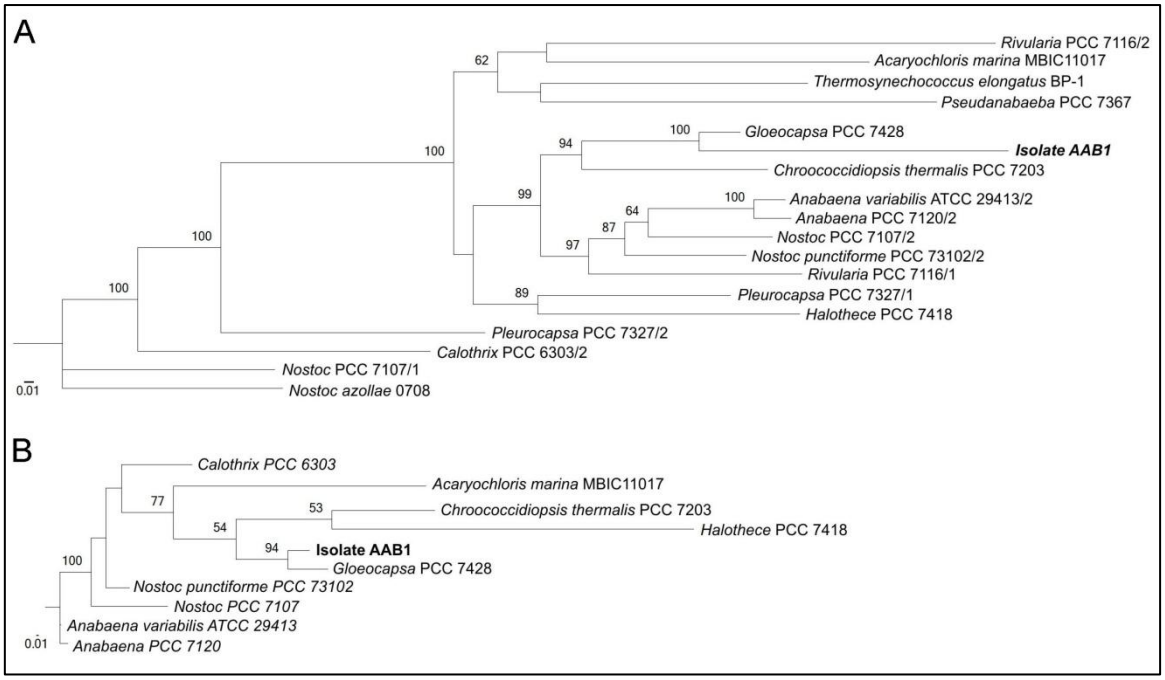

Figure 30.- Phylogenetic tree of sucrose-6-phosphate synthase and sucrose-6-phosphate phosphatase *Gloeocapsopsis* gene sequences. Maximum likelihood phylogenetic trees obtained from the aligned sucrose-6-phosphate synthase (A) and sucrose-6-phosphate phosphatase (B) *Gloeocapsopsis* gene sequences using BOSQUE. The numbers on the nodes represent bootstrap in % values with 1000 replicates. Grey pentagons besides names denote species from which sequences were obtained from its genomes.

Of these, two have been described in other Cyanobacteria, namely, the TreY (maltooligosyltrehalose synthase), TreZ (maltooligosyltrehalose trehalohydrolase) pathway and the TreS (trehalose synthase) pathway (Klähn and Hagemann, 2011). In spite of using no less than 200 different primer combinations based on known gene sequences reported for routes described in other cyanobacteria, we did not obtain positive results. Therefore, we decided not to continue with this approach as we expect to have the complete genome sequence of our isolate in the near future.

3.8. Quantification of mRNA levels of the candidate genes involved in sucrose synthesis under desiccation.

In the case of the sucrose synthase candidate gene, a notable seven-fold increase in mRNA levels was observed about one and a half hour after the onset of desiccation. One hour later, the amount of mRNA was negligible. A new, almost 14-fold increase was observed five hours later (Figure 31). No mRNA was detected during the following six days. After two weeks, mRNA levels were similar to those of the control and they decrease to disappear in the following weeks. For sucrose phosphatase, fluctations in mRNA levels were also observed (Figure 31). The responses shown by the candidate genes encoding for sucrose synthase and sucrose phosphatase are puzzling and require further work. However, it is possible to forward a few preliminary hypothesis, as follow.

Sucrose is known to be synthesized and used as a cell wall component under non stressed conditions in cyanobacteria (Curatti *et al.*, 2008). This may explain the levels of mRNA of both sucrose synthase and phosphatase found under our control conditions. This may also explain why sucrose is not observed in control conditions by HPLC

(Figure 29), as it is quickly used for cell wall synthesis. Sucrose is only observed about one week after the onset of the desiccation, when enough quantities are accumulated to be detected (Figure 29). During the onset of desiccation, cell wall synthesis should be halted, as it may be assumed that no cell growth is possible under this stressful condition. Nevertheless, the synthesis of sucrose is continued by the cell, as sucrose now takes its alternative role as compatible solute. In turn, another explanation might be that the synthesis of sucrose synthase follows a three stage response. First, immediately after the onset of desiccation, an initial increase in mRNA levels take place as water restriction is detected. This primary response may be of the type that is set in action by the cells in their natural environment when a decrease of water availability is sensed, which is in the hours range. It may be recalled that due to the typical input of water as fog dew at night in the Coastal Range, most of the time the biofilm has water available, with potential limitations between 10 AM in the morning and 3 PM in the afternoon (Figure 5). Then, as time goes by without additional inputs of water, a stronger secondary response is then activated, with a new and higher increase in mRNA levels of sucrose synthase. These augmentations in mRNA levels may be needed because either a) the sucrose synthase enzyme is damaged by the desiccation process or b) a higher requirement of enzyme units for a stronger response. Alternative b) seems more likely, as an enzyme that is part of the desiccation tolerance response would not be expected to be prone to desiccation damage. This possibility may be tested by determining the tertiary structure of the sucrose synthase enzyme and its functionality under increasing desiccating conditions and by determining the amount of enzyme available at different periods of desiccation by techniques like Western blotting.

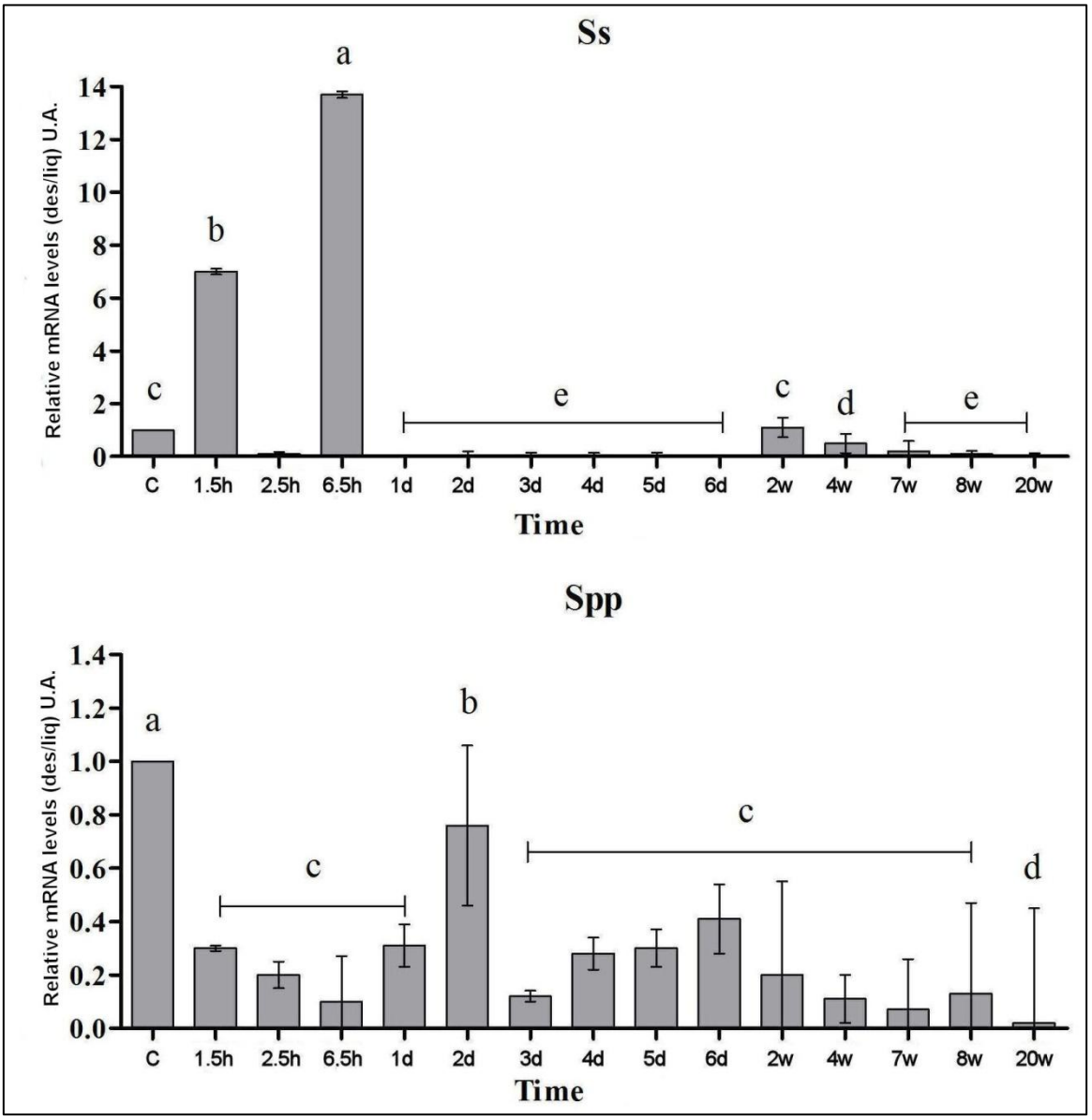

Figure 31.- Relative fold change (desiccated versus liquid control) in mRNA abundance of the sucrose synthase (Ss) and sucrose phosphate (Spp) genes in *Gloeocapsopsis* AAB1 desiccated cells. Relative fold change in mRNA abundance of sucrose synthase and sucrose phosphatase in *Gloeocapsopsis* cells under different times of desiccating conditions, as compared to non stressed cells in liquid media. h, hours. d, days. w, weeks. Means with different letters are statistically different ($P<0.05$; one way ANOVA, Tukey's post test) (a>b>c>d).

The set of primary and secondary responses explained above may be enough for the cell to be protected for a few days, as no further increases in mRNA levels are detected until more than a week later. At this period, the additional increase in mRNA may be required because the stressed cells cannot longer respond as strong as in the beginning, or maybe because a final "fine tuning" is needed in order to set the cells prepared for a longer period of desiccation.

In the case of sucrose phosphatase, its mRNA levels are much lower and more varied in magnitude, not reaching the values attained under normal hydration conditions. As water is needed as a substrate, the lower amounts of mRNA in comparison with the non-stressed control may be explained by a) a higher tolerance of this enzyme to desiccation and thus, new enzyme is not required. This latter possibility may in turn be explained by a) the enzyme being highly efficient and/or b) because there is already enough enzyme for the tolerance process. The determination of the kinetic parameters of sucrose phosphatase under increasing desiccating conditions, in particular *kcat/Km*, may give support to this alternative, as well as the measurement of the amount of enzyme at different times of desiccation.

As the determination of gene expression for long desiccation periods has not been reported, we wanted to have some confidence that the results obtained for sucrose synthesis candidate genes were reliable. Thus, we also measured the mRNA levels of additional gene whose response could be interpreted in our model. Given the results shown in Figures 22 to 25, in which a drop in the functional properties of the photosynthetic apparatus is observed, the mRNA levels of gene *psb*A4, which encodes the isoform 1:2 of the D1 subunit of photosystem II (Komenda *et al*., 2012), were also

determined. This protein is an indispensable component of the oxygenic photosynthesis apparatus. Due to the strongly oxidative chemistry of water splitting, photodamage of the D1 protein is unavoidable and therefore requires prompt replacement. In contrast, most of the other photosystem II subunits remain undamaged (Nishiyama *et al*., 2006). In the Cyanobacteria, the D1 protein is encoded by a *psbA* gene family, whose members are differentially expressed according to environmental stimuli (Mulo *et al*., 2009). Thus, if the method used for determining mRNA levels in the desiccated state is trustworthy, a decrease in the mRNA levels of the *psbA* gene should be observed, since less photosynthesis is taking place.

As expected, a decrease in *psbA*4 mRNA was found (Figure 32). Interestingly, this decrease was not linear in time, since various fluctuations were observed, similarly to the case of the sucrose synthesis genes. First, a strong decrease after one day of desiccation took place, followed by a 60% increase one day later. Then, a new decrease was observed at day three. This last response coincides with the time period in which the internal a_w of the desiccation chamber becomes stable. A new recovery was observed during the next two days until day five, when a new decline took place. Values in the range of two to twenty weeks were similar, with mRNA levels at about 5% of the control condition.

3.9. Determinations of ATP pools in desiccated cells

The biosynthesis of compatible solutes and the changing mRNA levels led us to consider the possibility that there might be some metabolic activity in the desiccated state.

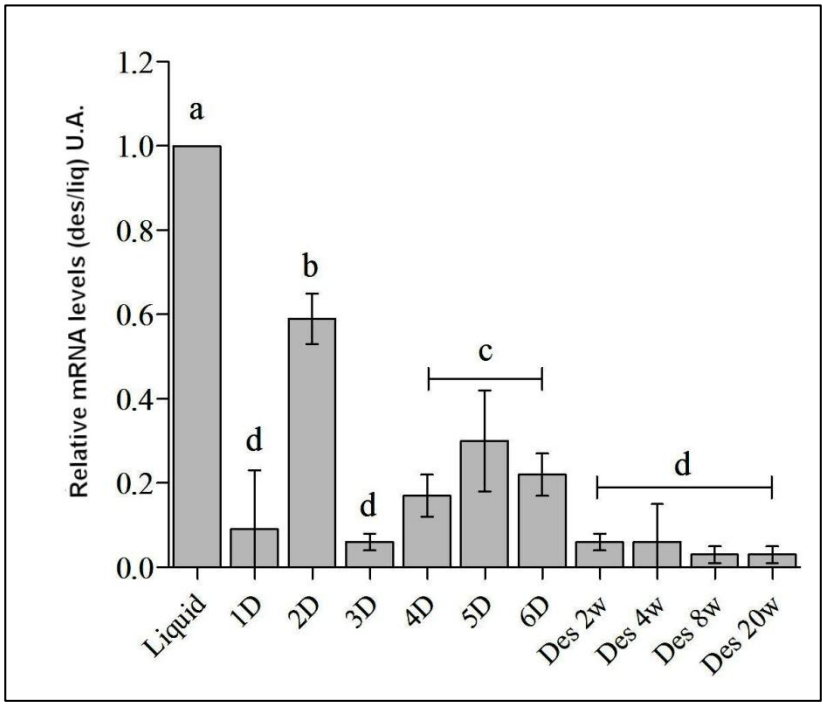

Figure 32.- Relative fold change (desiccated versus liquid control) in mRNA abundance of the *psbA*4 gene in *Gloeocapsopsis* AAB1 desiccated cells. d, days; w, weeks. Means with different letters are statistically different (P<0.05; one way ANOVA, Tukey's post test) (a>b>c>d).

In order to approach this possibility, we measured the intracellular levels of ATP in desiccated cells, as ATP quantification has been broadly used as an indicator of active metabolism in microorganisms (Crouch *et al.*, 1993; Hipler U-Ch *et al*., 1998), and in particular, in cyanobacterial cells (Shao *et al*., 2010; Lowery *et al*., 2009). Under the paradigm of "metabolic stasis" during the desiccated state, cells stop all metabolic activity until better conditions are sensed, in which case metabolism and growth reassume (Potts, 2001; Billi and Potts, 2002; Hand *et al*., 2011; Ricci and Perletti, 2006). If this was the case, ATP pools should be expected to be fixed in time at the beginning of the desiccation process.

ATP pools in AAB1 cells were measured after one week of desiccation at 0.3 a_w (the most stressfull desiccating condition used in this work), under the same conditions of light and temperature regularly used in other desiccation experiments, that is, 30 μmol m^{-2} s^{-1} and 30ºC, respectively. Strikingly, we detected a statistically significant drop of ATP after this period (white bar in Figure 33). This could be explained by ATP being used in damage response processes, which would indicate some metabolic activity in the desiccated state. To further improve this experiment, we re-distributed the one-week desiccated samples into four different conditions of light and temperature as follows: light at 30ºC, darkness at 30ºC, light at 4ºC and darkness at 4ºC. These were subjected to additional six weeks at 0.3 a_w. We chose these conditions of light and temperature since light availability should impact the energy budget of the treated cells. In turn, temperature changes should impact the enzymatic rates in general, as set by their q10 temperature coefficients. After this experiment, an additional drop in the ATP concentration was observed in all samples (Figure 33).

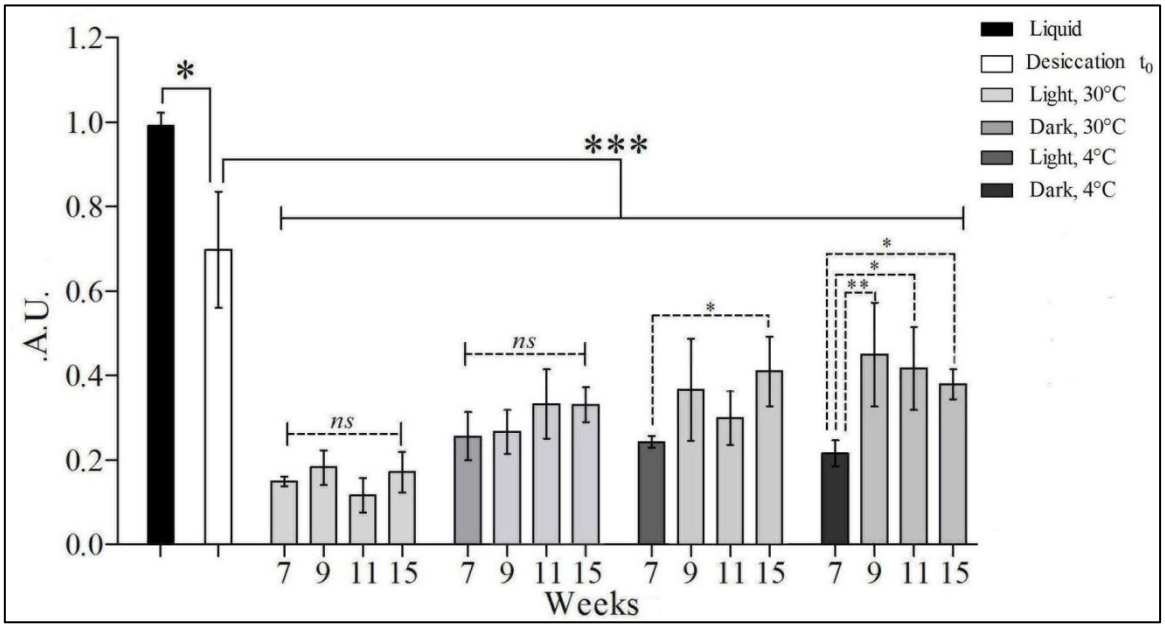

Figure 33.- Intracellular pools of ATP in *Gloeocapsopsis* AAB1 desiccated cells exposed to four environmental stimuli. The single big asterisk denotes a significant statistical difference between the control and the desiccated samples at t0. The three big asterisks denote a significant statistical difference between the desiccated samples at t0 and all subsequent treatments. Small asterisks denote intra-treatment significant statistical differences. Different number of asterisks denotes the magnitud of statistical difference between the groups. (* if $p<0.05$; ** if $p<0.01$; *** if $p<0.001$ and ns not significant.) One way ANOVA and Tukey's multiple comparison test was used. A.U., arbitrary units.

Although further experimentation is needed to fully understand these results, a preliminary interpretation may be proposed. As observed in Figure 33, the sample under light/30ºC shows the lowest concentration of ATP. In principle, ATP could not be generated due to phycobilisome uncoupling and to the lack of water available for photosynthesis. Thus, the lower levels may be explained by ATP being consumed in metabolic reactions. Lower ATP levels may also be caused by photorespiration, which has been proposed to act as a mechanism of light energy dissipation under conditions in which assimilatory processes are insufficient to dissipate the absorbed photons (Beardall *et al*., 2003). These assumptions agree with the higher pools of ATP observed in the illuminated sample at 4ºC, as lower temperatures may have caused the metabolic machinery to function at a slower rate, thus preserving the ATP. On the other hand, the relatively higher ATP pools in the dark samples could be explained by chlororespiration, which is only operative in the dark when the photosynthetic machinery is inactive. Chlororespiration has been suggested to be a mechanism that attenuates the generation of damaging superoxide and hydroxyl radicals caused by unused NADPH pools, which are then redirected to ATP synthesis (Beardall *et al*., 2003).

After seven weeks, all the samples were then returned to the original conditions of desiccation (light/30ºC) for additional eight weeks, thus totaling 15 weeks, with the premise that a recovery in ATP pools could be observed in some of these samples, if they were metabolically active. Measurements were taken at weeks 9, 11 and 15. In agreement with the hypothesis of active metabolism in the desiccated state, a recovery was observed in two of the experimental conditions, with the samples previously exposed to dark and 4ºC showing the most statistically significant increases.

These results constitute compelling evidence of metabolic activity in desiccated AAB1 cells. It seems that dark incubation allowed a better adaptation of the cell samples to desiccation, as ATP pool are higher in time in these cases (compare light/30ºC with dark/30ºC and light/4ºC with dark/4ºC). The same can be said for low temperatures (compare light/4ºC with dark/4ºC). Thus, the combinatory effect of dark and low temperatures may have caused the dark/4ºC cell samples to show the highest recoveries, which at week nine reach about 70% of the ATP pool detected at the beginning of the desiccating period (white bar). Active metabolism in AAB1 cells under extreme desiccating conditions could be further explored by $^{14}CO_2$ labeling.

4.- Conclusions

- In the extremely arid Atacama Desert, cyanobacteria of the *Gloeocapsopsis* genus are found in hypolithic biofilms under quartzes of the Coastal Range.
- After two years under desiccating conditions, 70% of the isolate *Gloeocapsopsis* AAB1 were viable, which indicates that this species is highly tolerant to desiccation.
- The desiccation tolerance shown by isolate *Gloeocapsopsis* AAB1 may be explained in part by the increasing accumulation in time of the compatible solutes sucrose and trehalose.
- Variable ATP levels measured in the desiccated state suggest that the *Gloeocapsopsis* AAB1 isolate is metabolically active during such state, an observation which has not been reported for other desert organisms. *Gloeocapsopsis* AAB1 may thus constitute a new model to understand the desiccation phenomenon.

5. References

Alpert, P. 2005. The limits and frontiers of desiccation-tolerant life. Integr. Comp. Biol. 45: 685-695.

Alpert P. 2006. Conisolatets of tolerance: why are desiccation-tolerant organisms so small or rare? J Exp Biol. 209:1575-1584.

Angeloni SV, Potts M. 1986. Polysome turnover in immobilized cells of *Nostoc commune* (cyanobacteria) exposed to water stress. J Bacteriol. 168:1036-1039.

Ashraf, M. 2010. Inducing drought tolerance in plants: recent advances. Biotechnol Adv. 28:169-183.

Avonce N, Mendoza-Vargas A, Morett E, Iturriaga G. 2006. Insights on the evolution of trehalose biosynthesis. BMC Evol Biol. 6:109.

Azúa-Bustos A, González-Silva C and Arenas-Fajardo C, Vicuña R. 2012. Extreme environments as drivers of convergent evolution: the Atacama Desert Coastal Range as a relevant model. Frontiers in Microbiology. In press. doi: 10.3389

Azúa-Bustos A, González-Silva C, Mancilla R.A., Salas, L., Gómez-Silva B, McKay CP and Vicuña R. 2011. Hypolithic cyanobacteria supported mainly by fog in the Coastal Range of the Atacama Desert. Microb Ecol, 61:568-581.

Azúa-Bustos A., González-Silva, C., Mancilla R.A., Salas L, Palma R.E., Wynne J.J., McKay, C.P. and Vicuña, R. 2009. Ancient photosynthetic eukaryote biofilms in an Atacama Desert coastal cave. Microb Ecol 58:485–496.

Azúa-Bustos, A., González-Silva, C., Salas L, Vicuña, R. 2010. A novel subaerial *Dunaliella* sp. growing on cave spiderwebs in the Atacama Desert. Extremophiles 14: 443-452.

Azúa-Bustos A., Urrejola C., and Vicuña R. 2012. Life at the dry edge: microorganisms of the Atacama Desert. FEBS Lett 586:2939-2945.

Azúa-Bustos A. and Vega-Martínez, C. 2013. The potential for detecting life as do don't know it by fractal complexity analysis. Int J Astrobiol. DOI: http://dx.doi.org/10.1017/S1473550413000177

Beardall J, Quigg A, and Raven JA. 2003. Photorespiration and Chlororespiration. In Photosynthesis in Algae. Advances in Photosynthesis and Oxygen Consumption. 14: 157-181. Larkum, A.W.D., Douglas, S.E. and Raven, J.A., editors. Springer Netherlands.

Bhatnagar-Mathur P, Vadez V, Sharma KK. 2008. Transgenic approaches for abiotic stress tolerance in plants: retrospect and prospects. Plant Cell Rep 27:411–424.

Billi D. 2009. Subcellular integrities in *Chroococcidiopsis* sp. CCMEE 029 survivors after prolonged desiccation revealed by molecular probes and genome stability assays. Extremophiles 13:49-57.

Billi D, Friedmann EI, Helm RF, Potts M. 2001. Gene transfer to the desiccation-tolerant cyanobacterium *Chroococcidiopsis*. J Bacteriol. 183:2298-2305.

Billi D, Potts M. 2002. Life and death of dried prokaryotes. Res Microbiol 153:7-12.

Billi D, Viaggiu E, Cockell CS, Rabbow E, Horneck G, Onofri S. 2011. Damage escape and repair in dried *Chroococcidiopsis* spp. from hot and cold deserts exposed to simulated space and martian conditions. Astrobiology. 11:65-73.

Billi D, Wright DJ, Helm RF, Prickett T, Potts M, Crowe JH. 2000. Engineering desiccation tolerance in *Escherichia coli*. Appl Environ Microbiol. 66:1680-1684.

Bruno L, Billi D and Albertano P. 2005. Optimization of molecular techniques applied to the taxonomy of epilithic *Leptolyngbya* isolates. Arch Hydrobiol Suppl Algol Stud 117:197–207.

Büdel, B., Karsten, U., and Garcia-Pichel, F. 1997. Ultraviolet-absorbing scytonemin and mycosporine-like amino acid derivatives in exposed, rock-inhabiting cyanobacterial lichens. Oecologia 112: 165–172.

Buitink, J. and Leprince, O. 2004. Glass formation in plant anhydrobiotes: survival in the dry state. Cryobiology 48: 215-228.

Bukhov NG, Carpentier R. 2004. Effects of water stress on the photosynthetic efficiency of plants. In Advances in Photosynthesis and Respiration. 19: 623-635. Papageorgiou GC and Govindjee G, Editors. Springer, Netherlands.

Campbell D, Hurry V, Clarke AK, Gustafsson P, Oquist G. 1998. Chlorophyll fluorescence analysis of cyanobacterial photosynthesis and acclimation. Microbiol Mol Biol Rev. 62:667-683.

Cereceda P, Osses P, Larraín H, Farias M, Schemenauer RS. 2002. Advective, orographic and radiation fog in the Tarapacá Region, Chile. Atmos Res 64:261–271.

Chen M, Wei H, Cao J, Liu R, Wang Y, Zheng C. 2007. Expression of *Bacillus subtilis proBA* genes and reduction of feedback inhibition of proline synthesis increases proline production and confers osmotolerance in transgenic Arabidopsis. J Biochem Mol Biol. 40:396-403.

Chorus, I & Bartram J (1999) Toxic Cyanobacteria in Water: a Guide to Public Health Significance, Monitoring and Management. Für WHO durch E & FN Spon. Chapman & Hall, London, 416 pp.

Close, TJ. 1997. Dehydrins: a commonality in the response of plants to dehydration and low temperature. Physiol Plant 100:291-296.

Close TJ, Lammers PJ. 1993. An osmotic stress protein of cyanobacteria is immunologically related to plant dehydrins. Plant Physiol. 101:773-779.

Cockell CS, Stokes MD. 2004. Widespread colonization by polar hypoliths. Nature 431:414.

Cortina C, Culianez-Macia F. 2005. Tomato abiotic stress enhanced tolerance by trehalose biosynthesis. Plant Sci 169:75–82.

Costerton, J.W., and Stoodley, P. 2003. Microbial biofilms: protective niches in ancient and modern microbiology. In Fossil and Recent Biofilms: A Natural History of Life on Earth. Krumbein, W.E., Paterson, D.M., and Zavarzin, G.A. (eds). Dordrecht, the Netherlands: Kluwer, pp. xv–xxi.

Coutinho PM, Deleury E, Davies GJ, Henrissat B. 2003. An evolving hierarchical family classification for glycosyltransferases. J Mol Biol. 328:307-317.

Crouch SPM, Kozlowski R, Slater KJ, Fletcher J. 1993. The use of ATP bioluminescence as a measure of cell proliferation and cytotoxicity. J Immunol Meth 160:81-88.

Curatti L, Giarrocco LE, Cumino AC, Salerno GL. 2008. Sucrose synthase is involved in the conversion of sucrose to polysaccharides in filamentous nitrogen-fixing cyanobacteria. Planta. 228:617-625

De Long EF. 1992. Archaea in coastal marine environments. Proc Natl Acad Sci USA 89:5685–5689.

de los Ríos A, Valea S, Ascaso C, Davila A, Kastovsky J, McKay CP, Gómez-Silva, B. and Wierzchos J. 2010. Comparative analysis of the microbial communities inhabiting halite evaporites of the Atacama Desert. Int Microbiol 13:79-89.

De Philippis, R. and M. Vincenzini. 1998. Exocellular polysaccharides from cyanobacteria and their possible applications. FEMS Microbiol Rev 22:151-175.

Drees KP, Neilson JW, Betancourt JL, Quade J, Henderson DA, Pryor BM, Maier RM 2006. Bacterial community structure in the hyperarid core of the Atacama Desert, Chile. Appl Environ Microbiol 72:7902-7908.

Edwards HGM, Moody CD, Villar SE, Wynn-Williams D. 2005. Raman spectroscopic detection of key biomarkers of Cyanobacteria and lichen symbiosis in extreme Antarctic habitats: Evaluation for Mars Lander missions. Icarus 174: 560-571.

Farías M, Cereceda P, Osses P, Nuñez R. 2005. Spatial and temporal behavior of the stratocumulus cloud, fog producer in the coast of the Atacama Desert (21° South lat., 70° West long.), during one month of winter and another of summer. Investig Geogr 56:43–61.

Garay-Arroyo A, Colmenero-Flores JM, Garciarrubio A and Covarrubias AA. 2000. Highly hydrophilic proteins in prokaryotes and eukaryotes are common during conditions of water deficit. J Biol Chem 275:5668-5674.

Ge LF, Chao DY, Shi M, Zhu MZ, Gao JP, Lin HX. 2008. Overexpression of the trehalose- 6-phosphate phosphatase gene OsTPP1 confers stress tolerance in rice and results in the activation of stress responsive genes. Planta. 228:191-201.

Gorbushina AA. 2007. Life on the rocks. Environ Microbiol. 9:1613-1631.

Goyal, K., Walton, L. J., Browne, J. A., Burnell, A. M. and Tunnacliffe, P. Alpert A. 2005. Conisolatets of desiccation toleranceMolecular anhydrobiology: identifying molecules implicated in invertebrate anhydrobiosis. Integr Comp Biol 45: 702-709.

Graf A, Kuttler W, Werner J. 2008. Mulching as a means of exploiting dew for arid agriculture? Atmos Res 87:369–376.

Gultepe I, Pagowski M, Ried J. 2007. A satellite-fog based detection scheme using screen air temperature. Weath Forec. 22:444–456.

Gupta S, Agrawal SC. 2006. Survival of blue-green and green algae under stress conditions. Folia Microbiol Praha 51:121–128.

Hagemann M and Marin K. 1998. Salt-induced sucrose accumulation is mediated by sucrose-phosphate-synthase in Cyanobacteria. J Plant Physiol. 155:424-430.

Hand SC, Menze MA, Borcar A, Patil Y, Covi JA, Reynolds JA, Toner M. 2011. Metabolic restructuring during energy-limited states: insights from *Artemia franciscana* embryos and other animals. J Insect Physiol. 57:584-594.

Harel Y, Ohad I, Kaplan A. 2004. Activation of photosynthesis and resistance to photoinhibition in cyanobacteria within biological desert crust. Plant Physiol. 136:3070-3079.

Hartley, A., Chong, G., Houston, J. and Mather, A. 2005. 150 million years of climatic stability: evidence from the Atacama Desert, northern Chile. J Geol Soc London. 162: 421-424.

Hershkovits N, Oren A, Cohen Y. 1991. Accumulation of trehalose and sucrose in cyanobacteria exposed to matric water stress. Appl Environ Microbiol. 57:645-648.

Higo A, Katoh H, Ohmori K, Ikeuchi M, Ohmori M. 2006. The role of a gene cluster for trehalose metabolism in dehydration tolerance of the filamentous cyanobacterium *Anabaena* sp. PCC 7120. Microbiology. 152:979-987.

Higo A, Suzuki T, Ikeuchi M, Ohmori M. 2007. Dynamic transcriptional changes in response to rehydration in *Anabaena* sp. PCC 7120. Microbiology 153:3685–3694.

Hipler U-Ch, Knöll B, Wollina U. 1998. The use of an ATP bioluminescence assay to quantify HaCaT cell cytotoxicity. Bioluminescence and chemiluminescence, Perspectives for the 21th century. pp 169-172. London Academic Press.

Holmstrom KO, Somersalo S, Mandal A, Palva ET, Welin B. 2000. Improved tolerance to salinity and low temperature in transgenic tobacco producing glycine betaine. J Exp Bot 51:177–185.

Hong-Bo S, Zong-Suo L, Ming-An S. 2005. LEA proteins in higher plants: structure, function, gene expression and regulation. Colloids Surf B Biointerfaces. 45:131-135.

Houston, J. and Hartley, A. 2003. The central Andean west-slope rainshadow and its potential contribution to the origin of hyper-aridity in the Atacama Desert. Desert. Int. J. Climatol. 23:1453–1464.

Jang IC, Oh SJ, Seo JS, Choi WB, Song SI, Kim CH, Kim YS, Seo HS, Choi YD, Nahm BH, Kim JK. 2003. Expression of a bifunctional fusion of the *Escherichia coli* genes for trehalose-6-phosphate synthase and trehalose-6-phosphate phosphatase in transgenic rice plants increases trehalose accumulation and abiotic stress tolerance without stunting growth. Plant Physiol. 131:516-524.

Janse I, Meima M, Kardinaal WE, Zwart G. 2003. High-resolution differentiation of Cyanobacteria by using rRNA-internal transcribed spacer denaturing gradient gel electrophoresis. Appl Environ Microbiol 69:6634-6643.

Kappen L, Lange OL, Schulze ED, Evenari M, Buschbom V. 1979. Ecophysiological investigations on lichens of the Negev Desert: IV. Annual course of the photosynthetic production of *Ramalina maciformis* (Del.) Bory. Flora 168:85–105.

Kaseke-Farai K. 2009. “Non-rainfall” atmospheric water in arid soil micro-hydrology and ecology. Master of Science Thesis, University of Stellenbosch.

Katra I, Lavee H, Sarah P. 2008. The effect of rock fragment size and position on topsoil moisture on arid and semi-arid hillslopes. Catena 72:49–55.

Kemper WD, Nicks AD, Corey AT. 1994. Accumulation of water in soils under gravel and sand mulches. Soil Sci Soc Am J 58:56–63.

Klähn S and Hagemann M. 2011. Compatible solute biosynthesis in cyanobacteria. Environ Microbiol. 13:551-562.

Komárek, J. 1993. Validation of the genera *Gloeocapsopsis* and *Asterocapsa* (Cyanoprokaryota) with regard to species from Japan, Mexico and Himalayas. Bull Natl Scie Museum, Tokyo, Ser. B (Botany) 19: 19-37.

Komárek J. 2003. Coccoid and Colonial Cyanobacteria. – In: Wehr J.D. & Sheath R.G. ed., Freshwater algae of North America, Academic Press, San Diego, pp. 59-116.

Komárek J. & Anagnostidis K. (1998): Cyanoprokaryota 1. Teil: Chroococcales. - In: Ettl H., Gärtner G., Heynig H. & Mollenhauer D. (eds): Süsswasserflora von Mitteleuropa 19/1, Gustav Fischer, Jena-Stuttgart-Lübeck-Ulm, 548 pp.

Komenda J, Sobotka R, Nixon PJ. 2012. Assembling and maintaining the photosystem II complex in chloroplasts and cyanobacteria. Curr Opin Plant Biol. 15:245-251.

Kovacs D, Agoston B, Tompa P. 2008. Disordered plant LEA proteins as molecular chaperones. Plant Signal Behav. 3:710-713.

Lacap DC, Warren-Rhodes KA, McKay CP, Pointing S.B. 2011. Cyanobacteria and chloroflexi-dominated hypolithic colonization of quartz at the hyper-arid core of the Atacama Desert, Chile. Extremophiles 15:31-38.

Lalley JS, Viles HA. 2006. Do vehicle track disturbances affect the productivity of soil-growing lichens in a fog desert? Funct Ecol 20:548–556.

Lange OL, Allen Green TG, Melzer B, Meyer A, Zellner H. 2006. Water relations and CO_2 exchange of the terrestrial lichen *Teloschistes capensis* in the Namib fog desert: measurements during two seasons in the field and under controlled conditions. Flora 201:268–280.

Lange OL and Bertsch A. 1965. Photosynthese der Wustenflechte Ramalina maciformis nach Wasserdampfaufnahme aus dem Luftraum. Naturwissenschaften, 52:215–216.

Larraín H, Velásquez F, Cereceda P, Espejo R, Pinto R, Osses P, Schemenauer RS. 2002. Fog measurements at the site 'Falda Verde' North of Chañaral (Chile) compared with other North Chilean fog stations. Atmos Res 64:273–284.

Li X. 2002. Effects of gravel and sand mulches on dew deposition in the semiarid region of China. J Hydrol 260:151–160.

Liu X, Wang Z, Wang L, Wu R, Phillips J, Deng X. 2009. LEA 4 group genes from the resurrection plant Boea hygrometrica confer dehydration tolerance in transgenic tobacco. Plant Sci 176: 90-98.

Lowery CA, Park J, Gloeckner C, Meijler MM, Mueller RS, Boshoff HI, Ulrich RL, Barry CE 3rd, Bartlett DH, Kravchenko VV, Kaufmann GF, Janda KD. 2009. Defining the mode of action of tetramic acid antibacterials derived from *Pseudomonas aeruginosa* quorum sensing signals. J Am Chem Soc. 131:14473-14479.

Luna GM, Stumm K, Pusceddu A, Danovaro R. 2009. Archaeal diversity in deep-sea sediments estimated by means of different terminal-restriction fragment length polymorphisms (T-RFLP) protocols. Curr Microbiol. 59:356-561.

Lunn JE, Ashton AR, Hatch MD, Heldt HW. 2000. Purification, molecular cloning, and sequence analysis of sucrose-6F-phosphate phosphohydrolase from plants. Proc Natl Acad Sci USA. 97:12914-12919.

Lunn JE. 2002. Evolution of sucrose synthesis. Plant Physiol. 128:1490-1500.

Malek E, McCurdy G, Giles G. 1999. Dew contribution to the annual water balances in semi-arid desert valleys. J Arid Environ 42:71–80.

Marchesi JR, Sato T, Weightman AJ, Martin TA, Fry JC, Hiom SJ, Dymock D & Wade WG (1998) Design and evaluation of useful bacterium-specific PCR primers that amplify genes coding for bacterial 16S rRNA. Appl Environ Microbiol 64:795-799

Marin K, Huckauf J, Fulda S, Hagemann M. 2002. Salt-dependent expression of glucosylglycerol-phosphate synthase, involved in osmolyte synthesis in the cyanobacterium *Synechocystis* sp. isolate PCC 6803. J Bacteriol. 184:2870-2877.

Mathlouthi M, Luu DV. 1980. Laser-raman spectra of d-glucose and sucrose in aqueous solution. Carbohyd Res. 81:203-212.

Maxwell K, Johnson GN. 2000. Chlorophyll fluorescence-a practical guide. J Exp Bot. 51:659-668.

McKay, C.P., Friedmann, E.I., Gómez- Silva, B., Cáceres-Villanueva, L., Andersen, D.T. and Landheim, R. 2003. Temperature and moisture conditions for life in the extreme arid region of the Atacama Desert: four years of observations including the El Niño of 1997-1998. Astrobiology 3:393-406.

McNeil SD, Nuccio ML, Ziemak MJ, Hanson AD. 2001. Enhanced synthesis of choline and glycine betaine in transgenic tobacco plants that overexpress phosphoethanolamine N-methyltransferase. Proc Natl Acad Sci U S A. 98:10001-10005.

Menze MA, Boswell L, Toner M, Hand SC. 2009. Occurrence of mitochondria-targeted Late Embryogenesis Abundant (LEA) gene in animals increases organelle resistance to water stress. J Biol Chem. 284:10714-10719.

Mulo P, Sicora C, Aro EM. 2009. Cyanobacterial *psbA* gene family: optimization of oxygenic photosynthesis. Cell Mol Life Sci. 66:3697-3710.

Navarro-González R, Rainey FA, Molina P, Bagaley DR, Hollen BJ, de la Rosa J, Small AM, Quinn RC, Grunthaner FJ, Cáceres L, Gomez-Silva B, McKay CP. 2003. Mars-like soils in the Atacama Desert, Chile, and the dry limit of microbial life. Science. 302:1018-1021.

Neu, T.R. 1996. Significance of bacterial surface–active compounds in interaction of bacteria with interfaces. Microbiol Rev 60: 151– 166.

Nishiyama Y, Allakhverdiev SI, Murata N. 2006. A new paradigm for the action of reactive oxygen species in the photoinhibition of photosystem II. Biochim Biophys Acta. 1757:742-749.

Noy-Meir, I. 1973. Desert ecosystems. I. Environment and producers. Annual Review of Ecology & Systematics 4: 25-52.

Nübel U, Garcia-Pichel F, Muyzer G. 1997. PCR primers to amplify 16S rRNA genes from cyanobacteria. Appl. Environ. Microbiol. 63:3327-3332.

Oraby H.F., Ransom C.B., Kravchenko A.N. & Sticklen M.B. 2005. Barley *HVA1* gene confers salt tolerance in R3 transgenic oat. Crop Science 45:2218–2227.

Page-Sharp M, Behm CA, Smith GD. 1999. Involvement of the compatible solutes trehalose and sucrose in the response to salt stress of a cyanobacterial *Scytonema* species isolated from desert soils. Biochim Biophys Acta. 1472:519-528.

Parro V, de Diego-Castilla G, Moreno-Paz M, Blanco Y, Cruz-Gil P, Rodríguez-Manfredi JA, Fernández-Remolar D, Gómez F, Gómez MJ, Rivas LA, Demergasso C, Echeverría A, Urtuvia VN, Ruiz-Bermejo M, García-Villadangos M, Postigo M, Sánchez-Román M, Chong-Díaz G, Gómez-Elvira J. 2011. A microbial oasis in the hypersaline Atacama Desert subsurface discovered by a life detector chip: implications for the search for life on Mars. Astrobiology 11:969-996.

Paulino-Lima I, Azúa-Bustos A, Vicuña R, González-Silva C, Salas L, Lia Teixeira, Rosado A, Leitão AC and Lage C. 2013. Isolation of UV-C tolerant bacteria from the hyperarid Atacama Desert, Chile. Microbial Ecol, 65:325–335.

Pointing SB, Warren-Rhodes KA, Lacap DC, Rhodes KL, McKay CP. 2007. Hypolithic community shifts occur as a result of liquid water availability along environmental gradients in China's hot and cold hyperarid deserts. Environ Microbiol. 2:414-424.

Potts M. 1999. Mechanisms of desiccation tolerance in cyanobacteria. Eur J Phycol. 34:319–328.

Potts M. 2001. Desiccation tolerance: a simple process? Trends Microbiol. 9:553-559.

Ramírez-Flandes S, Ulloa O. 2008. Bosque: integrated phylogenetic analysis software. Bioinformatics 24:2539-2541.

Reed RH, Stewart WDP. 1983 Physiological responses of *Rivularia atra* to salinity: osmotic adjustment in hyposaline media. New Phytol 95:595-603.

Reed RH, Borowitzka LJ, Mackay MA, Chudek JA, Foster R, Warr SRC, Moore DJ, Stewart WDP. 1986. Organic solute accumulation in osmotically stressed cyanobacteria. FEMS Microbiol Lett 39:51–56.

Reysenbach AL, Wickham GS and Pace NR. 1994. Phylogenetic analysis of the hyperthermophilic pink filament community in Octopus Spring, Yellowstone National Park. Appl Environ Microbiol 60:2113-2119.

Ricci C and Perletti F. 2006. Starve and survive: stress tolerance and life-history traits of a bdelloid rotifer. Funct Ecol 20: 340–346.

Rippka R, Deruelles J, Waterbury J B, Herdman M, Stanier RY. 1979. Generic assignments, isolate histories and properties of pure cultures of cyanobacteria. J Gen Microbiol 111:1-61.

Rundel P, Dillon MO, Palma B, Mooney HA, Gulmon SL, Ehleringer JR. 1990. The phytogeography and ecology of the coastal Atacama Desert and Peruvian deserts. Aliso 13:1–50.

Sakamoto T, Kumihashi K, Kunita S, Masaura T, Inoue-Sakamoto K, Yamaguchi M. 2011. The extracellular-matrix-retaining cyanobacterium *Nostoc verrucosum* accumulates trehalose, but is sensitive to desiccation. FEMS Microbiol Ecol.77:385-394.

Sakamoto T, Yoshida T, Arima H, Hatanaka Y, Takani Y, Tamaru Y. 2009. Accumulation of trehalose in response to desiccation and salt stress in the terrestrial cyanobacterium *Nostoc commune*. Phyc Res 57: 66–73.

Salerno GL, Curatti L. 2003. Origin of sucrose metabolism in higher plants: when, how and why? Trends Plant Sci. 8:63-69.

Scherer S, Potts M. 1989. Novel water stress protein from a desiccation-tolerant cyanobacterium. Purification and partial characterization. J Biol Chem 264:12546-12553.

Schlesinger WH, Pippen JS, Wallenstein MD, Hofmockel KS, Klepeis DM, Mahall BE. 2003. Community composition and photosynthesis by photoautotrophs under quartz pebbles, Southern Mojave desert. Ecology 84:3222–3231.

Shao J, Yu G, Wang Z, Wu Z, Peng X, Li R. 2010. Towards clarification of the inhibitory mechanism of wheat bran leachate on *Microcystis aeruginosa* NIES-843 (Cyanobacteria): physiological responses. Ecotoxicology. 19:1634-1641.

Stanier RY, Kunisawa M M and Cohen-Bazire G. 1971. Purification and properties of unicellular blue-green algae (order *Chroococcales*). Bact Res 35:171–201.

Shaw E, Hill DR, Brittain N, Wright DJ, Täuber U, Marand H, Helm RF, Potts M. 2003. Unusual water flux in the extracellular polysaccharide of the cyanobacterium *Nostoc commune*. Appl Environ Microbiol 69:5679–5684.

Singh J, Whitwill S, Lacroix G, Douglas J, Dubuc E, Allard G, Keller W, Schernthaner JP. 2009. The use of Group 3 LEA proteins as fusion partners in facilitating recombinant expression of recalcitrant proteins in *E. coli*. Protein Expr Purif. 67:15-22.

Sivamani E, Bahieldin A, Wraith JM, Al-Niemi T, Dyer WE, Ho THD, Qu R. 2000. Improved biomass productivity and water use efficiency under water deficit conditions in transgenic wheat constitutively expressing the barley *HVA1* gene. Plant Sci 155:1–9.

Smith M, Bowman J, Scott F, Line M. 2000. Sublithic bacteria associated with Antarctic quartz stones. Antarct Sci 12:177–184.

Stanier, R.Y., R. Kunisawa, M. Mandel, and G. Cohen-Bazier. 1971. Purification and properties of unicellular blue-green algae (*order Chroococcales*). Bacteriol Rev. 35:171-205.

Swire-Clark GA, Marcotte WR Jr. 1999. The wheat LEA protein Em functions as an osmoprotective molecule in *Saccharomyces cerevisiae*. Plant Mol Biol 39: 117–128.

Tarczynski MC, Jensen RG, Bohnert HJ. 1992. Expression of a bacterial *mtlD* gene in transgenic tobacco leads to production and accumulation of mannitol. Proc Natl Acad Sci USA. 89:2600-2604.

Thomas DN. 2005. Photosynthetic microbes in freezing deserts. Trends Microbiol 13:87–88.

Tweddle, J. C., J. B. Dickie, C. C. Baskin, and J. M. Baskin. 2003. Ecological aspects of seed desiccation sensitivity. J Ecol 91:294–304.

Walters, C., Hill, L. M. and Wheeler, L. J. 2005. Dying while dry: kinetics and mechanisms of deterioration in desiccated organisms. Integr Comp Biol 45: 751-758.

Warr SRC, Reed RH, Stewart WDP. 1987. Low-molecular-weight carbohydrate biosynthesis and the distribution of cyanobacteria (blue-green-algae) in marine environments. Br Phycol J 22:175-180.

Warren-Rhodes KA, Rhodes KL, Boyle LN, Pointing SB, Chen Y, Liu S, Zhuo P, McKay CP. 2007. Cyanobacterial ecology across environmental gradients and spatial scales in China's hot and cold deserts. FEMS Microbiol Ecol. 61:470-482.

Warren-Rhodes K.A., Rhodes, K.L., Pointing, S.B., Ewing, S.A., Lacap, D.C., Gómez-Silva, B., Amundson, R., Friedmann, E.I. and McKay, C.P. 2006. Hypolithic cyanobacteria, dry limit of photosynthesis, and microbial ecology in the hyperarid Atacama Desert. Microb Ecol. 52:389-398.

Whitford WG. 2002. Ecology of desert systems. Elsevier Science Ltd, San Diego.

Wierzchos J, Ascaso C, McKay CP. 2006. Endolithic cyanobacteria in halite rocks from the hyperarid core of the Atacama Desert. Astrobiology 6:415–422.

Wise MJ. 2003. LEAping to conclusions: a computational reanalysis of late embryogenesis abundant proteins and their possible roles. BMC Bioinformatics. 29:52.

Wise MJ, Tunnacliffe A. 2004. POPP the question: what do LEA proteins do? Trends Plant Sci. 9:13-17.

Yamada M, Morishita H, Urano K, Shiozaki N, Yamaguchi-Shinozaki K, Shinozaki K, Yoshiba Y. 2005. Effects of free praline accumulation in petunias under drought stress. J Exp Bot 56:1975–1981.

Yoshida T, Sakamoto T. 2009. Water-stress induced trehalose accumulation and control of trehalase in the cyanobacterium *Nostoc punctiforme* IAM M-15. J Gen Appl Microbiol. 55:135-45.

Yoshimura H, Okamoto S, Tsumuraya Y, Ohmori M. 2007. Group 3 sigma factor gene, *sigJ*, a key regulator of desiccation tolerance, regulates the synthesis of extracellular polysaccharide in cyanobacterium *Anabaena* sp. isolate PCC 7120. DNA Res. 14:13-24.

Zeng XQ, Hou YJ, Yang ZC, Pèli E, Peng Cl, Nie L. 2013. Opportunistic growth and desiccation tolerance: The ecological success of poikilohydrous sutotrophs. Nova Hedwigia 96:511-524.

6.- Publications of the author mentioned in this thesis work

1.- Azúa-Bustos A., Arenas, C., and Vicuña, R. 2013. *Gloeocapsopis* AAB1, a extremely desiccation tolerant cyanobacterium isolated from the Atacama Desert. Under review.

2.- Azúa-Bustos A. and Vega-Martínez, C. 2013. The potential for detecting life as do don't know it by fractal complexity analysis. Int. J. Astrobiol. In press.

3.- Paulino-Lima I, Azúa-Bustos A, Vicuña R, González-Silva C, Salas L, Lia Teixeira, Rosado A, Leitão AC and Lage C. 2013. Isolation of UV-C tolerant bacteria from the hyperarid Atacama Desert, Chile. Microb Ecol. 65:325–335.

4.- Azua-Bustos A., González-Silva C., and Arenas-Fajardo, C., Vicuña R. (2012). Extreme environments as drivers of convergent evolution: the Atacama Desert Coastal Range as a relevant model. Frontiers in Microbiology 3: 426.

5.- Azúa-Bustos A., Urrejola C., and Vicuña R. (2012). Life at the dry edge: microorganisms of the Atacama Desert. FEBS Lett. 586:2939–2945.

6.- Lage, C., Dalmaso, G., Teixeira, L., Bendia, A., Paulino-Lima, I., Galante, D., Janot-Pacheco, E., Abrevaya, X., Azua-Bustos, A., Pellizari V. and Rosado, A. (2012). Probing the limits of extremophilic life in extraterrestrial environment-simulated experiments. Int J Astrob 11:251-256.

7.- Azúa-Bustos A, González-Silva C, Mancilla R.A., Salas, L., Gómez-Silva B, McKay CP and Vicuña R. 2011. Hypolithic cyanobacteria supported mainly by fog in the Coastal Range of the Atacama Desert. Microb Ecol, 61:568-581.

8.- Azúa-Bustos, A., González-Silva, C., Salas L, Vicuña, R. 2010. A novel subaerial *Dunaliella* sp. growing on cave spiderwebs in the Atacama Desert. Extremophiles 14:443-452.

9.- Azúa-Bustos A., González-Silva, C., Mancilla R.A., Salas L, Palma R.E., Wynne J.J., McKay, C.P. and Vicuña, R. 2009. Ancient photosynthetic eukaryote biofilms in an Atacama Desert coastal cave. Microb Ecol. 58:485–496.